

# PNAS

www.pnas.org

Supplementary Information for

## **Immune evasion in HPV-negative head and neck precancer-cancer transition is driven by an aneuploid switch involving chromosome 9p loss**

William N. William Jr;<sup>1,2\*#</sup> Xin Zhao;<sup>3\*</sup> Joy J. Bianchi;<sup>3\*</sup> Heather Y. Lin;<sup>4</sup> Pan Cheng;<sup>3</sup> J. Jack Lee;<sup>4</sup> Hannah Carter;<sup>5,6</sup> Ludmil B. Alexandrov;<sup>5,7,8</sup> Jim P. Abraham;<sup>9</sup> David B. Spetzler;<sup>9</sup> Steven M. Dubinett;<sup>10</sup> Don W. Cleveland;<sup>5,7,11</sup> Webster Cavenee;<sup>5,6,11</sup> Teresa Davoli;<sup>3\$#</sup> Scott M. Lippman<sup>1,5,6\$</sup>

Departments of <sup>1</sup>Thoracic / Head and Neck Medical Oncology, <sup>4</sup>Biostatistics, The University of Texas MD Anderson Cancer Center; <sup>2</sup>Hospital BP, a Beneficência Portuguesa de São Paulo; <sup>3</sup>Institute for Systems Genetics, Department of Biochemistry and Molecular Pharmacology, NYU Langone Health; <sup>5</sup>Moores Cancer Center, Departments of <sup>6</sup>Medicine and <sup>7</sup>Cellular and Molecular Medicine, <sup>8</sup>Bioengineering, University of California San Diego; <sup>9</sup>Research and Development, Caris Life Sciences (United States); <sup>10</sup>Jonsson Comprehensive Cancer Center, University of California Los Angeles; <sup>11</sup>Ludwig Institute for Cancer Research

\* These authors contributed equally to this work

\$ These senior authors contributed equally to this work

# Corresponding Authors

Corresponding Authors:

Teresa Davoli, PhD  
Assistant Professor  
Department of Biochemistry and Molecular Pharmacology  
Institute for Systems Genetics  
NYU Langone Health  
New York, NY 10016  
Phone: 212-263-8081; email: [teresa.davoli@nyulangone.org](mailto:teresa.davoli@nyulangone.org)

William N. William Jr., MD  
Adjunct Associate Professor  
Department of Thoracic / Head and Neck Medical Oncology  
The University of Texas MD Anderson Cancer Center  
1515 Holcombe Blvd. unit 432  
Houston, TX 77030  
Phone: 713-792-6363; email: [william.william@bp.org.br](mailto:william.william@bp.org.br)

**This PDF file includes:**

Supplementary text (pages 3-7)  
Figures S1 to S12 (pages 8-19)  
SI References (page 20)  
Tables S1 to S25 (pages 21-88)

## Supplementary Information Text

### Methods – Extended Description

#### *Prospective Oral Precancer Cohort*

**SCNA and Multiplex immune profiling.** Chromosome gain was determined by fluorescence *in situ* hybridization, using a chromosome-7 centromeric probe, randomly selected marker of tri-/tetra-somy based on similar phenotypes with different chromosomes in this context (1). After specific PCR-DNA amplification, an automatic capillary DNA analyzer was used to separate microsatellite alleles and to quantify the peak height of individual alleles for each marker. Loss of at least one of the markers (using the criteria described in the statistical section) was considered as loss of that specific chromosomal site. We considered overall SCNA level as chr7 gain and loss at 7 chromosome arms, including 3p, 9p, and 17p and the following: 4q, 8p, 11q, and 13q.

As described in a prior methods report (2), we utilized a validated multiplex immunofluorescence (mIF) panel of five antibodies stained on the same tissue section, and labeled using a tyramide-signal amplification-based kit, including: anti-CD3 (Dako, T lymphocyte marker), anti-CD8 (clone C8/144B, Thermo Scientific, present on cytotoxic T cells), anti-CD68 (clone PG-M1, Dako, macrophage lineage marker), anti-cytokeratin (clone AE1/AE3, Dako), and DAPI (nuclear staining). Each antibody was labeled with a specific fluorophore. All antibodies had been optimized for mIF by examination of positive and negative controls and testing of the antibodies by Western blotting. We performed scanning and image capture with a multispectral microscope (Vectra™, PerkinElmer), and analyzed the images with a specialized software (InForm™, PerkinElmer) capable of counting the number of cells with positive staining for each marker in a specified area. For each sample, 1-10 representative areas (median 6) measuring 1 mm<sup>2</sup> each, were randomly selected for marker quantification. CD3+ and CD8+ T-cells and CD68+ macrophages were evaluated and reported as cell density (i.e., cells/mm<sup>2</sup>).

**Statistical considerations.** Wilcoxon rank-sum tests were used to compare the distribution of continuous variables between two groups defined by a binary variable. Fisher's exact tests were used to assess the association between binary markers and categorical factors. Spearman correlation coefficients were used to evaluate pair-wise correlations between two markers in continuous scale. When analyzing biomarkers assessed in a continuous scale, values from multiple areas were transformed into logarithm scale and were fit with linear mixed-effect models to account for within-patient variation (3). OCFS (model1) was defined as the time from protocol registration until development of the protocol-specified primary endpoint of invasive oral cancer, or death, and estimated by the Kaplan-Meier method. Cox proportional hazard model was used to study marker and OCFS associations. Log-rank test was performed to test the difference in OCFS between groups. All analyses were performed using SAS software (version 9.4; SAS Institute, Cary, NC) and R.

*Cox Model~ 9p21.3 Loss + 3p14 Loss + 17p13.1 Loss + Histology (model1)*

Throughout the paper, in the univariate (model2) and multivariable (model3) analyses performed to predict the level of a specific parameter (e.g., immune-cell level) based copy-number event, two different cutoffs were used (35 %-65 %, and confirmed with a 50 %). For example, in multivariable logistic regression of precancer cases, we divided the patients into the top and bottom 35 % in terms of percent of immune cells and used loss at 3p14, 9p21.3, or/and

17p13.1, and SCNA level, to determine the contribution of each parameter to the immune-cell landscape. The same cutoffs were used for the analysis of TCGA cases, including IS. The chromosome loss in precancer is defined as the ratio of the peak heights of the two alleles in lesion (L1/L2) DNA and in the corresponding normal lymphocytes (N1/N2) DNA >1.43 or <0.7, consistent with the same cutoffs utilized in the landmark clinical study that prospectively correlated precancer-specific SCNAs with prognosis (4).

The SCNA level was calculated based on the available information on the SCNA level at different genomic loci. More specifically, information was available on the presence of losses at the following loci: 3p21-14, 4q26-28, 4q31.1, 8p22-p23, 9p21.3, 11q13-q22, 13q21, 17p13.1 --SCNA level was calculated based on any SCNA (loss at all microsatellite loci in 3p21-14, 4q26-28, 4q31.1, 8p22, 8p23, 9p21.3, 11q13, 11q22, 13q21, or 17p13.1 and/or chromosome 7 gain):

$$SCNA.level^* = \begin{pmatrix} no\ SCNA & 0\ (none) \\ any\ Loss\ OR\ chr7\ gain & 1\ (low) \\ any\ Loss\ AND\ chr7\ gain & 2\ (high) \end{pmatrix}$$

$$Immune_{infiltrate} \sim 3p14\ Loss\ or\ 9p21.3\ Loss\ or\ 17p13.1\ Loss \times \beta + \varepsilon(\text{random effect})\ (model2)$$

$$Immune_{infiltrate} \sim 3p14\ Loss + 9p21.3\ Loss + 17p13.1\ Loss + SCNA.level\ (model3)$$

#### HPV-Negative HNSC in The Cancer Genome Atlas (TCGA)

**Statistical considerations.** Logistic regression was used to determine the variables most predictive of different parameters representing immune infiltrate (model4-5) and IS levels. All the findings were confirmed using two purity methods (pathology-based and ABSOLUTE, see main manuscript Methods) and reported in the supplemental tables. After purity adjustment, we consider a log2-transformed copy number ratio >0.3 as a gain and <(-0.3) as a loss. Gene expression, mutation and clinical data were downloaded from GDAC Firehose. Patients with nonsense, splice site, frame shift, and missense mutations with Polyphen2-HVAR score > 0.2 (5) were considered as *TP53* mutation-positive patients. HPV-status was determined using a cutoff of RPM >1 (viral reads per million) in tumors of oropharyngeal origin was used as a stringent definition of HPV-positive HNSC, for a limited subset analysis. We used the log2 transformed RSEM values to estimate differences in the immune cell content (different types of immune cells) using CIBERSORT (using the LM22 gene signature) (6). In order to recapitulate in HNSC what was done in oral precancers, RNA expression levels of specific immune markers were applied as a proxy of the level of the corresponding immune cells in the tumor. Previous studies have shown that RNA expression levels (e.g., CD8+) of immune-cell markers highly correlate with cell estimates based on immunofluorescence (7, 8) (see Results). We defined the tumors as having low or high gene expression level using the 35<sup>th</sup> and 65<sup>th</sup> percentiles; results were confirmed using a cutoff of 50%. We used the GISTIC2 algorithm to distinguish between the two major types of events--arm-level and focal-level events. When specified, logistic regression was performed after first selecting patients with a certain tumor stage or containing or not *TP53* mutations. In addition, 5-fold cross-validation and variable-importance (size-effect) evaluation (package caret) were also performed to evaluate the accuracy of multivariable logistic regression models, and the size effect of each covariate, respectively.

$$SCNA\ level = \sum arm\ gains + \sum arm\ losses$$

$$Immune_{infiltrate} \sim 3p14\ Loss + 9p21.3\ Loss + 17p13.1\ Loss + Chr\ 7\ Gain$$

$$+ SCNA\ level\ (normalized)\ (model4)$$

$$Immune_{infiltrate} \sim 9p21.3 \text{ Loss}(arm) + 9p21.3 \text{ Loss}(focal) + 9p21.3 \text{ Loss}(arm + focal) + 3p14 \text{ Loss} + SCNA \text{ level (normalized)} \text{ (model5)}$$

For the least absolute shrinkage and selection operator (*Lasso*) (9) classification, to determine the parameters most predictive of immune-infiltrate level, we defined tumors as having low or high IS levels using the 35<sup>th</sup> and 65<sup>th</sup> percentiles, as described previously (10), and used a binomial model. We also applied *Lasso* using 10-fold cross validation. As variables, we included the presence of loss or gain in all possible whole chromosome or chromosome arms across the genome and the overall arm/chromosome SCNA level.

For GSEA (Gene Set Enrichment Analysis) comparing tumor samples with or without the indicated SCNA, we first used DEseq2 package (11) to calculate the log2 fold change and adjusted p-value of differentially expressed genes. Then we calculated the differential-expression score [Exp. Score] based on the formula below. Exp. Score was then used to perform GSEA pathway analysis (pre-ranked model) (12).

$$Exp. \text{ Score} = \text{sign}(\log_2 \text{ FoldChange}) \times -\log_{10}(\text{adjusted } p\_value)$$

### *HPV-negative HNSC Cell Lines*

**Statistical considerations.** We used GSEA to investigate mechanisms of 9p21.3 or 3p14 (selected based on statistical significance in TCGA analyses) effects on gene- and pathway-change. To have similar numbers of cells in each group we split the cell lines into those having a copy-number level lower or higher than the median value (for example, as a threshold we used the median based on log2 copy-number ratio of -0.45 for 9p21.3 and -0.5 for 3p14 region). We used DEseq2 (11) to estimate the differential expression between the two groups of cell lines. We then used the formula above to calculate a score as input in GSEA (12). For GSEA, we used the comprehensive list of pathway and gene sets from BIOCARTA, KEGG and REACTOME databases. We performed logistic regression (model6) to determine the parameters most predictive of the expression of the SASP signature pathway (see below). We distinguished cell lines as having low or high SASP-signature scores using the 35<sup>th</sup>/65<sup>th</sup>, or 50<sup>th</sup> percentile cutoff (binary) or continuous variable of the distribution (all the continuous variables were normalized before being used in the multivariable models). We applied a logistic model on the dataset using as variables, 3p14 loss or 9p21.3 loss. To determine the contribution of chromosome loss encompassing whole 9p, 3p, and 17p arms as compared to focal losses, we used GISTIC2. Applying GISTIC2 algorithm to segment data derived from the cell lines, we determined the type of loss at 9p21.3 and 3p14: arm-level event versus focal-only event. As in TCGA analyses, a threshold of 70% of arm length (given in units of the fraction of chromosome arm) was used in GISTIC2 to distinguish between cell-line focal- and arm-level events.

$$SASP \text{ enrichment} \sim 9p21.3 \text{ Loss}(arm) + 9p21.3 \text{ Loss}(focal) \text{ (model6)}$$

**SASP and *IFN* gene set.** To derive an aneuploidy-associated SASP signature, we first considered the genes upregulated in SASP as previously reported (13). Then we crossed this gene list with the genes upregulated (log2FC of at least 1.5) in aneuploid cells versus control cells (reversine treated versus control) from (14). The derived list of 20 genes represents the SASP signature and is shown in Table S15. The *IFN* gene set contains the list of *IFN* genes that are located on chr 9p21.3 and shown in Table S15. To calculate the SASP gene-expression signature and *IFN* gene expression we used the single-sample GSEA (ssGSEA package) (12).

## Survival analysis of 9p loss in ICB treated HPV-negative HNSC

**Statistical, profiling considerations for real-world evidence (RWE) cohort.** We employed a novel “virtual karyotyping” platform that allowed interrogation of the associations between loss of genes/chromosomal regions in 9p or 3p and outcomes using linked biomarker-EMR-insurance claim-survival record data. The Caris Life Sciences CODEai database which contains over 215,000 molecular profiles combined with clinical outcomes was leveraged for this study. 2,761 HNSC cases were available of which 1,604 had results from the Caris 592-gene assay. These cases were then segregated by whether therapy was administered prior to the collection of the sample that was profiled. 479 cases were found to have therapy administration only after the collection date of the tumor profiled. The 479 cases were further subdivided into groups based on whether immunotherapy (nivolumab or pembrolizumab) was part of their treatment. An overall survival minimum of 30 days was selected to remove patients with incomplete outcomes records (filtered down to 455). 196 of the 455 cases were HPV negative assessed by p16 IHC status. 122 patients were treated with immunotherapy across various lines of treatments with and without chemotherapy. 74 patients were found to have no immunotherapy treatment (Consort diagram, Fig. S12). TMB in our 592-gene panel was found to be equivalent to the FDA-approved 324-gene companion diagnostic test related to the agnostic use of pembrolizumab for tumors with  $\geq 10$  mutations/megabase (15). The 592-gene MI Tumor Seek panel was used to validate anti-PD-1 therapy efficacy in relation to MSI status (16).

Microdissection was performed on all cases and only those that achieved a minimum of 20% of tumor content in the area selected for microdissection were sequenced. We derived the SCNA level by comparing the depth of sequencing of genomic loci to a diploid control as well as the known performance of these genomic loci from a CLIA-validated commercially available assay (MI Tumor Seek 592-gene panel; Caris Life Sciences), as recently described (17). The 592-gene panel arm loss algorithm was CAP/CLIA validated in a study comparing 436 patients with both 592-gene panel arm-loss predictions and FISH results for 1p/19q co-deletion, a pattern shown to be therapeutically relevant in glial-brain tumors, e.g., low-grade gliomas (18). There were 29 samples positive by FISH and 407 samples negative by FISH for 1p/19q co-deletion and the arm-loss algorithm predictions had a sensitivity of 96.6 % (95 % CI: 82.2-99.9) and specificity of 99.5 % (95 % CI: 98.2-99.9). The 592-gene panel arm loss algorithm was further validated against the Caris Life Sciences Whole Exome Sequencing (WES) assay on 369 cases with both 592-gene panel arm-loss predictions and WES arm-loss predictions. WES used a conservative copy-number estimate across entire chromosomes, excluding centromeres and telomeres. This estimate included ~50,000 intronic and intergenic SNPs which were present at minimum every 160,000 base intervals (6.25/megabase) along with depth data from every gene. The calculation used CNVKit (python 3.7, version 0.9.6) and provided confidence in deletion status by examining tens of thousands of data points and returning a call based on consecutive measurements of presence or absence of DNA. The Pearson's correlation between the two assays was 0.828 across 9p loss and 0.773 for 9p21.3 loss. *PD-L1*, *PD-L2*, and *JAK2* were evaluated for copy-number loss using 1.6 copies or less to determine if the gene is deleted as described previously (19). The 592-gene panel arm-loss algorithm evaluated large-scale gene deletions across both arms of all chromosomes where a gene was profiled. The mean copy number across all genes profiled on a region or arm was compared to the mean of all copies for genes profiled on the opposite arm. The resulting ratios for each chromosome must be  $\leq 0.8$  and the opposite arm cannot have an average copy number greater than 2.5 for the region or arm under consideration to be evaluated as lost. Larger cohorts using whole-exome or whole-genome sequencing data will be important to extend these findings, including to address the contribution of *TP53* mutations to ICB resistance, an analysis currently limited by statistical power due to the high *TP53* mutation-9p loss co-occurrence rates.

## **Contributions**

SML and TD conceived, planned and provided biologic and clinical (prevention, interception and immune therapy) intellectual input and insight into all aspects of this project, including all patient-cohort and cell-line studies and results—study design, statistical analyses and led the data interpretation, potential application and implications to HNSC, other cancers and aneuploid diseases—copy-number, aneuploid, -immune concept, balance and model development, and writing; WNW and SML planned, assembled and conducted the prospective precancer cohort; HYL and JJJ contributed to the design and analysis of the precancer cohort; XZ performed most of the statistical analyses for precancer and TCGA datasets; JJB provided essential contribution to the analyses and their interpretation. JPA, DBS, and SML provided the analysis, data interpretation and insight of the RWE cohort. WC provided essential insight into the development and conduct of the project, including the conception of the model concept. SML, TD, WNW and XZ wrote the manuscript. All the authors contributed to editing the manuscript.

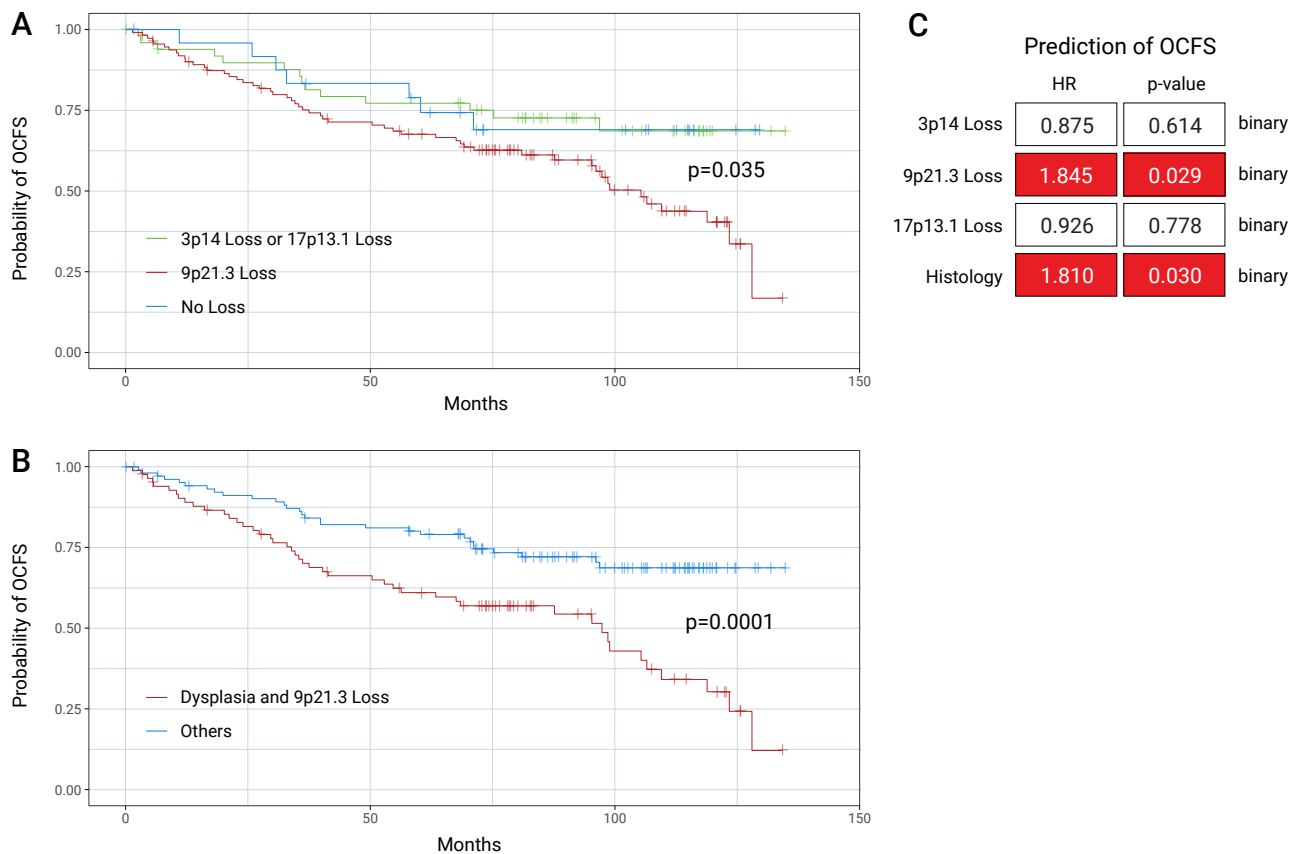


**Fig. S1. Predictors of cancer risk in prospective oral precancer cohort**

A) Kaplan-Meier curves of oral cancer-free survival (OCFS) by SCNAs (9p21.3, 3p14 or 17p13.1 loss, no chromosomal loss).

B) Kaplan-Meier curves of OCFS by combination of SCNA with histology status (dysplasia and 9p21.3 loss versus others).

C) Multivariable Cox-proportional hazard model for prediction of survival (OCFS).



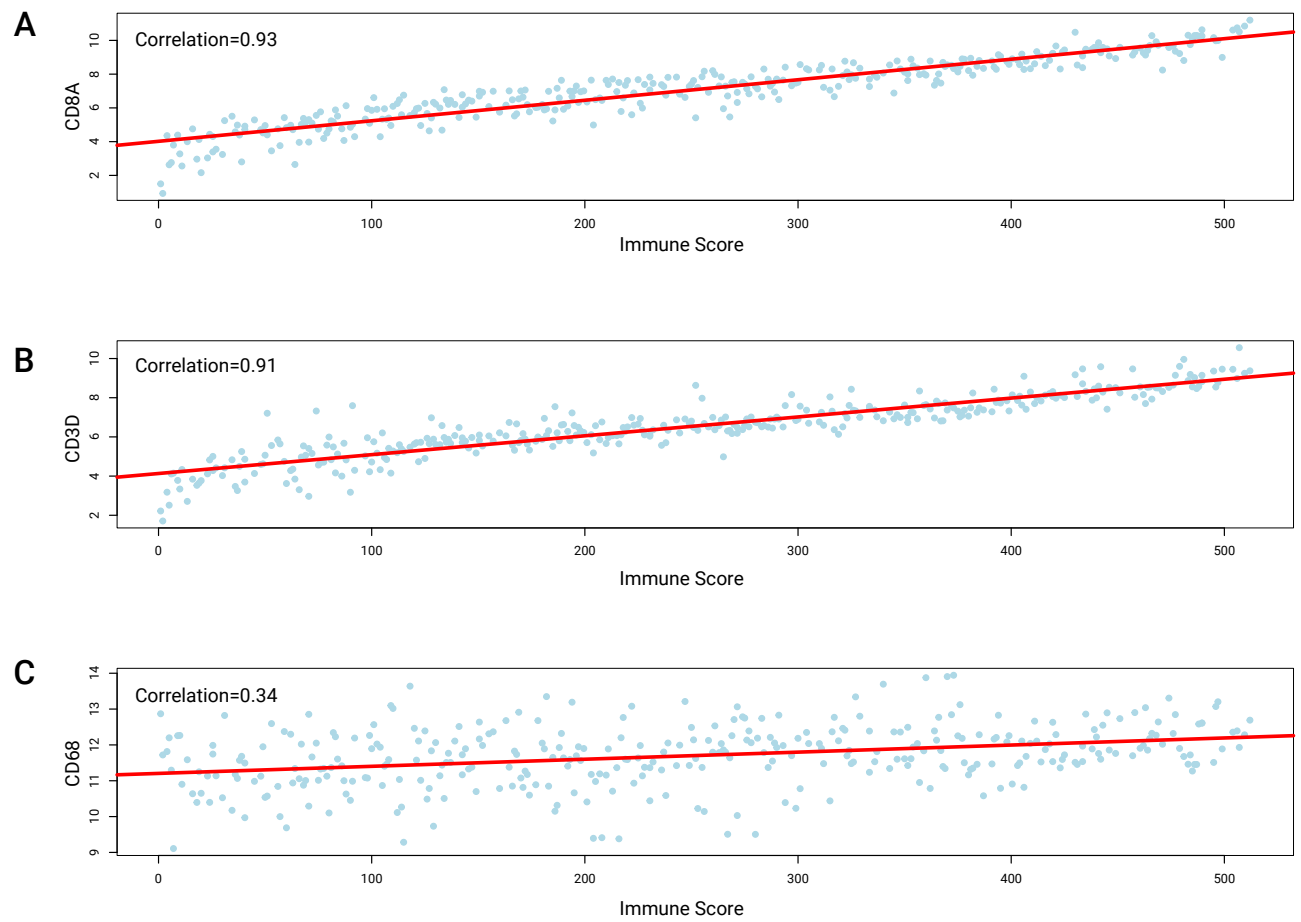
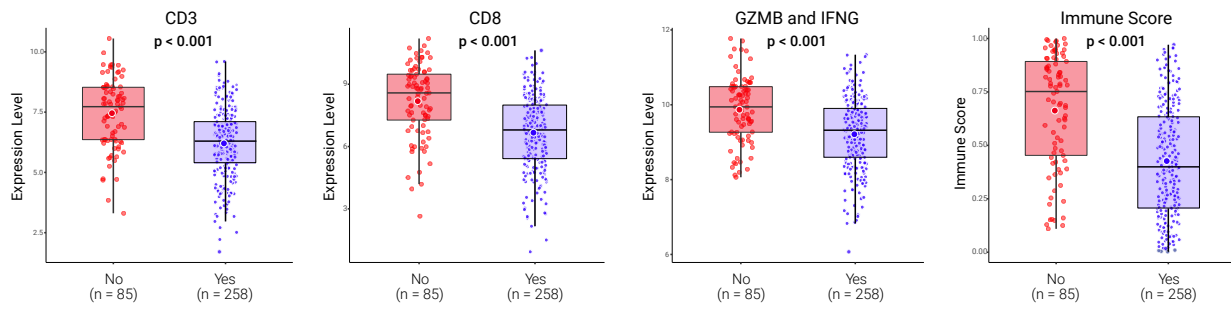
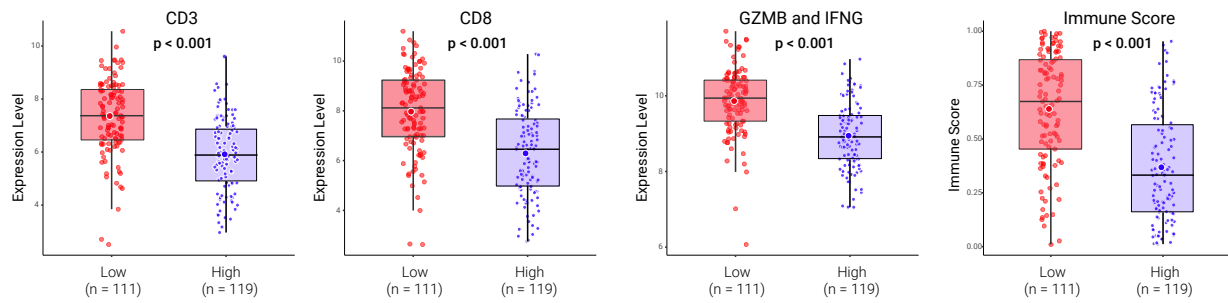


**Fig. S2. CD3+ (CD3D), CD8+ (CD8A) or CD68 expression and IS in HNSC**

**A** Loss at any site (3p14, 9p21.3 or 17p13.1)



**B** SCNA Level top 35% vs bottom 35%



**C** Chr 7 gain

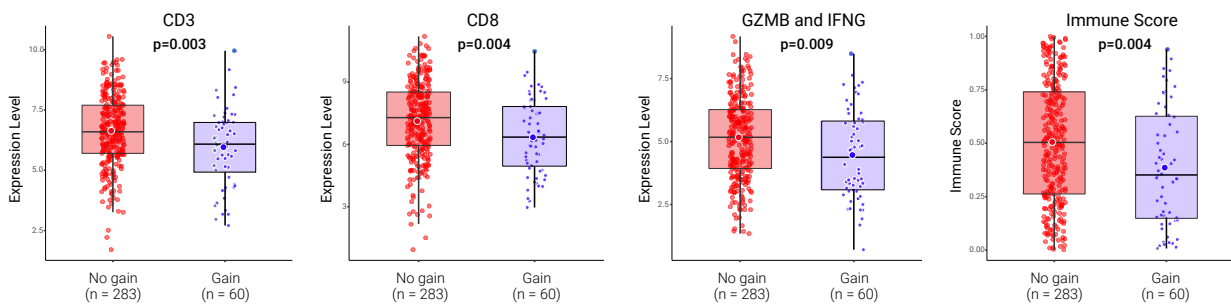


**Fig. S3. SCNA associations with CD3+, CD8+, GZMB/IFNg or IS in HNSC**

CD3+, CD8+ and GZMB/IFNg (average expression of the two genes) or IS associations with the presence of any loss (arm or focal) at 9p21.3, 3p14, or 17p13 (A), SCNA level (B), or chr7 gain (C).

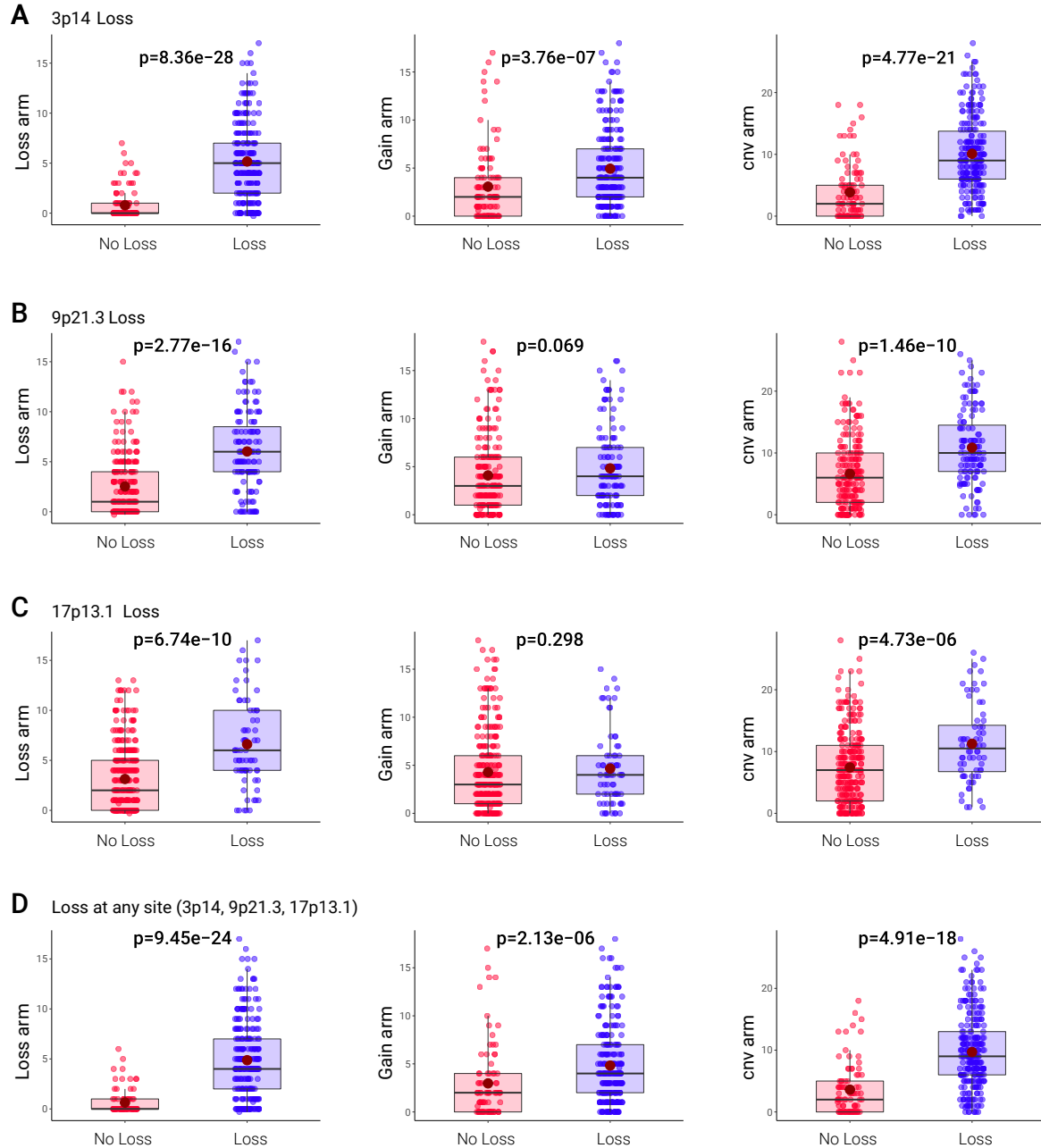


**Fig. S4. 3p14, 9p21.3 or 17p.13.1 loss (arm or focal) associated with SCNA level in HNSC**

A) Relationship between the number of arm loss (loss\_arm), gain (gain\_arm) and SCNA level (loss\_arm + gain\_arm, cnv\_Arm) between samples with and without 3p14 loss (arm or focal).

B) Arm loss, gain and SCNA level associations with and without 9p21.3 loss.

C) Arm loss, gain and SCNA level associations with or without 17p13.1 loss.

D) Arm loss, gain and SCNA level associations with or without loss (arm or focal) at any of the three sites (3p14, 9p21.3 or 17p13.1) (p-value is from Wilcoxon test).

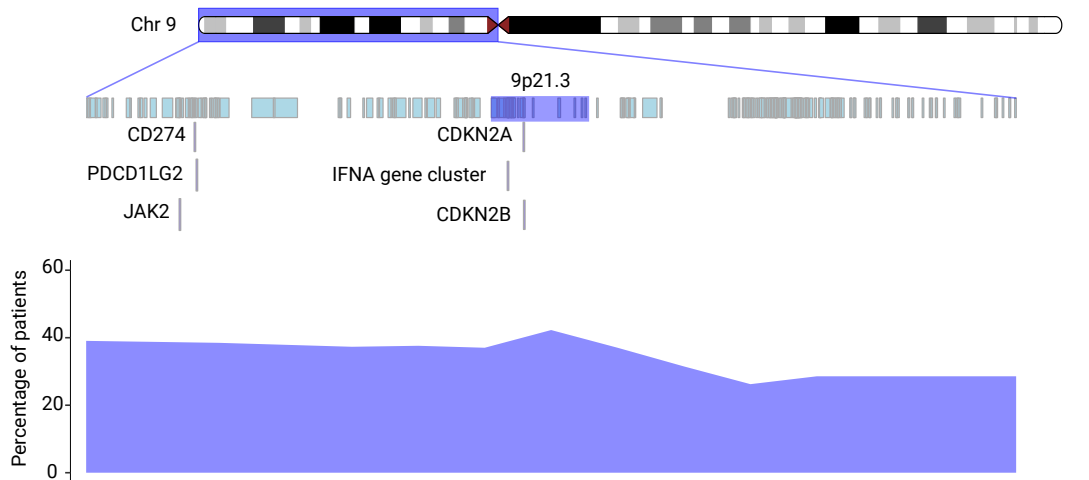


**Fig. S5. Percentage of loss on arm 9p in HNSC (based on cytoband regions)**

Representative genes indicated.

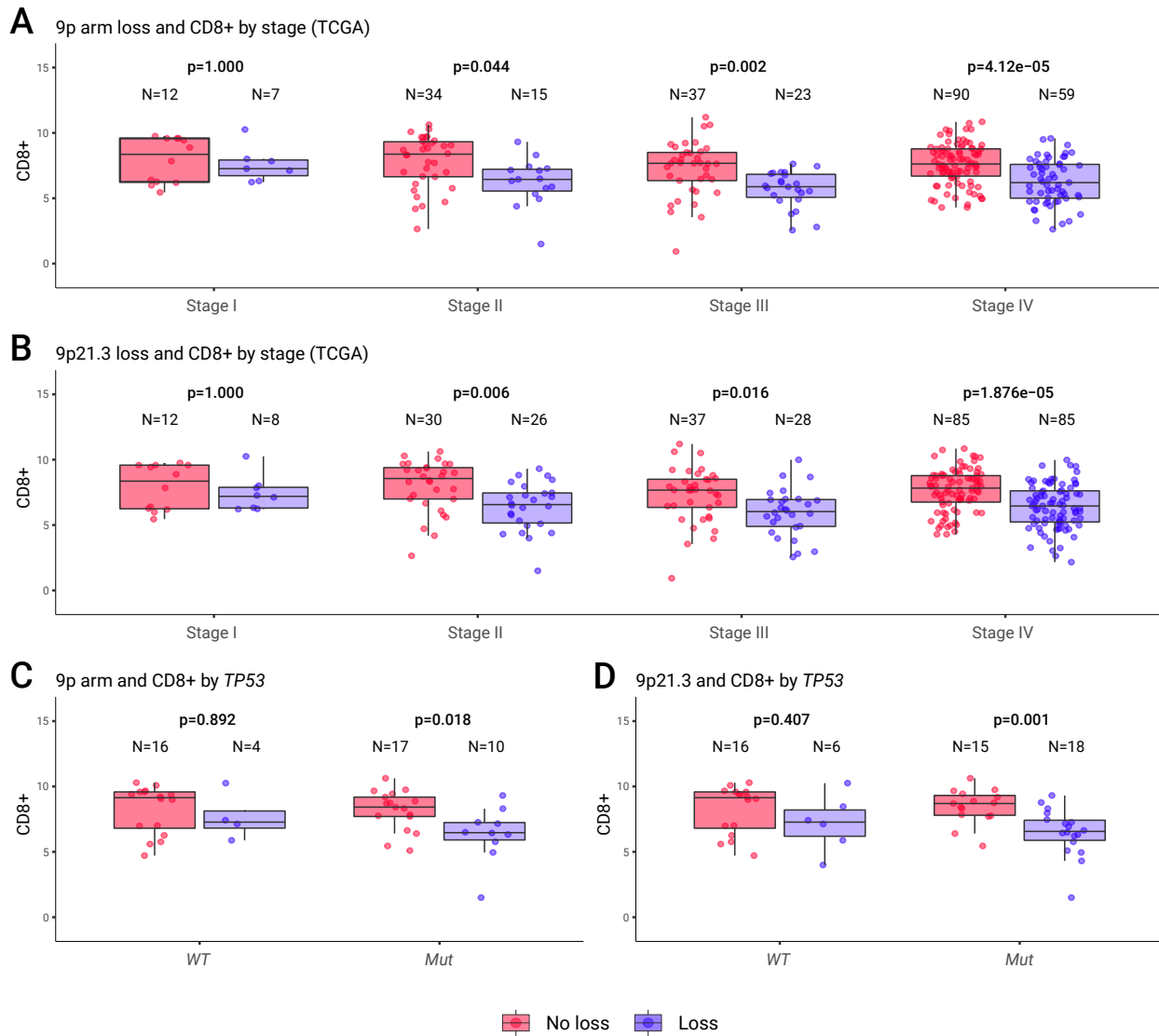


**Fig. S6. Chromosome-9p loss and CD8+ T-cell associations with HNSC stage and *TP53* status**

Association between CD8+ T-cell levels and 9p loss (A) and 9p21.3 loss (B), in relationship with tumor stage and *TP53* mutation status (C and D) in HPV-negative stage I or II HNSC tissue samples.

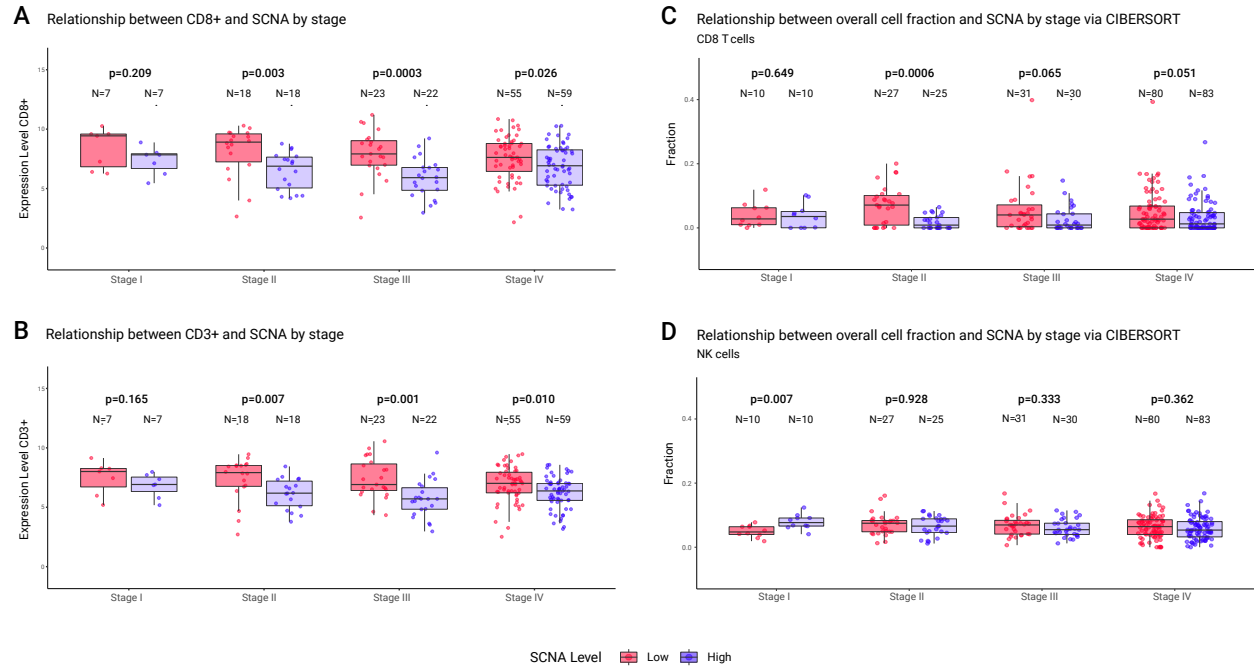


**Fig. S7. SCNA level to different HNSC tumor stage**

- A) SCNA level and CD8+ T cells in relation to tumor stage.
- B) SCNA level and CD3+ T cells in relation to tumor stage.
- C) SCNA level and CD8 T cells (via CIBERSORT) in relation to tumor stage.
- D) SCNA level and NK cells (via CIBERSORT) in relation to tumor stage.

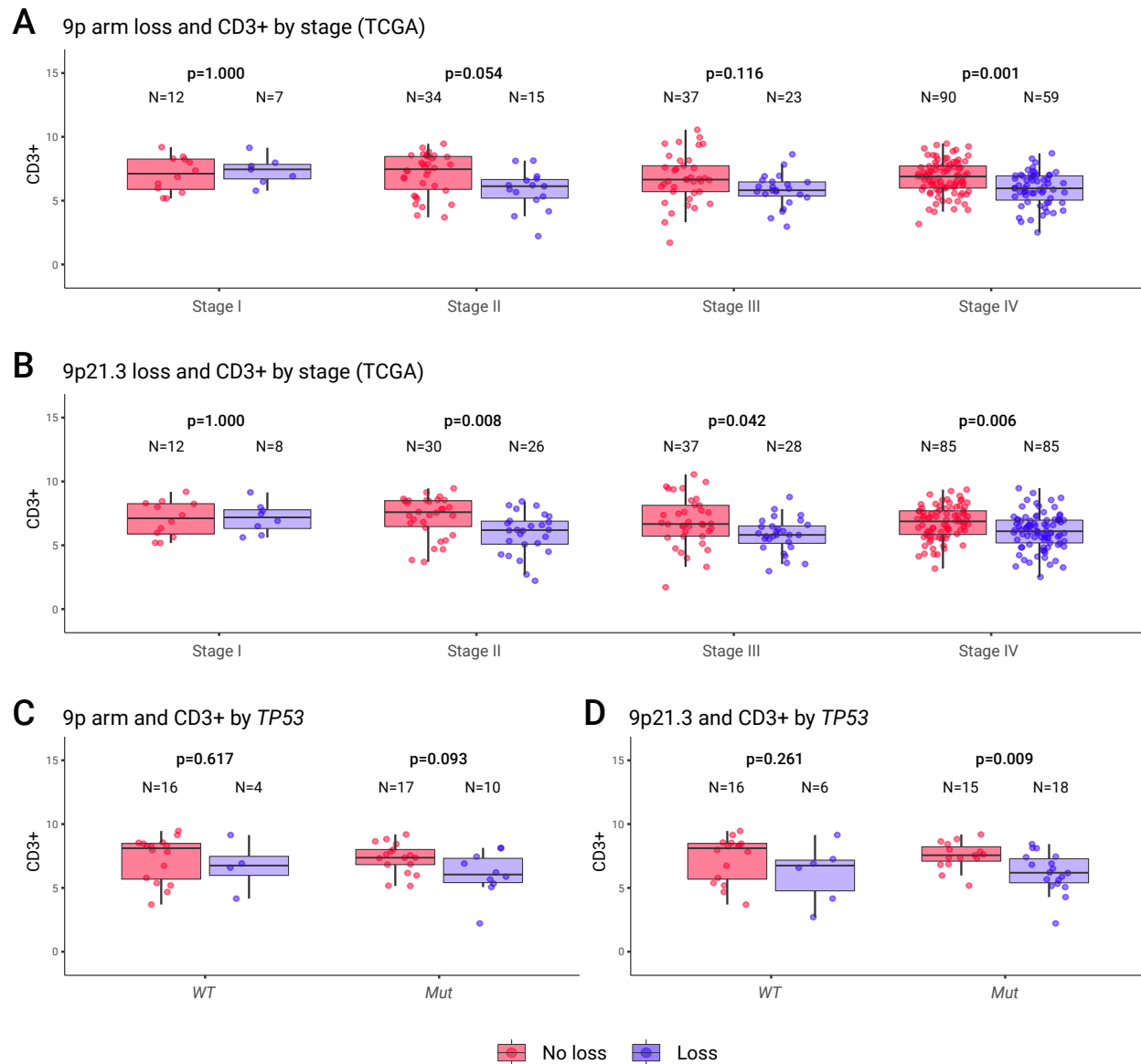


**Fig. S8. Chromosome 9p loss and CD3+ T-cell associations with HNSC stage and *TP53***

Association between CD3+ T-cell levels and 9p loss (A) and 9p21.3 loss (B), in relationship with tumor stage and *TP53* mutation status (C and D) in HPV-negative HNSC tissue samples, the latter focused on stage-I and -II samples.

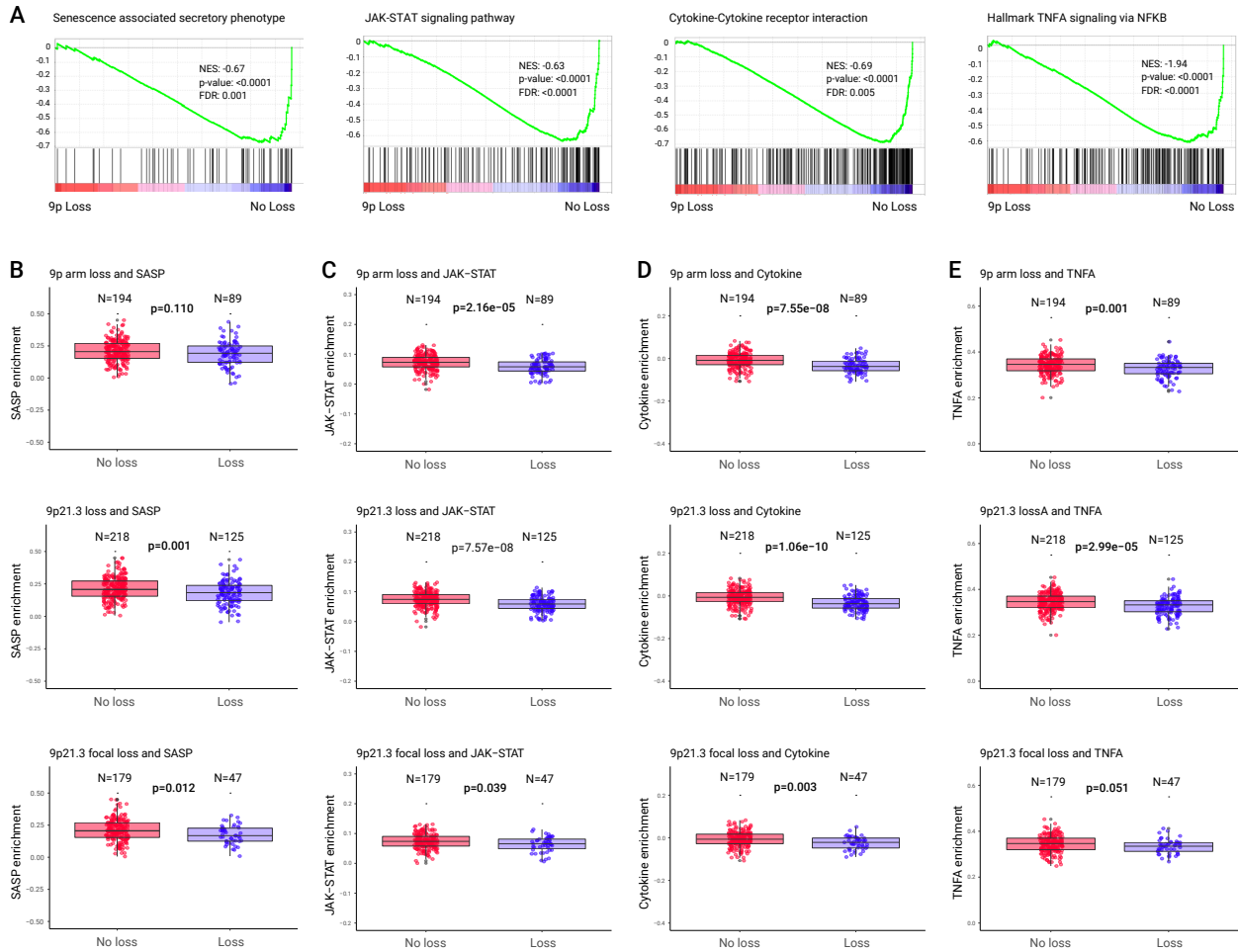


**Fig. S9. SASP, JAK/STAT and Cytokine receptor and TNFA Signaling via NFkB Pathways in relationship with 9p or 9p21.3 loss in HPV-negative HNSC tumors**

A) Pathway depletion from GSEA analysis of HPV-negative HNSC tumors comparing samples with and without 9p loss. GSEA plots, NES (normalized enrichment score), p-value and FDR.

B-E) Relationship between the gene expression of the SASP (B), JAK/STAT (C), Cytokine-cytokine receptor pathway (D) and TNFA Signaling via NFkB (E), and 9p arm loss, 9p21.3 loss, or 9p21.3 “focal” loss in HNSC tumors. p-value is from Wilcoxon test.



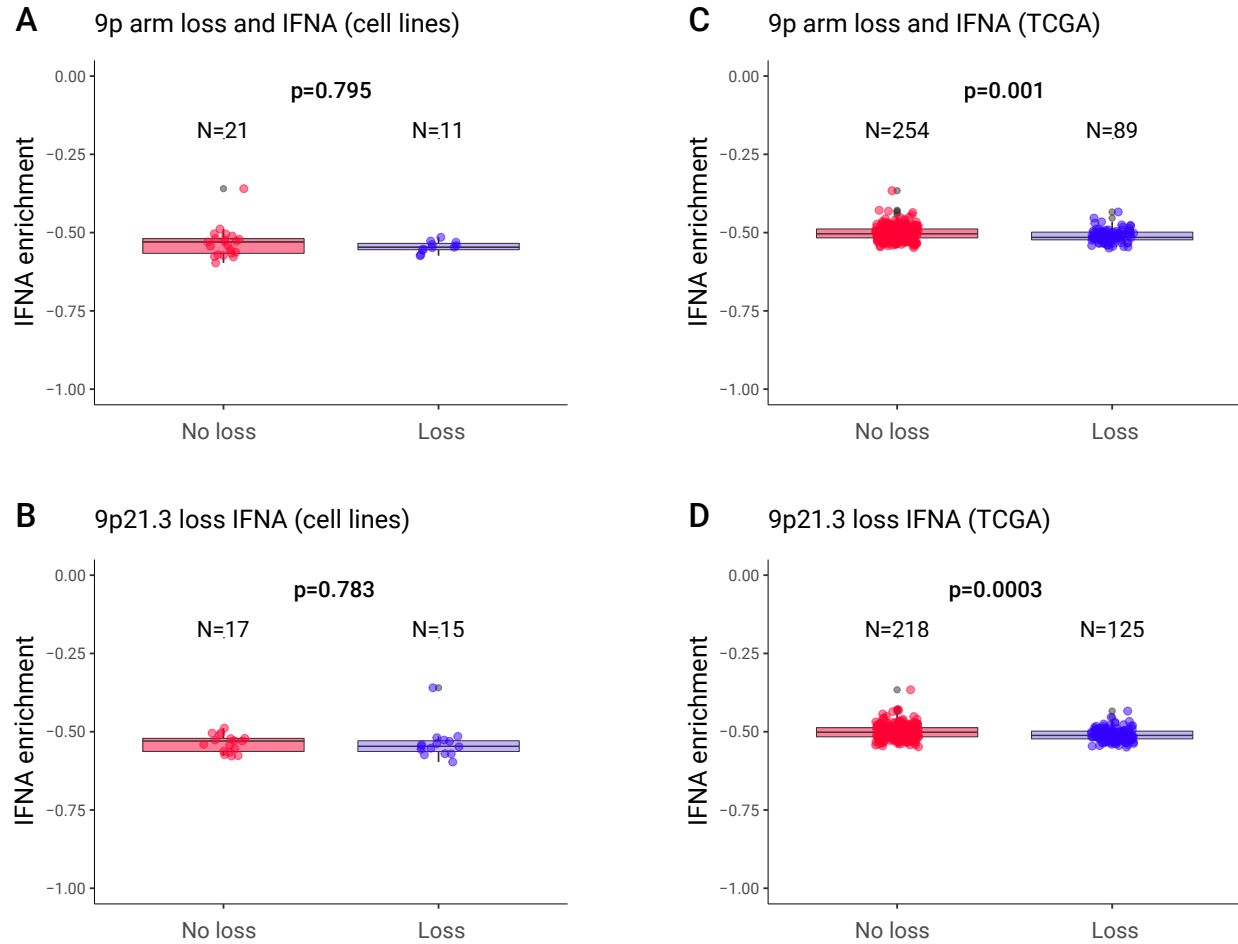


**Fig. S10. IFNA gene set enrichment in HPV-negative cell lines or tumors with or without 9p or 9p21.3 loss**

A-D) Relationship between *IFNA* gene set enrichment (through ssGSEA, see also Table S15 for gene set) and 9p arm or 9p21.3 loss in HPV-negative cell lines (A, B) or tumors (C, D). p-value is from Wilcoxon test.

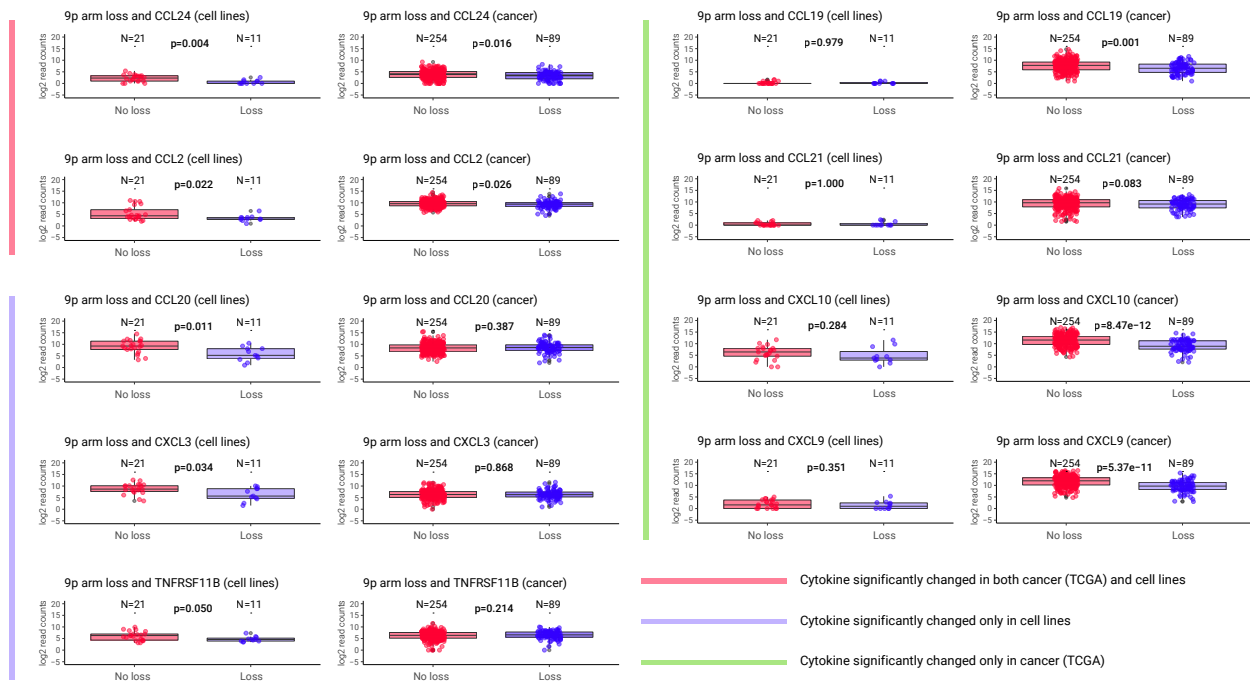


**Fig. S11. Representative genes differentially expressed in tumors or cell lines with or without 9p loss**

Relationship between the expression level of the indicated genes comparing HPV-negative cell lines or tumors with or without 9p arm-level. p-value is from Wilcoxon test.

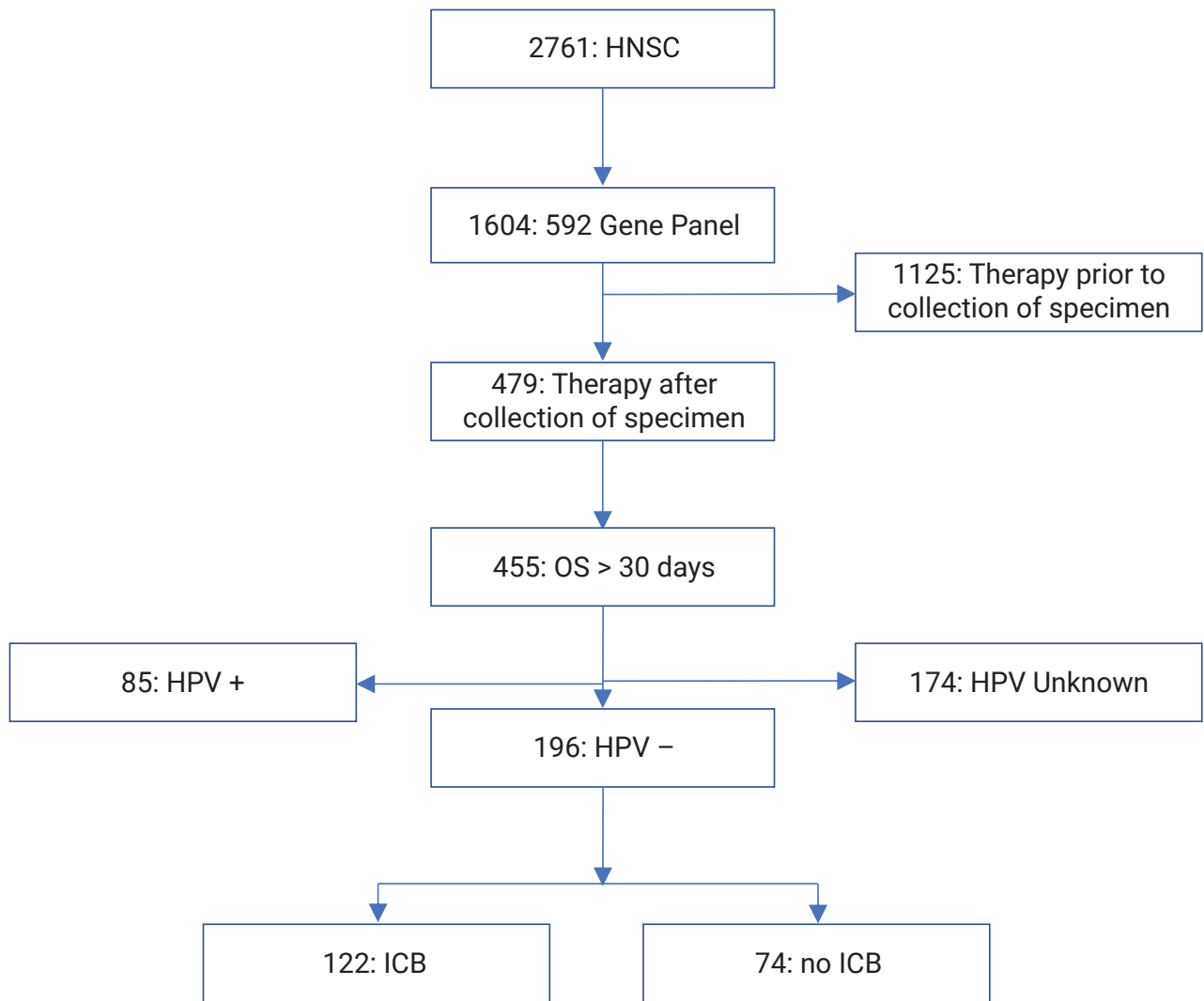


**Fig. S12. Consort diagram of Real-World Evidence (RWE) cohort**

Cohort of HPV-negative HNSC patients treated with nivolumab or pembrolizumab (or chemotherapy) whose tumors had been profiled using a next generation sequencing platform, as recently described (19).

## REFERENCES

1. W. N. Hittelman, Genetic instability in epithelial tissues at risk for cancer. *Ann N Y Acad Sci* **952**, 1-12 (2001).
2. E. R. Parra *et al.*, Validation of multiplex immunofluorescence panels using multispectral microscopy for immune-profiling of formalin-fixed and paraffin-embedded human tumor tissues. *Scientific Reports* **7**, 13380 (2017).
3. J. Jiang, *Linear and Generalized Linear Mixed Models and Their Applications*, Springer Series in Statistics (Springer-Verlag New York, ed. 1, 2007), 10.1007/978-0-387-47946-0, pp. 257.
4. W. N. William, Jr. *et al.*, Erlotinib and the Risk of Oral Cancer: The Erlotinib Prevention of Oral Cancer (EPOC) Randomized Clinical Trial. *JAMA oncology* **2**, 209-216 (2016).
5. I. A. Adzhubei *et al.*, A method and server for predicting damaging missense mutations. *Nat Methods* **7**, 248-249 (2010).
6. A. M. Newman *et al.*, Robust enumeration of cell subsets from tissue expression profiles. *Nat Methods* **12**, 453-457 (2015).
7. J. E. Beane *et al.*, Molecular subtyping reveals immune alterations associated with progression of bronchial premalignant lesions. *Nat Commun* **10**, 1856 (2019).
8. A. Mezheyeuski *et al.*, Multispectral imaging for quantitative and compartment-specific immune infiltrates reveals distinct immune profiles that classify lung cancer patients. *J Pathol* **244**, 421-431 (2018).
9. R. Tibshirani, Regression Shrinkage and Selection via the Lasso. *Journal of the Royal Statistical Society. Series B (Methodological)* **58**, 267-288 (1996).
10. T. Davoli, H. Uno, E. C. Wooten, S. J. Elledge, Tumor aneuploidy correlates with markers of immune evasion and with reduced response to immunotherapy. *Science* **355** (2017).
11. M. I. Love, W. Huber, S. Anders, Moderated estimation of fold change and dispersion for RNA-seq data with DESeq2. *Genome Biol* **15**, 550 (2014).
12. A. Subramanian *et al.*, Gene set enrichment analysis: a knowledge-based approach for interpreting genome-wide expression profiles. *Proceedings of the National Academy of Sciences of the United States of America* **102**, 15545-15550 (2005).
13. J. P. Coppé *et al.*, Senescence-associated secretory phenotypes reveal cell-nonautonomous functions of oncogenic RAS and the p53 tumor suppressor. *PLoS Biol* **6**, 2853-2868 (2008).
14. S. Santaguida, E. Vasile, E. White, A. Amon, Aneuploidy-induced cellular stresses limit autophagic degradation. *Genes Dev* **29**, 2010-2021 (2015).
15. D. M. Merino *et al.*, Establishing guidelines to harmonize tumor mutational burden (TMB): in silico assessment of variation in TMB quantification across diagnostic platforms: phase I of the Friends of Cancer Research TMB Harmonization Project. *J Immunother Cancer* **8** (2020).
16. D. T. Le *et al.*, Mismatch repair deficiency predicts response of solid tumors to PD-1 blockade. *Science* **357**, 409-413 (2017).
17. K. Zimmer *et al.*, WRN-Mutated Colorectal Cancer Is Characterized by a Distinct Genetic Phenotype. *Cancers (Basel)* **12** (2020).
18. A. M. Taylor *et al.*, Genomic and Functional Approaches to Understanding Cancer Aneuploidy. *Cancer Cell* **33**, 676-689 e673 (2018).
19. J. P. Abraham *et al.*, Clinical validation of a machine-learning derived signature predictive of outcomes from first-line oxaliplatin-based chemotherapy in advanced colorectal cancer. *Clinical Cancer Research* 10.1158/1078-0432.Ccr-20-3286, clincanres.3286.2020 (2020).

William et al.

## List of Supplemental Tables

### Table S1

- S1A** Selected patient characteristics and markers for oral precancer cohort.
- S1B** Co-occurrence analysis of SCNAs in oral precancer.

### Table S2

Association between immune parameters and copy number alterations or clinical parameters in oral pre-cancer.

- S2A** Distributions of CD3+, CD8+ and CD68+ by different parameters, and p-values for comparing between the two groups for each covariate using the linear mixed effect models on log-transformed data.
- S2B** Logistic regression analysis for the prediction of the indicated parameters (CD3+, CD8+ and CD68+) in precancer data.
- S2C** Univariate analysis for prediction of the indicated parameters (CD3+, CD8+ and CD68+) in precancer data.
- S2D** Univariate analysis for oral cancer-free survival according to clinical/demographic/biomarker characteristics
- S2E** Cox proportional hazards model for OCFS of the indicated parameters in precancer data.

### Table S3

Association between immune parameters and copy number alterations in HPV-negative HNSC tumor samples from TCGA.

- S3A** Logistic Regression for the prediction of immune infiltrate parameters in HNSC tumor samples ; binary definition of loss or gain.
- S3B** Logistic Regression for the prediction of immune infiltrate parameters in HNSC tumor samples ; copy number level considered as continuous variables.
- S3C** Logistic Regression for the prediction of CD8+ in HNSC tumor samples - after separating arm-level and focal-level loss at 9p21.3.
- S3D** Logistic Regression for the prediction of CD8+ in HNSC tumor samples - after separating arm-level and focal-level loss at 3p14.
- S3E** Logistic Regression for the prediction of CD8+ in HNSC tumor samples - after separating arm-level and focal-level loss at 17p13.1.
- S3F** Co-occurrence analysis of immune infiltrate parameters in HPV-neg HNSC tumor samples.
- S3G** Logistic Regression for the prediction of CD3+ in HNSC tumor samples - after separating arm-level and focal-level loss at 9p21.3.
- S3H** Logistic Regression for the prediction of CD3+ in HNSC tumor samples - after separating arm-level and focal-level loss at 3p14.
- S3I** Logistic Regression for the prediction of CD3+ in HNSC tumor samples - after separating arm-level and focal-level loss at 17p13.1.

**S3J** Logistic Regression for the prediction of immune infiltrate parameters in HNSC tumor samples with additional clinical parameters binary definition of loss or gain.

**S3K** 5-fold cross validation of Logistic Regression for the prediction of immune infiltrate parameters in HNSC tumor samples with extra clinical information, binary definition of loss or gain.

**S3L** Logistic Regression for the prediction of CD8+ in HNSC tumor samples, binary definition of loss or gain.

#### **Table S4**

Association between immune parameters and copy number alterations in HPV-negative oral tumor samples from TCGA.

**S4A** Logistic Regression for the prediction of immune infiltrate parameters in oral tumor samples.

**S4B** Logistic Regression for the prediction of CD8+ in oral tumor samples - after separating arm-level and focal-level loss at 9p21.3.

**S4C** Logistic Regression for the prediction of CD8+ in oral tumor samples - after separating arm-level and focal-level loss at 3p14.

**S4D** Logistic Regression for the prediction of CD8+ in oral tumor samples - after separating arm-level and focal-level loss at 17p13.1.

#### **Table S5**

Lasso-based prediction model of Immune Score in HNSC tumor samples (TCGA). Variable Selection.

#### **Table S6**

Association between immune parameters and copy number alterations and other parameters in HPV-negative HNSC tumor samples from TCGA.

**S6A** Logistic Regression for the prediction of CD8+ in HNSC tumor samples after considering the tumor stage.

**S6B** Logistic Regression for the prediction of CD8+ in HNSC tumor samples after considering the *TP53* status.

**S6C** Pearson's correlation analysis between CD8+/CD3+ and 9p arm loss in HNSC tumor samples after considering the *TP53* status.

**S6D** Wilcoxon Signed Rank Test between CD8+/CD3+ and 9p arm loss/9p21.3 loss in HNSC tumor samples after considering the *TP53* status.

#### **Table S7**

Relationship between Immune Markers and SCNA Events in HPV-positive HNSC (N=36).

**S7A** Comparison of the frequencies of different copy number events in HPV positive and negative HNSC.

**S7B** Logistic Regression for the prediction of immune infiltrate parameters in HPV-positive HNSC tumor samples; binary definition of loss or gain.

**S7C** Logistic Regression for the prediction of immune infiltrate parameters in HPV-positive HNSC tumor samples; copy number level considered as continuous data.

#### **Table S8**

HPV-negative HNSC cell lines and corresponding CNV for different genomic regions.

**Table S9**

GSEA Analysis on HNSC cancer cell lines comparing cell lines with or without 9p21.3 loss (arm or focal), Pathways Enriched.

**Table S10**

GSEA Analysis on HNSC cancer cell lines comparing cell lines with or without 9p21.3 loss (arm or focal), Pathways Depleted.

**Table S11**

GSEA Analysis on HNSC cancer cell lines comparing cell lines with or without 3p14 loss (arm or focal), Pathways Enriched.

**Table S12**

GSEA Analysis on HNSC cancer cell lines comparing cell lines with or without 3p14 loss (arm or focal), Pathways Depleted.

**Table S13**

GSEA Analysis on HNSC cancer cell lines comparing cell lines with or without 9p loss, Pathways Enriched.

**Table S14**

GSEA Analysis on HNSC cancer cell lines comparing cell lines with or without 9p loss, Pathways Depleted.

**Table S15**

List of Aneuploidy-associated SASP genes and IFNA gene set.

**Table S16**

GSEA Analysis on TCGA HNSC comparing tumors with or without 9p21.3 loss (arm or focal), Pathways Enriched.

**Table S17**

GSEA Analysis on TCGA HNSC comparing tumors with or without 9p21.3 loss (arm or focal), Pathways Depleted.

**Table S18**

GSEA Analysis on TCGA HNSC comparing tumors with or without 9p loss, Pathways Enriched.

**Table S19**

GSEA Analysis on TCGA HNSC comparing tumors with or without 9p loss, Pathways Depleted.

**Table S20**

Association between SASP signature pathway and copy number alterations in HPV-negative HNSC cell lines.

**S20A** Logistic Regression for the prediction of SASP enrichment in HNSC cell lines (CCLE) - after separating arm-level and focal-level loss at 9p21.3

**S20B** Logistic Regression for the prediction of SASP enrichment in HNSC cell lines (CCLE) - after separating arm-level and focal-level loss at 3p14.

**Table S21**

GSEA Analysis on TCGA HNSC comparing tumors with or without 9p21.3 focal loss, Pathways Depleted.

**Table S22**

GSEA Analysis on HNSC cancer cell lines comparing cell lines with or without 9p21.3 focal loss, Pathways Depleted.

**Table S23**

GSEA Analysis (Hallmark gene sets) on TCGA HNSC comparing tumors with or without 9p loss, Pathways Depleted.

**Table S24**

GSEA Analysis (Hallmark gene sets) on HNSC cancer cell lines comparing cell lines with or without 9p loss, Pathways Depleted.

**Table S25**

Cox proportional hazards model for OCFS of the indicated parameters in Real-World Evidence Cohort.



**Table S1****S1A**

Selected patient characteristics and markers for oral precancer cohort.\*

<b>N=188</b>	
<b>Prior oral cancers, N (%)</b>	
No	69 (37%)
Yes	119 (63%)
<b>Histology, N (%)</b>	
Hyperplasia	68 (36%)
Mild/moderate dysplasia	107 (57%)
Severe dysplasia	13 (7%)
<b>3p14 Loss, N (%)</b>	
No Loss	105 (56%)
Loss	82 (43%)
<b>9p21.3 Loss, N (%)</b>	
No Loss	76 (40%)
Loss	112 (60%)
<b>17p13.1 Loss, N (%)</b>	
No Loss	62 (33%)
Loss	126 (67%)
<b>Chromosome 7 Gain, N (%)**</b>	
No	114 (61%)
Yes	72 (38%)
<b>Smoking, N (%)</b>	
Current	23 (12%)
Former	71 (38%)
<b>Alcohol, N (%)</b>	
Light drinker	81 (43%)
Moderate, Heavy drinkers	23 (12%)
<b>Gender, N (%)</b>	
Male	94 (50%)
Female	94 (50%)

\* See Results section for details

\*\*Missing values (N=2).

**S1B****Co-occurrence analysis of SCNAs in oral precancer**

<b>Event 1</b>	<b>Event 2</b>	<b>p-Value Mutual Exclusivity</b>	<b>p-Value Co-occurrence</b>
3p14 Loss	9p21.3 Loss	1	1.29302E-07
3p14 Loss	17p13.1 Loss	0.9999976	1.15549E-05
9p21.3 Loss	17p13.1 Loss	0.9939178	0.01424003
3p14 Loss	Chr 7 Gain	0.9999877	4.64218E-05
9p21.3 Loss	Chr 7 Gain	0.9999911	3.62777E-05
17p13.1 Loss	Chr 7 Gain	0.9974528	0.006866455
Major risk loci	Minor risk loci	0.9991201	0.003799281



**Table S3**  
Association between immune parameters and copy number alterations in HPV-negative HNSC tumor samples from TCGA.

Unless otherwise specified, '9p21.3 loss', '3p14 loss', or '17p13.1 loss' refer to the presence of a loss at this region irrespective of the length of the deletion (whether the loss encompasses the entire arm or is a focal event).

**S3A**  
Logistic Regression for the prediction of immune infiltrate parameters in HNSC tumor samples ; binary definition of loss or gain.  
Top and bottom 35% of the distributions were considered to divide the tumors into those with high or low levels of immune markers.  
Thresholded values were used to define loss and gain

purely method/Pathology	$\beta$ coefficient	z value	P< z	FDR	OR
CD8+	-0.3447693	-0.8907451	0.373069598	0.73416	0.708584 binary
3p14 Loss	-1.2851964	-3.5119797	0.00044782	0.00226	0.051313 continuous
9p21.3 Loss	-0.4864328	-1.0348338	0.3005979	0.73416	0.64816 binary
Chr 7 Gain	-0.4301541	-0.990093	0.37341501	0.73416	0.650409 continuous
SCNA level	-0.5920483	-3.0591518	0.002219846	0.00549	0.553193 continuous

**S3B**  
Logistic Regression for the prediction of immune infiltrate parameters in HNSC tumor samples ; copy number level considered as continuous variables.  
Top and bottom 35% of the distributions were considered to divide the tumors into those with high or low levels of immune markers.  
For each copy number event, we used copy number level after standardization.

purely method/Pathology	$\beta$ coefficient	z value	P< z	FDR	OR
CD8+	0.5620057	2.6801579	0.007358744	0.0184	1.790779 continuous
3p14 scale	0.9922856	4.125259	2.649420E-05	0.000125	2.697239 continuous
9p21.3 scale	-0.1904378	-0.6542167	0.5126147	1.842	0.870213 continuous
Chr 7 scale	-0.4613918	-1.0757769	0.2860852	0.70878	0.630426 continuous
SCNA level	-0.4925233	-2.429203	0.01497931	0.025	0.611077 continuous

**S3C**  
Logistic Regression for the prediction of CD8+ in HNSC tumor samples - after separating arm-level and focal-level loss at 9p21.3  
Top and bottom 35% of the distributions were considered to divide the tumors into those with high or low levels of immune markers.  
Distinction between tumors showing arm-only, focal-only events and a combination of both.

purely method/Pathology	$\beta$ coefficient	z value	P< z	FDR	OR
9p21.3 Loss: ARM (N=80)	-1.7946255	-3.7209207	0.000198488	0.00002	0.186119 binary
9p21.3 Loss: FOCAL (N=40)	-0.6307587	-1.3710268	0.06053996	0.15085	0.450729 binary
9p21.3 Loss: ARM+FOCAL (N=15)	-0.9878614	-1.9720706	0.04849153	0.10585	0.593975 binary
3p14 Loss	-0.2839986	-0.7154122	0.4738768	0.76805	0.788051 binary
SCNA level	-0.6306161	-3.5184969	0.000433999	0.01085	0.529397 continuous

**S3D**  
Logistic Regression for the prediction of CD8+ in HNSC tumor samples - after separating arm-level and focal-level loss at 3p14.  
Top and bottom 35% of the distributions were considered to divide the tumors into those with high or low levels of immune markers.  
Distinction between tumors showing arm-only, focal-only events and a combination of both.

purely method/Pathology	$\beta$ coefficient	z value	P< z	FDR	OR
3p14 Loss: ARM Level	-1.5614052	-1.3802814	0.16750007	0.23201	0.570730 binary
3p14 Loss: FOCAL Level	-0.6243176	-1.3481234	0.17781706	0.23201	0.535207 binary
3p14 Loss: ARM+FOCAL	-0.4484294	-0.9842548	0.3242548	0.73416	0.598929 binary
9p21.3 Loss	-1.2971362	-3.6417872	0.000285127	0.00343	0.273133 binary
SCNA level	-0.6120982	-3.3376742	0.000844827	0.01103	0.542212 continuous

**S3E**  
Logistic Regression for the prediction of CD8+ in HNSC tumor samples - after separating arm-level and focal-level loss at 17p13.1  
Top and bottom 35% of the distributions were considered to divide the tumors into those with high or low levels of immune markers.  
Distinction between tumors showing arm-only, focal-only events and a combination of both.

purely method/Pathology	$\beta$ coefficient	z value	P< z	FDR	OR
17p13.1 Loss: ARM Level	0.2224102	0.4211548	0.6737787	1.41611	0.880097 binary
17p13.1 Loss: FOCAL Level	0.0208666	0.0278069	0.9778139	0.78761	1.021085 binary
17p13.1 Loss: ARM+FOCAL	-0.4484294	-0.9842548	0.3242548	0.73416	0.598929 binary
9p21.3 Loss	-1.39586102	-4.0886441	4.37243E-05	1.09E-04	0.247894 binary
SCNA level	-0.1792939	-0.3373242	1.45276E-05	7.25E-05	0.482094 continuous

**S3F**  
Co-occurrence analysis of immune infiltrate parameters in HPV-neg HNSC tumor samples .

Event 1	Event 2	p-Value	Mutual Exclusivity	p-Value	Co-occurrence	FDR
3p14 Loss	17p13.1 Loss	1	3.56E-11	1.72E-11		
9p21.3 Loss	17p13.1 Loss	1	1.73E-06	1.04E-05		
9p21.3 Loss	3p Am Loss	1	3.39E-08	5.09E-08		
9p Am Loss	17p Am Loss	1	3.2E-11	1.72E-11		
9p Am Loss	3p Am Loss	1	9.9999978	1.10E-05		
9p Am Loss	17p Am Loss	1	0.9939966	1.86E-03	0.01186	
3p14 Loss	Chr 7 Gain	1	4.13E-01	4.13E-01		
17p13.1 Loss	Chr 7 Gain	1	0.971026	6.72E-02	2.02E-01	
9p21.3 Loss	Chr 7 Gain	1	0.8313768	2.66E-01	3.99E-01	

**S3G**  
Logistic Regression for the prediction of CD8+ in HNSC tumor samples - after separating arm-level and focal-level loss at 9p21.3  
Top and bottom 35% of the distributions were considered to divide the tumors into those with high or low levels of immune markers.  
Distinction between tumors showing arm-only, focal-only events and a combination of both.

purely method/Pathology	$\beta$ coefficient	z value	P< z	FDR	OR
9p21.3 Loss: ARM (N=80)	-1.5977906	-3.3393469	0.000987566	0.00002	0.208905 binary
9p21.3 Loss: FOCAL (N=40)	-0.7797818	-1.6979718	0.0948098	0.23201	0.591311 binary
9p21.3 Loss: ARM+FOCAL (N=15)	-0.3383003	-0.7414703	0.4583662	0.78761	1.402662 binary
3p14 Loss	-0.2852683	-0.7598933	0.4486989	0.56141	0.715182 binary
SCNA level	-0.7397484	-2.4748091	0.0130159	0.03405	0.450461 continuous

**S3H**  
Logistic Regression for the prediction of CD8+ in HNSC tumor samples - after separating arm-level and focal-level loss at 3p14.  
Top and bottom 35% of the distributions were considered to divide the tumors into those with high or low levels of immune markers.  
Distinction between tumors showing arm-only, focal-only events and a combination of both.

purely method/Pathology	$\beta$ coefficient	z value	P< z	FDR	OR
9p21.3 copy number ARM Level	0.1620283	3.0858467	0.00229734	0.06033	2.050744 continuous
9p21.3 copy number FOCAL Level	-0.0473708	-0.9319286	0.3527065	0.763E-01	0.853728 continuous
3p14 copy number	0.0426939	0.9278958	0.3527065	0.763E-01	0.853728 continuous
SCNA level	0.7781581	1.4634373	0.1398505	0.125E-04	0.495251 continuous

**S3I**  
Logistic Regression for the prediction of CD8+ in HNSC tumor samples - after separating arm-level and focal-level loss at 17p13.1  
Top and bottom 35% of the distributions were considered to divide the tumors into those with high or low levels of immune markers.  
Distinction between tumors showing arm-only, focal-only events and a combination of both.

purely method/Pathology	$\beta$ coefficient	z value	P< z	FDR	OR
17p13.1 Loss: ARM Level	-0.3861063	-0.8607013	0.38700603	0.2272	0.617594 binary
17p13.1 Loss: FOCAL Level	-0.2849578	-0.6095738	0.542144776	0.542144	0.702846 binary
17p13.1 Loss: ARM+FOCAL	-0.6390007	-1.3957758	0.338175841	0.2272	0.504796 binary
9p21.3 Loss	-1.0420025	-2.257214	0.0249828	0.007874	0.351973 binary
SCNA level	-0.8093191	-4.3246247	1.52792E-05	6.64E-05	0.45161 continuous

**S3J**  
Logistic Regression for the prediction of CD8+ in HNSC tumor samples - after separating arm-level and focal-level loss at 3p14.  
Top and bottom 35% of the distributions were considered to divide the tumors into those with high or low levels of immune markers.  
Distinction between tumors showing arm-only, focal-only events and a combination of both.

purely method/Pathology	$\beta$ coefficient	z value	P< z	FDR	OR
9p21.3 copy number ARM Level	0.6263493	2.1662478	0.03003883	0.04089	1.870788 continuous
9p21.3 copy number FOCAL Level	-0.1760768	-0.3638438	0.7160768	1.72606	0.853728 continuous
3p14 copy number	0.3494518	2.3618369	0.0184553	0.03639	1.412929 continuous

**S3K**  
Logistic Regression for the prediction of CD8+ in HNSC tumor samples - after separating arm-level and focal-level loss at 17p13.1  
Top and bottom 35% of the distributions were considered to divide the tumors into those with high or low levels of immune markers.  
Distinction between tumors showing arm-only, focal-only events and a combination of both.

purely method/Pathology	$\beta$ coefficient	z value	P< z	FDR	OR
17p13.1 Loss: ARM Level	-0.12487	-0.26399	0.791389	1.688	0.88012 binary
17p13.1 Loss: FOCAL Level	0.07095	0.095	0.9244	0.9244	1.073288 binary
17p13.1 Loss: ARM+FOCAL	-0.6390007	-1.3957758	0.338175841	0.2272	0.504796 binary
9p21.3 Loss	-1.0420025	-2.257214	0.0249828	0.007874	0.351973 binary
SCNA level	-0.8093191	-4.3246247	1.52792E-05	6.64E-05	0.45161 continuous

**S3L**  
Logistic Regression for the prediction of CD8+ in HNSC tumor samples - after separating arm-level and focal-level loss at 3p14.  
Top and bottom 35% of the distributions were considered to divide the tumors into those with high or low levels of immune markers.  
Distinction between tumors showing arm-only, focal-only events and a combination of both.

purely method/Pathology	$\beta$ coefficient	z value	P< z	FDR	OR
9p21.3 copy number ARM Level	0.0826228	0.56091	0.574859	0.574859	1.086132 continuous
9p21.3 copy number FOCAL Level	-0.1760768	-0.3638438	0.7160768	1.72606	0.853728 continuous
3p14 copy number	0.3494518	2.3618369	0.0184553	0.03639	1.412929 continuous



**Table S4**

**Association between immune parameters and copy number alterations in HPV-negative oral tumor samples from TCGA.**

Unless otherwise specified, '9p21.3 loss', '3p14 loss' or '17p13.1 loss' refer to the presence of a loss at this region irrespective of the length of the deletion (whether the loss encompasses the entire arm or is a focal event).'

**S4A**

**Logistic Regression for the prediction of immune infiltrate parameters in oral tumor samples**

Top and bottom 35% of the distributions were considered to divide the tumors into those with high or low levels of immune markers.

Binary definition of loss or gain.

**purity method=Pathology**

For each copy number event, we used copy number values after standardization.

**purity method=Pathology**

	$\beta$ coefficient	z value	Pr(> z )	FDR	OR		$\beta$ coefficient	z value	Pr(> z )	FDR	OR
<b>CD8+</b>						<b>CD8+</b>					
3p14 Loss	-0.0927768	-0.181646	8.56E-01	8.56E-01	0.911397	3p14 scale	0.6456285	2.152065	3.14E-02	5.23E-02	1.907185
9p21.3 Loss	-2.0425244	-3.970332	7.18E-05	3.59E-04	0.129701	9p21.3 scale	1.5603175	4.257302	2.07E-05	1.04E-04	4.760332
17p13.1 Loss	-0.9482032	-1.15309	2.49E-01	4.03E-01	0.387437	17p13.1 scale	-0.3221382	-1.117982	2.64E-01	3.30E-01	0.724598
Chr 7 Gain	0.7283416	0.990505	3.22E-01	4.03E-01	2.071642	Chr 7 scale	-0.2573763	-0.709606	4.78E-01	4.78E-01	0.773077
SCNA level	-0.9097892	-3.296963	9.77E-04	2.44E-03	0.402609	SCNA level	-0.6239998	-2.166146	3.03E-02	5.23E-02	0.535797
<b>CD3+</b>						<b>CD3+</b>					
3p14 Loss	-0.4973584	-1.013056	0.311033	0.311033	0.608135	3p14 scale	0.94246865	3.422997	0.000619	0.003097	2.566309
9p21.3 Loss	-1.6183061	-3.2009	0.00137	0.003425	0.198234	9p21.3 scale	0.45085749	2.285872	0.022262	0.037103	1.569658
17p13.1 Loss	-1.4036496	-1.516095	0.129495	0.215825	0.245699	17p13.1 scale	0.03674168	0.147436	0.882788	0.882788	1.037425
Chr 7 Gain	0.7122948	1.015339	0.309944	0.311033	2.038664	Chr 7 scale	-0.1710354	-0.551452	0.581324	0.726655	0.842792
SCNA level	-0.9353222	-3.304707	0.000951	0.003425	0.392459	SCNA level	-0.64705579	-2.364806	0.01804	0.037103	0.523585
<b>CD68+</b>						<b>CD68+</b>					
3p14 Loss	0.4460938	0.940225	0.347102	0.433878	1.562198	3p14 scale	-0.19870062	-0.854913	0.392599	0.490749	0.819795
9p21.3 Loss	-0.6193774	-1.442211	0.149243	0.248738	0.538279	9p21.3 scale	-0.09582344	-0.545602	0.58534	0.58534	0.908624
17p13.1 Loss	-0.9026873	-1.815994	0.069371	0.248738	0.405479	17p13.1 scale	0.63795188	2.999854	0.002701	0.013505	1.892601
Chr 7 Gain	0.2935597	0.443107	0.657689	0.657689	1.341193	Chr 7 scale	0.38044836	1.306076	0.191527	0.319212	1.46294
SCNA level	-0.3435666	-1.463083	0.143445	0.248738	0.709236	SCNA level	-0.48139622	-2.005555	0.044904	0.112259	0.61792
<b>Immune Score</b>						<b>Immune Score</b>					
3p14 Loss	-0.07727523	-0.147538	0.882707	0.882707	0.925635	3p14 scale	0.71445954	2.36427	0.018066	0.045164	2.043082
9p21.3 Loss	-1.84823056	-3.607866	0.000309	0.001544	0.157501	9p21.3 scale	1.390649	4.036392	5.43E-05	0.000271	4.017457
17p13.1 Loss	-1.12998716	-1.552851	0.120459	0.200765	0.323037	17p13.1 scale	-0.07017032	-0.254492	0.799115	0.799115	0.932235
Chr 7 Gain	0.94756411	1.30175	0.193002	0.241252	2.579419	Chr 7 scale	-0.09509775	-0.273664	0.784343	0.799115	0.909284
SCNA level	-0.96903058	-3.392153	0.000693	0.001734	0.379451	SCNA level	-0.63000651	-2.192166	0.028368	0.047279	0.532588

**S4B**

**Logistic Regression for the prediction of CD8+ in oral tumor samples - after separating arm-level and focal-level loss at 9p21.3**

Top and bottom 35% of the distributions were considered to divide the tumors into those with high or low levels of immune markers.

Distinction between tumors showing arm-only, focal-only events and a combination of both.

Binary definition of loss or gain.

**purity method=Pathology**

For each copy number event, we used copy number values after standardization.

**purity method=Pathology**

	$\beta$ coefficient	z value	Pr(> z )	FDR	OR		$\beta$ coefficient	z value	Pr(> z )	FDR	OR
9p21.3 Loss: ARM (N=80)	-3.7291933	-3.45977	0.000541	0.002703	0.024012	9p21.3 copy number ARM Level	2.3099844	4.450053	8.58E-06	3.43E-05	10.07427
9p21.3 Loss: FOCAL (N=40)	-0.9835497	-1.801873	0.071565	0.119276	0.373981	9p21.3 copy number FOCAL Level	0.412355	1.451957	1.47E-01	1.96E-01	1.510371
9p21.3 Loss: ARM+FOCAL (N=15)	-16.6563876	-0.012475	0.990046	0.990047	5.84E-08	3p14 copy number	0.3604761	1.216953	2.24E-01	2.24E-01	1.434012
3p14 Loss	-0.1119033	-0.229746	0.818289	0.990047	0.894131	SCNA level	-0.7464163	-2.484486	1.30E-02	2.60E-02	0.474062
SCNA level	-0.7339896	-2.826584	0.004705	0.011762	0.47999						

**S4C**

**Logistic Regression for the prediction of CD8+ in oral tumor samples - after separating arm-level and focal-level loss at 3p14.**

Top and bottom 35% of the distributions were considered to divide the tumors into those with high or low levels of immune markers.

Distinction between tumors showing arm-only, focal-only events and a combination of both.

Binary definition of loss or gain.

**purity method=Pathology**

For each copy number event, we used copy number values after standardization.

**purity method=Pathology**

	$\beta$ coefficient	z value	Pr(> z )	FDR	OR		$\beta$ coefficient	z value	Pr(> z )	FDR	OR
3p14 Loss: ARM Level	-0.5338593	-1.030897	3.03E-01	3.03E-01	0.586338	3p14 copy number ARM Level	0.8072066	1.728135	8.40E-02	1.12E-01	2.241637
3p14 Loss: FOCAL Level	-0.5939564	-1.031031	3.03E-01	3.03E-01	0.552138	3p14 copy number FOCAL Level	0.4955731	1.083639	2.79E-01	2.79E-01	1.641439
3p14 Loss: ARM+FOCAL	-1.4998566	-1.217132	2.24E-01	3.03E-01	0.223162	9p21.3 copy number	1.4691859	4.356877	1.32E-05	5.28E-05	4.345696
9p21.3 Loss	-2.0023121	-3.988118	6.66E-05	3.33E-04	0.135023	SCNA level	-0.7858527	-2.75483	5.87E-03	1.17E-02	0.455731
SCNA level	-0.766696	-3.062019	2.20E-03	5.50E-03	0.464545						

**S4D**

**Logistic Regression for the prediction of CD8+ in oral tumor samples - after separating arm-level and focal-level loss at 17p13.1.**

Top and bottom 35% of the distributions were considered to divide the tumors into those with high or low levels of immune markers.

Distinction between tumors showing arm-only, focal-only events and a combination of both.

Binary definition of loss or gain.

**purity method=Pathology**

For each copy number event, we used copy number values after standardization.

**purity method=Pathology**

	$\beta$ coefficient	z value	Pr(> z )	FDR	OR		$\beta$ coefficient	z value	Pr(> z )	FDR	OR
17p13.1 Loss: ARM Level	-0.6573481	-0.716571	4.74E-01	6.91E-01	0.518224	17p13.1 copy number ARM Level	-0.2824384	-1.091784	2.75E-01	3.67E-01	0.753943
17p13.1 Loss: FOCAL Level	0.6678774	0.593938	5.53E-01	6.91E-01	1.950094	17p13.1 copy number FOCAL Level	0.1523539	0.478366	6.32E-01	6.32E-01	1.164572
17p13.1 Loss: ARM+FOCAL	-16.085137	-0.016596	9.87E-01	9.87E-01	1.03E-07	9p21.3 copy number	1.7523208	4.896996	9.73E-07	3.89E-06	5.767973
9p21.3 Loss	-2.1347942	-4.270594	1.95E-05	9.75E-05	0.118269	SCNA level	-1.0356635	-4.436121	9.16E-06	1.83E-05	0.354991
SCNA level	-0.9148237	-3.919697	8.87E-05	2.22E-04	0.400587						

**Table S5****Lasso-based prediction model of Immune Score in HNSC tumor samples (TCGA). Variable Selection.**

<b>Parameters</b>	<b><math>\beta</math> coefficient</b>	<b>Pvalue</b>
Chr 1	0	NA
Chr 2	0	NA
Chr 3	0	NA
Chr 4	0	NA
Chr 5	0	NA
Chr 6	0	NA
Chr 7	0	NA
Chr 8	0	NA
Chr 9	-0.72(0.18,1.26)	0.0078
Chr 10	-0.22(-1,1.44)	0.7209
Chr 11	0	NA
Chr 12	0	NA
Chr 13	0	NA
Chr 14	0	NA
Chr 15	0	NA
Chr 16	0	NA
Chr 17	0	NA
Chr 18	0	NA
Chr 19	0	NA
Chr 20	0	NA
Chr 21	0	NA
Chr 22	0.24(-0.78,0.3)	0.3764
1p Arm	0	NA
2p Arm	0	NA
3p Arm	0	NA
4p Arm	0	NA
5p Arm	0	NA
6p Arm	-0.43(-0.27,1.13)	0.2108
7p Arm	0	NA
8p Arm	0	NA
9p Arm	-1.13(0.47,1.79)	7.00E-04
10p Arm	0	NA
11p Arm	0	NA
12p Arm	0	NA
16p Arm	0	NA
17p Arm	0	NA
18p Arm	0	NA
19p Arm	0	NA
20p Arm	0	NA
1q Arm	0	NA
2q Arm	0	NA
3q Arm	0	NA
4q Arm	0	NA
5q Arm	0	NA
6q Arm	0	NA
7q Arm	-0.83(-3.57,1.91)	0.5445
8q Arm	0	NA
9q Arm	0	NA
10q Arm	0	NA
11q Arm	0	NA
12q Arm	0	NA
16q Arm	0	NA
17q Arm	0	NA
18q Arm	0	NA
19q Arm	0	NA
20q Arm	0	NA
SCNA level	-1.12(-1.6,-0.64)	0

---

**Table S6**

Association between immune parameters and copy number alterations and other parameters in HPV-negative HNSC tumor samples from TCGA. Unless otherwise specified, '9p21.3 loss', '3p14 loss' or '17p13.1 loss' refer to the presence of a loss at this region irrespective of the length of the deletion (whether the loss encompasses the entire arm or is a focal event).

**S6A**

Logistic Regression for the prediction of CD8+ in HNSC tumor samples after considering the tumor stage.

Top and bottom 35% of the distributions were considered to divide the tumors into those with high or low levels of immune markers.

purity method=ABSOLUTE

stage I or II (N=76)

	$\beta$ coefficient	z value	Pr(> z )	OR
3p14 Loss (samples with loss=49)	0.1751775	0.2176969	0.827665	1.191458 binary
9p21.3 Loss (samples with loss=33)	-1.6968636	-2.3427388	0.019143	0.183257 binary
17p13.1 Loss (samples with loss=20)	-1.214868	-1.3559012	0.175131	0.296749 binary
SCNA level	-0.5542126	-1.2550551	0.209459	0.574524 continuous

stage III (N=65)

	$\beta$ coefficient	z value	Pr(> z )	OR
3p14 Loss (samples with loss=50)	-1.538657	-1.0086105	0.313161	0.214669 binary
9p21.3 Loss (samples with loss=25)	-2.064968	-1.9344592	0.053057	0.126822 binary
17p13.1 Loss (samples with loss=16)	2.017373	1.8246672	0.068051	7.518548 binary
SCNA level	-1.353899	-1.8978269	0.057719	0.258231 continuous

stage IV (N=163)

	$\beta$ coefficient	z value	Pr(> z )	OR
3p14 Loss (samples with loss=137)	-0.48979533	-0.7251495	0.46836	0.612752 binary
9p21.3 Loss (samples with loss=77)	-1.77733416	-3.8753118	0.000106	0.169088 binary
17p13.1 Loss (samples with loss=32)	-0.00592329	-0.0106613	0.991494	0.994094 binary
SCNA level	-0.29755493	-1.1531567	0.248846	0.742632 continuous

**S6B**

Logistic Regression for the prediction of CD8+ in HNSC tumor samples after considering the TP53 status.

Top and bottom 35% of the distributions were considered to divide the tumors into those with high or low levels of immune markers.

purity method=ABSOLUTE

TP53 WT (N=22) (stage I or II)

	$\beta$ coefficient	z value	Pr(> z )	OR
3p14 Loss	-16.021672	-0.004619	0.996315	1.1E-07 binary
9p21.3 Loss	-0.70451	-0.4432798	0.657563	0.494351 binary
SCNA level	-2.565948	-1.3362557	0.181466	0.076846 continuous

TP53 Mut (N=33) (stage I or II)

	$\beta$ coefficient	z value	Pr(> z )	OR
3p14 Loss	-1.0983191	-0.7301274	0.465312	0.333431 binary
9p21.3 Loss	-2.5883793	-2.4649196	0.013704	0.075142 binary
SCNA level	-0.2980467	-0.5378871	0.590655	0.742267 continuous

**S6C**

Pearson's correlation analysis between CD8+/CD3+ and 9p arm loss in HNSC tumor samples after considering the TP53 status.

purity method=ABSOLUTE

TP53 WT (N=22) (stage I or II)

	cor	p-value	FDR
CD8+ ~9p Arm Loss	0.41	0.06	0.12 continuous
CD3+ ~9p Arm Loss	0.32	0.15	0.3 continuous

TP53 Mut (N=33) (stage I or II)

	cor	p-value	FDR
CD8+ ~9p Arm Loss	0.51	0.002	0.004 continuous
CD3+ ~9p Arm Loss	0.36	0.03	0.06 continuous

**S6D**

Wilcoxon signed rank test between CD8+/CD3+ and 9p arm loss/9p21.3 loss in HNSC tumor samples after considering the TP53 status.

purity method=ABSOLUTE

TP53 WT (N=70) (stage I ~ IV)

	p-value	FDR
CD8+ ~9p Arm Loss	0.00446	0.01784
CD8+ ~9p21.3 focal Loss	0.127	0.1693333
CD3+ ~9p Arm Loss	0.0563	0.1126
CD3+ ~9p21.3 focal Loss	0.309	0.309

TP53 Mut (N=146) (stage I ~ IV)

	p-value	FDR
CD8+ ~9p Arm Loss	0.00286	0.01144
CD8+ ~9p21.3 focal Loss	0.864	0.864
CD3+ ~9p Arm Loss	0.0194	0.0388
CD3+ ~9p21.3 focal Loss	0.755	0.864

Table S7

## Relationship between Immune Markers and SCNA Events in HPV-positive HNSC (N=36)

Unless otherwise specified, '9p21.3 loss', '3p14 loss' or '17p13.1 loss' refer to the presence of a loss at this region irrespective of the length of the deletion (whether the loss encompasses the entire arm or is a focal event).

## S7A

## Comparison of the frequencies of different copy number events in HPV positive and negative HNSC

Events	Frequency in HPV positive HNSC (oropharynx, N=36)	Frequency in HPV negative HNSC (all, N=343)	Frequency in HPV negative HNSC (oral pharynx, N=232)
17p13.1 Loss	0.167	0.167	0.138
3p14 Loss	0.306	0.558	0.621
9p21.3 Loss	0.056	0.367	0.388
17p13.1 Focal Loss	0.028	0.027	0.031
3p14 Focal Loss	0.139	0.039	0.022
9p21.3 Focal Loss	0	0.116	0.094
3p Arm Loss	0.139	0.388	0.406
9p Arm Loss	0.056	0.26	0.281
9p Arm Gain	0.121	0.125	0.137
17p Arm Loss	0.167	0.122	0.138
Chr 7 Gain	0	0.125	0.08
Average number of arm-level Gain	4.69	5.05	4.46
Average number of arm-level Loss	3.18	4.74	4.12

## S7B

## Logistic Regression for the prediction of immune infiltrate parameters in HPV-positive HNSC tumor samples; binary definition of loss or gain

Thresholded values were used to define Loss and Gain in HPV-positive samples

## HPV positive HNSC (oropharynx)

CD8+	$\beta$ coefficient	z value	Pr(> z )	OR
3p14 Loss		0.5177	0.537	0.592 1.6781634 binary
9p21.3 Loss		-35.4044	-0.007	0.994 4.208E-16 binary
17p13.1 Loss		18.0518	0.005	0.996 69150787 binary
Chr 7 Gain	NA	NA	NA	NA binary
SCNA level		0.2352	0.443	0.658 1.2651618 continuous 1
CD3+	$\beta$ coefficient	z value	Pr(> z )	OR
3p14 Loss		-0.02513	-0.025	0.98 0.9751831 binary
9p21.3 Loss		-17.62253	-0.006	0.995 2.221E-08 binary
17p13.1 Loss		-0.31789	-0.204	0.838 0.7276828 binary
Chr 7 Gain	NA	NA	NA	NA binary
SCNA level		-0.31853	-0.568	0.57 0.7272173 continuous 1
CD68+	$\beta$ coefficient	z value	Pr(> z )	OR
3p14 Loss		-0.34485	-0.371	0.711 0.7083266 binary
9p21.3 Loss		-16.25612	-0.007	0.995 8.711E-08 binary
17p13.1 Loss		-0.48031	-0.405	0.685 0.6185916 binary
Chr 7 Gain	NA	NA	NA	NA binary
SCNA level		-0.92103	-1.474	0.141 0.3981088 continuous

## S7C

## Logistic Regression for the prediction of immune infiltrate parameters in HPV-positive HNSC tumor samples; copy number level considered as continuous data.

For each copy number event (HPV-positive), we used copy number values after standardization.

## HPV positive HNSC (oropharynx)

CD8+	$\beta$ coefficient	z value	Pr(> z )	OR
3p14 scale		0.009591503	0.022416157	0.982116 1.0096376 continuous
9p21.3 scale		1.261262916	1.339749544	0.1803268 3.5298766 continuous
17p13.1 scale		-0.182965451	-0.303090653	0.7618208 0.8327969 continuous
Chr 7 scale		-3.988996857	-0.006119591	0.9951173 0.0185183 continuous
SCNA level		-0.183671061	-0.34096679	0.7331286 0.8322095 continuous
CD3+	$\beta$ coefficient	z value	Pr(> z )	OR
3p14 scale		0.2581585	0.49707339	0.6191373 1.294544 continuous
9p21.3 scale		0.2347384	0.498746708	0.6179578 1.2645779 continuous
17p13.1 scale		1.0354722	1.081391702	0.2795229 2.8164358 continuous
Chr 7 scale		-4.7208476	-0.00677584	0.9945937 0.0089076 continuous
SCNA level		-0.6893639	-0.985145189	0.3245528 0.5018952 continuous
CD68+	$\beta$ coefficient	z value	Pr(> z )	OR
3p14 scale		0.1582568	0.342368875	0.73207331 1.171467 continuous
9p21.3 scale		1.1535477	0.976983156	0.32857749 3.1694171 continuous
17p13.1 scale		0.2566075	0.490022554	0.62411794 1.2925377 continuous
Chr 7 scale		-4.2568355	-0.006530487	0.99478946 0.0141671 continuous
SCNA level		-1.2051899	-1.656786082	0.09756273 0.2996351 continuous



Table S8

HPV-negative HNSC cell lines and corresponding CNV for different genomic regions

CCLE name	3p Arm cnv	9p Arm cnv	17p Arm cnv	17p13.1 cnv	3p14 cnv	9p21.3 cnv	TP53 mutation	SASP_enrichment
SCC9_UPPER_AERODIGESTIVE_TRACT	0	-0.614	0	0.559	-0.645	-0.693	0	0.138674957
SCC25_UPPER_AERODIGESTIVE_TRACT	-0.504	-0.841	-0.009	0.24	-0.82	-0.859	1	0.311574821
DETROIT562_UPPER_AERODIGESTIVE_TRACT	-0.638	-0.586	0.059	0.687	-0.648	-0.628	1	0.229371271
BICR31_UPPER_AERODIGESTIVE_TRACT	-0.888	-0.438	-0.264	-0.264	-0.888	-0.59	1	0.299130188
SCC4_UPPER_AERODIGESTIVE_TRACT	-0.748	-0.437	-0.356	-0.356	-0.748	-0.437	1	0.24427235
SCC15_UPPER_AERODIGESTIVE_TRACT	0.083	-0.409	0.929	0.955	-0.46	-0.443	1	0.403180505
BICR6_UPPER_AERODIGESTIVE_TRACT	-0.586	-0.606	0	-0.049	-0.673	-0.606	1	0.154112043
HSC2_UPPER_AERODIGESTIVE_TRACT	-0.276	0.105	0.91	0.91	-0.276	0.105	1	0.269425399
SNU46_UPPER_AERODIGESTIVE_TRACT	-0.523	0	0.624	0.689	-0.523	-0.018	1	0.024359176
BICR16_UPPER_AERODIGESTIVE_TRACT	-0.596	0.178	-0.223	0.371	-0.596	-0.53	1	0.162163423
CAL33_UPPER_AERODIGESTIVE_TRACT	0.005	0	0	-0.017	-0.997	0.015	1	0.2549407
HSC4_UPPER_AERODIGESTIVE_TRACT	0.402	0.464	0.498	0.498	-0.113	1.095	1	0.158259287
BHY_UPPER_AERODIGESTIVE_TRACT	-0.274	0.635	-0.25	-0.392	-0.274	0.528	1	0.285596712
SNU1076_UPPER_AERODIGESTIVE_TRACT	-0.576	0.071	-0.326	-0.326	-0.576	-0.951	1	0.20324502
PECAPJ34CLONEC12_UPPER_AERODIGESTIVE_TRACT	0.011	0	0.879	-0.094	-0.978	-0.027	1	0.223535876
SNU1041_UPPER_AERODIGESTIVE_TRACT	0	0	0	-0.071	-0.902	-0.133	1	0.166218258
PECAPJ15_UPPER_AERODIGESTIVE_TRACT	-0.531	-0.744	0.239	0.239	-0.819	-0.744	1	0.098837199
YD8_UPPER_AERODIGESTIVE_TRACT	0	0.509	1.045	1.045	-0.633	0.478	1	0.093072471
SNU1066_UPPER_AERODIGESTIVE_TRACT	-0.82	0.123	0.135	0.112	-0.82	-0.797	1	0.236743808
SNU899_UPPER_AERODIGESTIVE_TRACT	-0.531	0	0	-0.018	-0.531	-0.036	1	0.278886299
SNU1214_UPPER_AERODIGESTIVE_TRACT	-0.979	-0.964	0	-0.007	-0.979	-0.967	1	0.11958324
YD10B_UPPER_AERODIGESTIVE_TRACT	-0.676	-0.218	0.152	0.152	-0.676	0.898	1	0.186047685
PECAPJ41CLONED2_UPPER_AERODIGESTIVE_TRACT	-0.956	-0.978	0	-0.002	-0.963	-0.978	1	0.280160386
PECAPJ49_UPPER_AERODIGESTIVE_TRACT	-0.954	0	0	0.003	-0.98	0.004	1	0.33584896
A253_SALIVARY_GLAND	-0.626	-0.541	0	0.487	-0.462	-0.541	1	0.004138976
YD38_UPPER_AERODIGESTIVE_TRACT	-0.639	0	0.214	0.214	-0.639	-0.003	1	0.310609016
BICR56_UPPER_AERODIGESTIVE_TRACT	-0.978	0	0	0.011	-0.978	-0.001	1	0.263762592
HSC3_UPPER_AERODIGESTIVE_TRACT	-0.582	0.448	0.149	0.392	-0.582	0.448	1	0.336701744
CAL27_UPPER_AERODIGESTIVE_TRACT	-0.953	0	0	-0.035	-0.964	0.07	1	0.31333995
YD15_SALIVARY_GLAND	-0.615	-0.637	0.502	0.658	-0.65	-0.675	1	0.118655673
FADU_UPPER_AERODIGESTIVE_TRACT	0	-0.65	0	0.045	-0.64	-0.65	1	0.04112478
BICR18_UPPER_AERODIGESTIVE_TRACT	-0.573	-0.543	0	0.087	-0.573	-0.575	1	-0.039028669

Table S9

GSEA Analysis on HNSC cancer cell lines comparing cell lines with or without 9p21.3 loss (arm or focal), Pathways Enriched

NAME	SIZE	ES	NES	NOM p-Value	FDR q-Value	FWER p-Value	RANK AT MAX	LEADING EDGE
BIOCARTA_EDG1_PATHWAY	26	0.770171	1.732077	0.005163511	1	1	0.923	3988 tags=50%, list=16%, signal=59%
REACTOME_STRIATED_MUSCLE_CONTRACTION	23	0.747589	1.675122	0.005067567	1	1	0.989	2947 tags=17%, list=12%, signal=20%
KEGG_TASTE_TRANSDUCTION	33	0.716086	1.662948	0.013675214	1	1	0.993	516 tags=12%, list=13%, signal=12%
BIOCARTA_BARRESTIN_SRC_PATHWAY	15	0.778297	1.621138	0.028725315	1	1	0.999	3223 tags=27%, list=23%, signal=31%
REACTOME_METAL_ION_SLC_TRANSPORTERS	21	0.722715	1.573749	0.037487074	1	1	1	769 tags=19%, list=3%, signal=20%
REACTOME_THE_ROLE_OF_NEF_IN_HIV1_REPLICATION_AND_DISEASE_PATHOGENESIS	25	0.689001	1.570837	0.027350428	1	1	1	17 tags=4%, list=0%, signal=4%
REACTOME_TIGHT_JUNCTION_INTERACTIONS	28	0.686324	1.569755	0.021885522	1	1	1	99 tags=7%, list=0%, signal=7%
KEGG_CELL_ADHESION_MOLECULES_CAMS	102	0.564584	1.564531	0.020057306	1	1	1	508 tags=9%, list=2%, signal=9%
KEGG_STEROID_HORMONE_BIOSYNTHESIS	40	0.645129	1.56117	0.028428094	1	1	1	2719 tags=30%, list=11%, signal=34%
REACTOME_GAP_JUNCTION_TRAFFICKING	23	0.722779	1.559818	0.038206897	1	1	1	2479 tags=35%, list=10%, signal=38%
REACTOME_CELL_CELL_JUNCTION_ORGANIZATION	49	0.626491	1.557937	0.02728732	1	1	1	247 tags=9%, list=1%, signal=8%
KEGG_PENTOSE_AND_GLYCUCURONATE_INTERCONVERSIONS	22	0.700953	1.528772	0.051194537	1	1	1	5667 tags=50%, list=22%, signal=64%
KEGG_ASCORBATE_AND_ALDARATE_METABOLISM	20	0.707971	1.51637	0.05263158	1	1	1	2719 tags=30%, list=11%, signal=34%
KEGG_PARKINSONS_DISEASE	93	0.55174	1.489339	0.033282906	1	1	1	5910 tags=30%, list=23%, signal=39%
REACTOME_CELL_JUNCTION_ORGANIZATION	70	0.550621	1.462215	0.037936267	1	1	1	247 tags=6%, list=1%, signal=6%
KEGG_ARACHIDONIC_ACID_METABOLISM	45	0.593656	1.450863	0.039808918	1	1	1	2830 tags=27%, list=11%, signal=30%
REACTOME_REGULATORY_RNA_PATHWAYS	21	0.670205	1.448237	0.078397214	1	1	1	5076 tags=57%, list=22%, signal=71%
REACTOME_ABORTIVE_ELONGATION_OF_HIV1_TRANSCRIPT_IN_THE_ABSENCE_OF_TAT	19	0.669201	1.441679	0.08148148	1	1	1	3876 tags=42%, list=15%, signal=50%
REACTOME_ASSEMBLY_OF_THE_PRE_REPLICATIVE_COMPLEX	63	0.556189	1.429341	0.046104927	1	1	1	7464 tags=49%, list=29%, signal=69%
KEGG_DRUG_METABOLISM_OTHER_ENZYMES	40	0.595014	1.426465	0.07017544	1	1	1	2719 tags=28%, list=11%, signal=31%
KEGG_TYPE_II_DIABETES_MELLITUS	41	0.580994	1.418746	0.068515494	1	1	1	1927 tags=17%, list=8%, signal=18%
KEGG_ALDOSTERONE_REGULATED_SODIUM_REABSORPTION	38	0.592241	1.418961	0.07692308	1	1	1	4083 tags=50%, list=24%, signal=54%
REACTOME_VOLTAGE_GATED_POTASSIUM_CHANNELS	34	0.596848	1.409571	0.07826087	1	1	1	324 tags=9%, list=1%, signal=9%
BIOCARTA_RHO_PATHWAY	32	0.604687	1.405141	0.07272727	1	1	1	1084 tags=13%, list=4%, signal=13%
KEGG_FC_GAMMA_R_MEDIATED_PHAGOCYTOSIS	91	0.521835	1.403979	0.055072464	1	1	1	4013 tags=22%, list=16%, signal=26%
REACTOME_MICRORNA_MIRNA_BIOGENESIS	18	0.672858	1.400063	0.10124334	1	1	1	5810 tags=61%, list=23%, signal=79%
BIOCARTA_BAD_PATHWAY	24	0.628961	1.399039	0.087628864	1	1	1	4674 tags=38%, list=18%, signal=46%
REACTOME_M_G1N_TRANSITION	78	0.526321	1.395061	0.07969925	1	1	1	6059 tags=35%, list=24%, signal=45%
REACTOME_CDT1_ASSOCIATION_WITH_THE_CDC6_ORC_ORIGIN_COMPLEX	54	0.554225	1.390763	0.07042254	1	1	1	7464 tags=50%, list=29%, signal=71%
REACTOME_RNA_POL_I_PROMOTER_OPENING	55	0.556454	1.386885	0.07605178	1	1	1	6397 tags=38%, list=25%, signal=51%
REACTOME_REGULATION_OF_SIGNALING_BY_CBL	18	0.657341	1.379645	0.11599257	1	1	1	2481 tags=22%, list=10%, signal=25%
REACTOME_SORSK2_MEDIATED_DEGRADATION_OF_P27_P21	54	0.480333	1.370444	0.07981565	1	1	1	6059 tags=39%, list=24%, signal=51%
REACTOME_RECYCLING_PATHWAY_OF_L1	26	0.611553	1.373821	0.114817944	1	1	1	2286 tags=23%, list=9%, signal=25%
REACTOME_PACKAGING_OF_TELOMERE_ENDS	42	0.555223	1.373576	0.07820299	1	1	1	6397 tags=40%, list=25%, signal=54%
REACTOME_FANCONI_ANEMIA_PATHWAY	20	0.622841	1.366789	0.104166664	1	1	1	4032 tags=30%, list=16%, signal=36%
REACTOME_DESTABILIZATION_OF_MRNA_BY_AUF1_HNRNP_D0	50	0.551495	1.365638	0.08796296	1	1	1	7428 tags=50%, list=29%, signal=70%
REACTOME_OXYGEN_DEPENDENT_PROLINE_HYDROXYLATION_OF_HYPOXIA_INDUCIBLE_FACTOR_ALPHA	15	0.658078	1.361504	0.11900533	1	1	1	2363 tags=27%, list=9%, signal=29%
REACTOME_NCAM1_INTERACTIONS	36	0.576865	1.35965	0.10305958	1	1	1	1496 tags=17%, list=6%, signal=18%
KEGG_STARCH_AND_SUCROSE_METABOLISM	37	0.563694	1.354787	0.097087376	1	1	1	2719 tags=19%, list=11%, signal=21%
REACTOME_PHASE_I_CONJUGATION	56	0.534087	1.35351	0.0913242	1	1	1	2719 tags=20%, list=11%, signal=22%
REACTOME_ORC1_REMOVAL_FROM_CHROMATIN	65	0.526172	1.353487	0.08926597	1	1	1	7464 tags=48%, list=29%, signal=67%
REACTOME_DEPOSITION_OF_NEW_CENPA_CONTAINING_NUCLEOSOMES_AT_THE_CENTROMERE	56	0.532127	1.351076	0.10108865	1	1	1	8555 tags=50%, list=24%, signal=58%
REACTOME_NITRIC_OXIDE_STIMULATES_GUANYLATE_CYCLASE	22	0.608178	1.335548	0.14089656	1	1	1	2871 tags=45%, list=11%, signal=51%
BIOCARTA_VEGF_PATHWAY	29	0.579152	1.335398	0.13866232	1	1	1	1927 tags=21%, list=8%, signal=22%
BIOCARTA_GSK3_PATHWAY	25	0.603801	1.333843	0.122689076	1	1	1	2309 tags=16%, list=9%, signal=18%
REACTOME_CDK_MEDIATED_PHOSPHORYLATION_AND_REMOVAL_OF_CDC6	46	0.543932	1.331843	0.111821085	1	1	1	7925 tags=54%, list=31%, signal=79%
REACTOME_CYCLIN_E_ASSOCIATED_EVENTS_DURING_G1_S_TRANSITION	63	0.51879	1.331077	0.09968847	1	1	1	6059 tags=37%, list=24%, signal=48%
BIOCARTA_GCR_PATHWAY	19	0.624814	1.32915	0.1465798	1	1	1	1927 tags=21%, list=8%, signal=23%
REACTOME_G1_S_TRANSITION	108	0.471804	1.32304	0.08840227	1	1	1	7925 tags=44%, list=31%, signal=63%
REACTOME_APOPTIC_EXECUTION_PHASE	51	0.520198	1.320914	0.09693053	1	1	1	3278 tags=18%, list=13%, signal=20%
REACTOME_INFLAMMASOMES	16	0.628617	1.320492	0.16187051	1	1	1	2021 tags=19%, list=8%, signal=20%
CANCER-TESTIS-ANTIGEN	54	0.480333	1.320344	0.091871346	1	1	1	2265 tags=18%, list=9%, signal=20%
REACTOME_STEROID_HORMONES	20	0.609023	1.316482	0.15412845	1	1	1	1767 tags=10%, list=7%, signal=11%
REACTOME_VIF_MEDIATED_DEGRADATION_OF_APOBEC3G	47	0.534553	1.315992	0.12480499	1	1	1	6059 tags=36%, list=24%, signal=47%
KEGG_SMALL_CELL_LUNG_CANCER	84	0.491926	1.315584	0.10644678	1	1	1	3948 tags=26%, list=15%, signal=31%
REACTOME_PLATELET_HOMEOSTASIS	71	0.505701	1.315359	0.1036036	1	1	1	3010 tags=24%, list=12%, signal=27%
REACTOME_P53_INDEPENDENT_G1_S_DNA_DAMAGE_CHECKPOINT	48	0.532281	1.314497	0.11568938	0.9915861	1	1	7428 tags=46%, list=29%, signal=65%
REACTOME_MEIOTIC_RECOMBINATION	75	0.494345	1.309656	0.11179173	0.9995672	1	1	6099 tags=35%, list=24%, signal=45%
KEGG_PORPHYRIN_AND_CHLOROPHYLL_METABOLISM	34	0.553904	1.306764	0.14214046	0.9971052	1	1	2719 tags=21%, list=11%, signal=23%
REACTOME_NEUTRIN_INTERACTIONS	19	0.610365	1.303367	0.14160839	0.99678326	1	1	2927 tags=21%, list=11%, signal=24%
BIOCARTA_HCMV_PATHWAY	17	0.634228	1.299367	0.1598023	1	1	1	3223 tags=29%, list=13%, signal=34%
REACTOME_CITRIC_ACID_CYCLE_TCA_CYCLE	20	0.603066	1.295536	0.17750439	1	1	1	5080 tags=45%, list=20%, signal=56%
REACTOME_IL_3_5_AND_GM-CSF_SIGNALING	39	0.545913	1.285037	0.135878	0.98893344	1	1	2481 tags=18%, list=10%, signal=20%
REACTOME_LYSOSOME_VESICLE_BIOGENESIS	23	0.583281	1.285098	0.15939598	0.9745598	1	1	4103 tags=22%, list=16%, signal=26%
BIOCARTA_AKT_PATHWAY	20	0.595165	1.283943	0.17875211	0.96540487	1	1	1927 tags=15%, list=8%, signal=16%
BIOCARTA_MCM_PATHWAY	18	0.599264	1.287011	0.17572464	0.9850114	1	1	7581 tags=61%, list=30%, signal=87%
REACTOME_SIGNALING_BY_ERBB2	95	0.478423	1.285279	0.10237389	0.9792291	1	1	726 tags=5%, list=3%, signal=5%
KEGG_B_CELL_RECEPTOR_SIGNALING_PATHWAY	73	0.482904	1.28432	0.12708019	0.96953064	1	1	2517 tags=12%, list=10%, signal=14%
REACTOME_MITOTIC_M_M_G1_PHASES	160	0.441203	1.281349	0.0945758	0.9704232	1	1	7832 tags=41%, list=31%, signal=59%
REACTOME_ADHERENS_JUNCTIONS_INTERACTIONS	21	0.590084	1.278812	0.17190082	0.968655	1	1	1534 tags=14%, list=6%, signal=15%
BIOCARTA_BCELLSURVIVAL_PATHWAY	16	0.608918	1.275065	0.18053098	0.9731757	1	1	1927 tags=25%, list=8%, signal=27%
REACTOME_GMP_PATHWAYS	18	0.606413	1.273005	0.1842162	0.9688615	1	1	2871 tags=50%, list=18%, signal=56%
BIOCARTA_IL2RB_PATHWAY	37	0.542148	1.26937	0.16221035	0.97210085	1	1	1927 tags=14%, list=8%, signal=15%
BIOCARTA_IL7_PATHWAY	17	0.610943	1.263801	0.20344828	0.98673224	1	1	3068 tags=20%, list=12%, signal=22%
REACTOME_SEMAPHORIN_INTERACTIONS	64	0.489497	1.262914	0.14198473	0.9766299	1	1	1993 tags=9%, list=8%, signal=10%
REACTOME_S_PHASE	106	0.456783	1.260745	0.12957746	0.97360575	1	1	6059 tags=34%, list=24%, signal=44%
BIOCARTA_ACH_PATHWAY	15	0.610333	1.258094	0.19604316	0.9735438	1	1	4191 tags=33%, list=16%, signal=40%
BIOCARTA_RAS_PATHWAY	23	0.566833	1.25686	0.19765495	0.96747756	1	1	3223 tags=17%, list=13%, signal=20%
REACTOME_SYNTHESIS_OF_PIP3_AT_THE_PLASMA_MEMBRANE	29	0.548324	1.25185	0.19410746	0.9778379	1	1	819 tags=14%, list=3%, signal=14%
REACTOME_GPIV_MEDIATED_ACTIVATION_CASCADE	29	0.547522	1.25035	0.19966997	0.9721544	1	1	1927 tags=17%, list=8%, signal=19%
REACTOME_ANTIEN_PROCESSING_CROSS_PRESENTATION	66	0.485244	1.245534	0.14678898	0.98283905	1	1	7428 tags=39%, list=29%, signal=55%
REACTOME_AUTODEGRADATION_OF_THE_E3_UBIQUITIN_LIGASE_COP1	46	0.505773	1.242985	0.16666667	0.9822829	1	1	7428 tags=46%, list=29%, signal=64%
REACTOME_P53_DEPENDENT_G1_DNA_DAMAGE_RESPONSE	52	0.496983	1.24226	0.1827957	0.9738304	1	1	6059 tags=35%, list=24%, signal=45%
REACTOME_METABOLISM_OF_STEROID_HORMONES_AND_VITAMINS_A_AND_D	22	0.567338	1.238708	0.208991	0.9784806	1	1	1767 tags=9%, list=7%, signal=10%
REACTOME_POTASSIUM_CHANNELS	81	0.483439	1.234446	0.16228747	0.98690908	1	1	3010 tags=20%, list=12%, signal=22%
KEGG_PROTEASOMES	40	0.515849	1.233867	0.19936204	0.97698897	1	1	8930 tags=63%, list=35%, signal=96%
REACTOME_G_BETA_PROTEIN_BETA_GAMMA_SIGNALING	26	0.554316	1.233243	0.19400352	0.96881586	1	1	4894 tags=38%, list=19%, signal=48%
REACTOME_SYNTHESIS_OF_DNA	90	0.455107	1.232121	0.15889212	0.9633374	1	1	726 tags=46%, list=30%, signal=65%
BIOCARTA_ARF_PATHWAY	17	0.592508	1.230947	0.22459893	0.9579939	1	1	2516 tags=24%, list=10%, signal=26%
REACTOME_FACTORS_INVOLVED_IN_MEGAKARYOCYTE_DEVELOPMENT_AND_PLATELET_PRODUCTION	111	0.441511	1.23074	0.13439307	0.94826597	1	1	1697 tags=10%, list=7%, signal=11%
REACTOME_MRNA_SPLICING	104	0.440185	1.229712	0.13960114	0.9422683	1	1	4609 tags=24%, list=18%, signal=29%
REACTOME_G_BETA_GAMMA_SIGNALING_THROUGH_PI3K_GAMMA	23	0.549386	1.224801	0.20950705	0.9532556	1	1	4894 tags=35%, list=19%, signal=43%
REACTOME_AMP_PATHWAYS	67	0.471208	1.221272	0.18045112	0.9564032	1	1	6460 tags=36%, list=25%, signal=48%
KEGG_ECM_RECEPTOR_INTERACTION	60	0.461412	1.220852	0.17557251	0.9504806	1	1	4121 tags=26%, list=16%, signal=31%
REACTOME_PYRUVATE_METABOLISM	18	0.573971	1.218216	0.24551971	0.95051475	1	1	214 tags=17%, list=1%, signal=17%
REACTOME_CELL_CELL_COMMUNICATION	109	0.439852	1.216262	0.16550764	0.94906795	1	1	2482 tags=10%, list=10%, signal=11%
BIOCARTA_CXCR4_PATHWAY	24	0.533307	1.214863	0.24377224	0.94516504	1	1	3948 tags=29%, list=15%, signal=34%
BIOCARTA_HDAC_PATHWAY	26	0.545908	1.214384	0.21631205	0.93753886	1	1	3171 tags=27%, list=12%, signal=31%
REACTOME_MEIOSIS	102	0.4471	1.210212	0.17914832	0.94591445	1	1	6397 tags=35%, list=25%, signal=47%
REACTOME_CROSS_PRESENTATION_OF_SOLUBLE_EXOGENOUS_ANTIGENS_ENDOSOMES	45	0.501203	1.209037	0.21753247	0.9411948	1	1	8930 tags=58%, list=35%, signal=89%
KEGG_RETINOL_METABOLISM	47	0.488926	1.20459	0.20414673	0.951021	1	1	6361 tags=43%, list=25%, signal=57%
REACTOME_FORMATION_OF_THE_HIV1_EARLY_ELONGATION_COMPLEX	29	0.527094	1.202129	0.2359736	0.9519279	1	1	3876 tags=28%, list=15%, signal=32%
REACTOME_DNA_REPLICATION	180	0.415707	1.200826	0.14171124	0.9478919	1	1	7832 tags=41%, list=31%, signal=59%
REACTOME_MITOTIC_G1_G1_S_PHASES	133	0.423975	1.198573	0.17574932	0.9486619	1	1	6059 tags=32%, list=24%, signal=41%
BIOCARTA_LOCAL_PAIN_PATHWAY	18	0.571252	1.197948	0.260177	0.9428095	1	1	3948 tags=22%, list=15%, signal=26%
REACTOME_PI_METABOLISM	45	0.48635	1.194814	0.2194745	0.9468292	1	1	819 tags=9%, list=3%, signal=9%
REACTOME_APOPTOTIC_CLEAVAGE_OF_CELLULAR								

REACTOME_ER_PHAGOSOME_PATHWAY	53	0.479617	1.183286	0.21677215	0.93497497	1	7428 tags=42%, list=29%, signal=58%
REACTOME_O_LINKED_GLYCOSYLATION_OF_MUCINS	47	0.479964	1.178353	0.23557693	0.94732136	1	1296 tags=17%, list=5%, signal=18%
REACTOME_PLATELET_CALCIIUM_HOMEOSTASIS	15	0.567257	1.176389	0.2621528	0.94686437	1	826 tags=20%, list=3%, signal=21%
REACTOME_HIV_INFECTION	183	0.398153	1.175642	0.16425756	0.94178862	1	6059 tags=27%, list=24%, signal=35%
REACTOME_COMPLEMENT_CASCADE	19	0.533815	1.175389	0.25215888	0.93473417	1	3193 tags=16%, list=13%, signal=18%
REACTOME_NEURONAL_SYSTEM	237	0.388085	1.172839	0.16216215	0.93711651	1	3010 tags=20%, list=12%, signal=14%
REACTOME_HOST_INTERACTIONS_OF_HIV_FACTORS	116	0.420565	1.172216	0.20735294	0.931804	1	6059 tags=20%, list=24%, signal=36%
BIOCARTA_MEF2D_PATHWAY	18	0.556291	1.171223	0.28347826	0.92817926	1	3657 tags=17%, list=14%, signal=19%
REACTOME_INCRETIN_SYNTHESIS_SECRETION_AND_INACTIVATION	17	0.561425	1.17102	0.29491526	0.9245167	1	1065 tags=18%, list=4%, signal=18%
REACTOME_REGULATION_OF_ORNITHINE_DECARBOXYLASE_ODC	47	0.47508	1.169553	0.24052718	0.9195563	1	8524 tags=53%, list=33%, signal=80%
REACTOME_G0_AND_EARLY_G1	24	0.529691	1.168521	0.26206896	0.9161775	1	1794 tags=13%, list=7%, signal=13%
REACTOME_MRNA_CAPPING	29	0.506602	1.167014	0.2487725	0.9145512	1	3876 tags=24%, list=15%, signal=28%
REACTOME_MUSCLE_CONTRACTION	42	0.476894	1.165613	0.2540453	0.9128417	1	272 tags=5%, list=1%, signal=5%
REACTOME_AUTODEGRADATION_OF_CDH1_BY_CDH1_APC_C	57	0.459249	1.163865	0.2643857	0.912247	1	8524 tags=49%, list=33%, signal=74%
KEGG_METABOLISM_OF_XENOBIOTICS_BY_CYTOCHROME_P450	53	0.463973	1.157116	0.240625	0.9311158	1	2719 tags=23%, list=11%, signal=25%
BIOCARTA_PTEN_PATHWAY	17	0.543969	1.156405	0.2967628	0.92647946	1	4756 tags=41%, list=19%, signal=51%
REACTOME_APC_C_CDCC20_MEDIATED_DEGRADATION_OF_MITOTIC_PROTEINS	65	0.45395	1.153899	0.2435464	0.92903095	1	8524 tags=49%, list=33%, signal=74%
BIOCARTA_GLEEVEC_PATHWAY	23	0.526525	1.151111	0.28500825	0.93255705	1	4756 tags=32%, list=19%, signal=32%
REACTOME_CELL_SURFACE_INTERACTIONS_AT_THE_VASCULAR_WALL	77	0.438799	1.143079	0.24707602	0.95709497	1	3193 tags=21%, list=13%, signal=24%
REACTOME_RNA_POL_II_TRANSCRIPTION_PRE_INITIATION_AND_PROMOTER_OPENING	40	0.469304	1.142999	0.285956	0.9502089	1	3876 tags=20%, list=15%, signal=24%
REACTOME_ELONGATION_ARREST_AND_RECOVERY	24	0.516869	1.140171	0.30633804	0.9542445	1	4298 tags=38%, list=17%, signal=45%
BIOCARTA_CDC42RAC_PATHWAY	16	0.542043	1.140007	0.28849557	0.9474684	1	1927 tags=19%, list=8%, signal=20%
KEGG_ANTIGEN_PROCESSING_AND_PRESENTATION	41	0.474302	1.139683	0.267101	0.94232595	1	1847 tags=12%, list=7%, signal=13%
REACTOME_MRNA_SPLICING_MINOR_PATHWAY	40	0.47257	1.138542	0.28805238	0.93947893	1	4517 tags=28%, list=18%, signal=33%
REACTOME_MEIOTIC_SYNAPSIS	64	0.445869	1.137998	0.24423963	0.93476504	1	6397 tags=38%, list=25%, signal=50%
REACTOME_HEMOSTASIS	408	0.359955	1.137715	0.15441176	0.9311093	1	3223 tags=15%, list=13%, signal=17%
BIOCARTA_PPARG_PATHWAY	55	0.445039	1.136978	0.28526148	0.92507076	1	2410 tags=19%, list=9%, signal=19%
REACTOME_E2F_MEDIATED_REGULATION_OF_DNA_REPLICATION	34	0.47618	1.13461	0.2821369	0.92696977	1	8198 tags=44%, list=32%, signal=65%
REACTOME_TIE2_SIGNALING	17	0.538143	1.134483	0.29965752	0.9211186	1	4756 tags=41%, list=19%, signal=51%
KEGG_INTESTINAL_IMMUNE_NETWORK_FOR_IGA_PRODUCTION	32	0.522251	1.133356	0.30981067	0.91860086	1	3317 tags=17%, list=13%, signal=20%
BIOCARTA_GH_PATHWAY	26	0.509876	1.131194	0.30819672	0.91998446	1	4756 tags=35%, list=19%, signal=43%
REACTOME_CD28_DEPENDENT_PI3K_AKT_SIGNALING	20	0.513814	1.12831	0.31088084	0.9238655	1	4488 tags=40%, list=18%, signal=48%
REACTOME_IRON_UPTAKE_AND_TRANSPORT	35	0.484411	1.127345	0.29307568	0.92074007	1	6543 tags=34%, list=26%, signal=46%
REACTOME_NEGATIVE_REGULATION_OF_FGFR_SIGNALING	31	0.477726	1.121135	0.30882353	0.93722785	1	1943 tags=16%, list=8%, signal=17%
REACTOME_ACYL_CHAIN_REMODELLING_OF_PE	17	0.530067	1.117459	0.32841328	0.9444429	1	3133 tags=29%, list=12%, signal=34%
BIOCARTA_SPPA_PATHWAY	21	0.513941	1.113905	0.3249054	0.9511328	1	3948 tags=24%, list=15%, signal=28%
REACTOME_BASIGIN_INTERACTIONS	24	0.50102	1.11295	0.3272553	0.9400991	1	2842 tags=21%, list=10%, signal=23%
REACTOME_REGULATION_OF_APOPTOSIS	66	0.44852	1.111617	0.31104198	0.946298	1	7428 tags=40%, list=29%, signal=62%
BIOCARTA_CTCF_PATHWAY	23	0.50002	1.107803	0.316609	0.9540625	1	1927 tags=13%, list=8%, signal=14%
REACTOME_PYRIMIDINE_METABOLISM	19	0.51103	1.10762	0.33854166	0.948499	1	2530 tags=21%, list=10%, signal=23%
BIOCARTA_ALK_PATHWAY	34	0.465284	1.107515	0.31764707	0.94270605	1	3367 tags=18%, list=13%, signal=20%
REACTOME_TCA_CYCLE_AND_RESPIRATORY_ELECTRON_TRANSPORT	104	0.397397	1.100761	0.29555237	0.9611441	1	6187 tags=39%, list=26%, signal=53%
BIOCARTA_MTA3_PATHWAY	18	0.516858	1.100322	0.33862433	0.9565695	1	5750 tags=50%, list=23%, signal=64%
REACTOME_CA_DEPENDENT_EVENTS	26	0.488411	1.096338	0.3416252	0.96457756	1	4010 tags=15%, list=16%, signal=18%
REACTOME_RESPIRATORY_ELECTRON_TRANSPORT_ATP_SYNTHESIS_BY_CHEMIOSMOTIC_COUPLING_A	67	0.422136	1.092489	0.31455398	0.9719719	1	7617 tags=49%, list=30%, signal=70%
ND_HEAT_PRODUCTION_BY_UNCOUPLING_PROTEINS	2	0.494251	1.089206	0.35294212	0.97816294	1	1337 tags=13%, list=5%, signal=14%
KEGG_PROTEIN_EXPORT	65	0.417693	1.08915	0.32758713	0.9721706	1	7617 tags=49%, list=30%, signal=70%
REACTOME_RESPIRATORY_ELECTRON_TRANSPORT	75	0.409058	1.089129	0.3023952	0.98613574	1	2564 tags=13%, list=10%, signal=15%
REACTOME_PHOSPHATIDYLINOSITOL_SIGNALING_SYSTEM	34	0.460313	1.088953	0.33663365	0.96076256	1	3223 tags=24%, list=13%, signal=27%
REACTOME_SIGNAL_TRANSDUCTION_BY_L1	22	0.485985	1.086738	0.35643566	0.9625683	1	2363 tags=18%, list=9%, signal=20%
REACTOME_REGULATION_OF_HYPOXIA_INDUCIBLE_FACTOR_HIF_BY_OXYGEN	53	0.425152	1.085944	0.3146965	0.95960766	1	2719 tags=21%, list=11%, signal=23%
KEGG_DRUG_METABOLISM_CYTOCHROME_P450	44	0.444373	1.08424	0.3418124	0.959853	1	136 tags=7%, list=1%, signal=7%
REACTOME_PHOSPHOLIPASE_C_MEDIATED_CASCADE	24	0.483548	1.083424	0.35049835	0.9570774	1	1296 tags=17%, list=5%, signal=18%
REACTOME_KERATAN_SULFATE_BIOSYNTHESIS	35	0.454853	1.083222	0.32495812	0.95202965	1	3837 tags=17%, list=15%, signal=20%
BIOCARTA_TOLL_PATHWAY	229	0.363818	1.082009	0.2859025	0.9508083	1	2286 tags=10%, list=9%, signal=11%
REACTOME_AXON_GUIDANCE	155	0.374026	1.081834	0.30769232	0.94576424	1	2602 tags=15%, list=10%, signal=17%
KEGG_CALCIIUM_SIGNALING_PATHWAY	21	0.440625	1.077388	0.33774835	0.9557531	1	798 tags=10%, list=3%, signal=10%
REACTOME_PYRUVATE_METABOLISM_AND_CITRIC_ACID_TCA_CYCLE	64	0.416151	1.075217	0.35407406	0.9576428	1	798 tags=10%, list=3%, signal=10%
REACTOME_CLASS_B_2_SECRETIN_FAMILY_RECEPTORS	79	0.405248	1.074662	0.35103244	0.9543587	1	6099 tags=30%, list=24%, signal=40%
REACTOME_RNA_POL_I_TRANSCRIPTION	21	0.497225	1.074358	0.37122557	0.9497413	1	4756 tags=33%, list=19%, signal=41%
BIOCARTA_INSULIN_PATHWAY	22	0.487966	1.072629	0.383821	0.95029545	1	3948 tags=23%, list=15%, signal=21%
REACTOME_CCR3_PATHWAY	28	0.47399	1.072008	0.37221268	0.94695824	1	9190 tags=61%, list=36%, signal=95%
BIOCARTA_PROTEASOME_PATHWAY	81	0.397911	1.071451	0.33576643	0.9433855	1	7731 tags=37%, list=30%, signal=53%
REACTOME_REGULATION_OF_MRNA_STABILITY_BY_PROTEINS_THAT_BIND_AU_RICH_ELEMENTS	29	0.463083	1.070106	0.36963695	0.94279945	1	5080 tags=31%, list=20%, signal=39%
KEGG_CITRATE_CYCLE_TCA_CYCLE	28	0.474424	1.06765	0.37024793	0.94543433	1	1296 tags=14%, list=5%, signal=15%
REACTOME_KERATAN_SULFATE_KERATIN_METABOLISM	49	0.436154	1.065596	0.34923077	0.946852	1	3840 tags=22%, list=15%, signal=26%
KEGG_OLFACTORY_TRANSDUCTION	70	0.408192	1.064866	0.35603714	0.9445531	1	3704 tags=21%, list=15%, signal=25%
REACTOME_TRANSPORT_OF_GLUCOSE_AND_OTHER_SUGARS_BILE_SALTS_AND_ORGANIC_ACIDS_MET	108	0.340311	1.062898	0.34705882	0.9345967	1	2830 tags=13%, list=10%, signal=16%
AL_IONS_AND_AMINE_COMPOUNDS	30	0.464579	1.06164	0.38758388	0.9441915	1	5860 tags=30%, list=23%, signal=39%
REACTOME_BIOLOGICAL_OXIDATIONS	22	0.4875	1.061318	0.39826086	0.94015795	1	3223 tags=27%, list=13%, signal=31%
REACTOME_ACTIVATION_OF_THE_PRR_REPLIATIVE_COMPLEX	162	0.363005	1.058879	0.33065596	0.94288766	1	2038 tags=12%, list=8%, signal=13%
BIOCARTA_HER2_PATHWAY	110	0.374502	1.056504	0.36947218	0.9454774	1	7774 tags=38%, list=30%, signal=55%
REACTOME_TRANSMISSION_ACROSS_CHEMICAL_SYNAPSES	29	0.460851	1.052341	0.38039866	0.95361567	1	5810 tags=45%, list=23%, signal=58%
REACTOME_CELL_CYCLE_CHECKPOINTS	132	0.369415	1.051145	0.34051725	0.9525287	1	7887 tags=39%, list=31%, signal=56%
KEGG_RNA_POLYMERASE	94	0.387534	1.046157	0.37896255	0.96397644	1	5865 tags=27%, list=23%, signal=34%
REACTOME_PROCESSING_OF_CAPPED_INTRON_CONTAINING_PRE_MRNA	15	0.50879	1.043892	0.42105263	0.96637994	1	410 tags=2%, list=2%, signal=7%
REACTOME_RNA_POL_II_TRANSCRIPTION	27	0.463726	1.042353	0.42708334	0.96646893	1	4032 tags=22%, list=16%, signal=26%
REACTOME_TGF_BETA_RECEPTOR_SIGNALING_IN_EMT_EPITHELIAL_TO_MESENCHYMAL_TRANSITION	87	0.379157	1.04131	0.3636387	0.9646104	1	6397 tags=30%, list=25%, signal=40%
REACTOME_ENDOSOMAL_SORTING_COMPLEX_REQUIRED_FOR_TRANSPORT_ESCRT	62	0.399687	1.038993	0.393468	0.9673461	1	7428 tags=40%, list=29%, signal=62%
KEGG_SYSTEMIC_IP3_ERYTHEMATOSUS	50	0.419264	1.038868	0.39556962	0.96267295	1	708 tags=6%, list=3%, signal=6%
REACTOME_SIGNALING_BY_WNT	110	0.368148	1.038594	0.38152012	0.95862854	1	6799 tags=33%, list=27%, signal=44%
REACTOME_CHROMOSOME_MAINTENANCE	17	0.497442	1.037893	0.4424599	0.9560122	1	4592 tags=41%, list=18%, signal=50%
REACTOME_SYNTHESIS_OF_PC	17	0.49187	1.03777	0.41696113	0.95153594	1	5216 tags=35%, list=20%, signal=44%
REACTOME_POST_CHAPERONIN_TUBULIN_FOLDING_PATHWAY	24	0.476274	1.035872	0.43674177	0.9528378	1	1879 tags=21%, list=7%, signal=22%
KEGG_GLYCOPHINGOLIPID_BIOSYNTHESIS_LACTO_AND_NEOLACTO_SERIES	49	0.422384	1.03521	0.3984	0.9501987	1	6059 tags=37%, list=24%, signal=48%
REACTOME_SCF_BETA_TRCP_MEDIATED_DEGRADATION_OF_EM11	189	0.34948	1.030321	0.40684932	0.96073335	1	6099 tags=30%, list=24%, signal=39%
REACTOME_TERMINATION_OF_O_GLYCAN_BIOSYNTHESIS	20	0.483378	1.028077	0.43463498	0.96298033	1	2030 tags=25%, list=8%, signal=27%
BIOCARTA_NGF_PATHWAY	18	0.481127	1.025717	0.45360824	0.96555406	1	4756 tags=33%, list=19%, signal=41%
REACTOME_SYNTHESIS_OF_PA	21	0.470951	1.024683	0.4214047	0.9640597	1	2145 tags=14%, list=8%, signal=16%
REACTOME_SYNTHESIS_OF_P2	33	0.435858	1.0239	0.41373533	0.9617074	1	5390 tags=30%, list=21%, signal=38%
KEGG_FRUCTOSE_AND_MANNOSE_METABOLISM	16	0.497575	1.02388	0.44181818	0.9570173	1	136 tags=13%, list=1%, signal=13%
REACTOME_FGFR_LIGAND_BINDING_AND_ACTIVATION	193	0.347182	1.022012	0.41888297	0.9584095	1	4571 tags=22%, list=18%, signal=27%
KEGG_FOCAL_ADHESION	21	0.466664	1.021347	0.43816254	0.9560218	1	8247 tags=52%, list=32%, signal=77%
REACTOME_INSULIN_RECEPTOR_RECYCLING	54	0.407431	1.018268	0.41259843	0.96085806	1	1084 tags=6%, list=4%, signal=6%
REACTOME_PATHOGENIC_ESCHERICHIA_COLI_INFECTION	70	0.382542	1.017559	0.41768292	0.95853245	1	5120 tags=24%, list=20%, signal=30%
REACTOME_OPIOID_SIGNALLING	52	0.404349	1.01641	0.43393394	0.9575536	1	5810 tags=27%, list=23%, signal=35%
REACTOME_MRNA_POL_II_PRE_TRANSCRIPTION_EVENTS	22	0.458125	1.014745	0.46192053	0.9581807	1	136 tags=9%, list=1%, signal=9%
REACTOME_SHC_MEDIATED_CASCADE	50	0.407264	1.013426	0.43670887	0.95767987	1	6181 tags=30%, list=24%, signal=40%
REACTOME_GOLGI_ASSOCIATED_VESICLE_BIOGENESIS	21	0.469802	1.012779	0.44821733	0.9550803	1	4756 tags=33%, list=19%, signal=41%
BIOCARTA_IGF1_PATHWAY	24	0.469896	1.011766	0.45502645	0.95375943	1	6412 tags=33%, list=25%, signal=44%
REACTOME_TRANSFERRIN_ENDOCYTOSIS_AND_RECYCLING	385	0.323822	1.00				

KEGG_REGULATION_OF_ACTIN_CYTOSKELETON	196	0.330343	0.997316	0.4654498	0.9216861	1	1985 tags=9%, list=8%, signal=9%
KEGG_OXIDATIVE_PHOSPHORYLATION	93	0.364322	0.992618	0.46439168	0.9314307	1	7617 tags=44%, list=30%, signal=63%
KEGG_BIOPHYSICS_PATHWAY	24	0.454314	0.992603	0.4645799	0.92744845	1	4401 tags=29%, list=17%, signal=35%
KEGG_BIOPHYSICS_PATHWAY	26	0.453136	0.991781	0.47058824	0.92596346	1	3918 tags=19%, list=15%, signal=23%
KEGG_RAS_ACTIVATION_UOPN_CA2_INFUX_THROUGH_NMDA_RECEPTOR	17	0.46121	0.980672	0.4642857	0.9256176	1	3001 tags=18%, list=12%, signal=20%
KEGG_NUCLEAR_RECEPTOR_TRANSCRIPTION_PATHWAY	44	0.40635	0.989672	0.4752	0.9238713	1	2125 tags=16%, list=12%, signal=17%
KEGG_TPO_PATHWAY	24	0.445407	0.987427	0.47582606	0.9282785	1	4756 tags=33%, list=19%, signal=41%
KEGG_FORMATION_OF_RNA_POL_II_ELONGATION_COMPLEX	36	0.415403	0.98679	0.46042004	0.92431706	1	4298 tags=25%, list=17%, signal=30%
KEGG_PI_3K_CASCADE	48	0.401157	0.981814	0.4648986	0.93463576	1	1943 tags=13%, list=8%, signal=14%
KEGG_BETA_GAMMA_SIGNALING_THROUGH_PL_C_BETA	19	0.464643	0.979319	0.48776224	0.9378079	1	4894 tags=37%, list=19%, signal=46%
KEGG_REGULATION_OF_MITOTIC_CELL_CYCLE	77	0.369116	0.977297	0.4673748	0.9396402	1	7428 tags=42%, list=29%, signal=58%
KEGG_PAR1_PATHWAY	35	0.424061	0.976889	0.5024793	0.9369703	1	2564 tags=14%, list=10%, signal=16%
KEGG_CREB_PHOSPHORYLATION_THROUGH_THE_ACTIVATION_OF_RAS	27	0.42986	0.974219	0.4788494	0.9408243	1	3972 tags=19%, list=16%, signal=22%
KEGG_PROXIMAL_TUBULE_BICARBONATE_RECLAMATION	20	0.49045	0.970033	0.516696	0.94877034	1	4887 tags=40%, list=19%, signal=49%
KEGG_IMMUNOREGULATORY_INTERACTIONS_BETWEEN_A_LYMPHOID_AND_A_NON_LYMPHOID_CELL	38	0.409589	0.969931	0.49447078	0.9451058	1	1515 tags=5%, list=6%, signal=6%
KEGG_NEUROACTIVE_LIGAND_RECEPTOR_INTERACTION	181	0.328012	0.969148	0.49395972	0.9435023	1	2405 tags=13%, list=9%, signal=15%
KEGG_HUNTINGTONS_DISEASE	151	0.340599	0.967813	0.52136755	0.94318163	1	5910 tags=29%, list=23%, signal=38%
KEGG_ECM_PATHWAY	24	0.44006	0.965659	0.49834436	0.9452904	1	4488 tags=25%, list=18%, signal=30%
KEGG_ENDOCYTOSIS	166	0.32825	0.96221	0.52387846	0.95091015	1	2194 tags=10%, list=9%, signal=10%
KEGG_GLYCOSAMINOGLYCAN_METABOLISM	102	0.352034	0.962175	0.5138282	0.9472084	1	1296 tags=9%, list=5%, signal=9%
KEGG_TID_PATHWAY	18	0.454762	0.961406	0.5103448	0.9455111	1	1146 tags=11%, list=4%, signal=12%
KEGG_KINESINS	23	0.435081	0.960266	0.5	0.94502604	1	1697 tags=13%, list=7%, signal=14%
KEGG_APOPTOSIS	141	0.337335	0.958305	0.53781515	0.94667584	1	5068 tags=20%, list=20%, signal=25%
KEGG_GENERIC_TRANSCRIPTION_PATHWAY	323	0.310894	0.95458	0.5613809	0.953517	1	5127 tags=22%, list=20%, signal=28%
KEGG_GALACTOSE_METABOLISM	22	0.444307	0.922272	0.48861647	0.955984	1	3026 tags=16%, list=12%, signal=21%
KEGG_DNA_REPAIR	103	0.383417	0.932014	0.57294766	0.9589869	1	6105 tags=26%, list=24%, signal=31%
KEGG_MET_PATHWAY	37	0.402348	0.950428	0.5190972	0.9534686	1	4943 tags=27%, list=19%, signal=34%
KEGG_MRNA_3_END_PROCESSING	33	0.407936	0.94884	0.5281457	0.954141	1	6491 tags=30%, list=25%, signal=41%
KEGG_GABA_B_RECEPTOR_ACTIVATION	35	0.406812	0.94576	0.5472637	0.95902675	1	458 tags=9%, list=2%, signal=9%
KEGG_TRANS_GOLGI_NETWORK_VESICLE_BUDDING	57	0.368225	0.944629	0.53051645	0.95847267	1	6181 tags=30%, list=24%, signal=39%
KEGG_ACTIVATION_OF_NF_KAPPAB_IN_B_CELLS	61	0.367968	0.943634	0.55007946	0.95736504	1	6059 tags=33%, list=24%, signal=43%
KEGG_HEPARAN_SULFATE_HEPARIN_HS_GAG_METABOLISM	48	0.386106	0.943418	0.5378549	0.9542804	1	3308 tags=17%, list=13%, signal=19%
KEGG_GLUCCOSE_METABOLISM	61	0.366172	0.942956	0.5504732	0.95180583	1	5231 tags=26%, list=21%, signal=33%
KEGG_LEUKOCYTE_TRANSENDOTHELIAL_MIGRATION	111	0.338788	0.941693	0.52949643	0.9517764	1	1927 tags=8%, list=8%, signal=9%
KEGG_FORMATION_OF_TUBULIN_FOLDING_INTERMEDIATES_BY_CCT_TRIC	20	0.473371	0.94157	0.5253378	0.94488484	1	5216 tags=40%, list=20%, signal=50%
KEGG_SIGNALING_BY_FGFR	100	0.346699	0.935948	0.5431366	0.96144003	1	1943 tags=8%, list=6%, signal=9%
KEGG_FRSL_MEDIATED_CASCADE	30	0.405340	0.931791	0.5519591	0.96775407	1	1943 tags=8%, list=6%, signal=9%
KEGG_DEVELOPMENTAL_BIOLOGY	351	0.299815	0.931634	0.6528436	0.9645708	1	2286 tags=10%, list=9%, signal=10%
KEGG_PROCESSING_OF_CAPPED_INTRONLESS_PRE_MRNA	23	0.411626	0.928894	0.5457627	0.9683162	1	3814 tags=26%, list=15%, signal=31%
KEGG_FORMATION_OF_TRANSCRIPTION_COUPLED_NER_TC_NER_REPAIR_COMPLEX	29	0.404948	0.928306	0.56435645	0.9662625	1	3876 tags=24%, list=15%, signal=28%
KEGG_TRANSLATION	170	0.318631	0.927793	0.5813953	0.964087	1	2012 tags=9%, list=8%, signal=10%
KEGG_NON_SMALL_CELL_LUNG_CANCER	54	0.362061	0.927255	0.5629984	0.9619992	1	1993 tags=15%, list=8%, signal=16%
KEGG_HEMATOPOIETIC_CELL_LINEAGE	65	0.353527	0.926227	0.5602504	0.9611508	1	3317 tags=23%, list=13%, signal=26%
KEGG_NEUROTRANSMITTER_RECEPTOR_BINDING_AND_DOWNSTREAM_TRANSMISSION_IN_THE_P	120	0.327145	0.92525	0.5872781	0.9601035	1	4894 tags=27%, list=19%, signal=33%
KEGG_OSTSYNAPTIC_CELL	124	0.324293	0.924517	0.5905849	0.9585844	1	4167 tags=19%, list=16%, signal=22%
KEGG_INFLUENZA_VIRAL_RNA_TRANSCRIPTION_AND_REPLICATION	103	0.383426	0.923014	0.57294766	0.9589869	1	2913 tags=13%, list=11%, signal=15%
KEGG_PL_C_BETA_MEDIATED_EVENTS	36	0.390879	0.923345	0.54545456	0.95721847	1	3756 tags=22%, list=15%, signal=28%
KEGG_FLMP_PATHWAY	24	0.422422	0.921434	0.55126053	0.9580874	1	4894 tags=25%, list=19%, signal=31%
KEGG_GLUCAAGON_TYPE_LIGAND_RECEPTORS	53	0.365426	0.917878	0.5771605	0.96197516	1	2999 tags=19%, list=12%, signal=21%
KEGG_COLLAGEN_FORMATION	204	0.308082	0.917777	0.6464516	0.9588161	1	3130 tags=14%, list=12%, signal=16%
KEGG_SL_C_MEDIATED_TRANSMEMBRANE_TRANSPORT	78	0.346136	0.917552	0.58651024	0.9589898	1	7832 tags=38%, list=31%, signal=55%
KEGG_MITOTIC_PROMETAPHASE	17	0.427161	0.914478	0.57699114	0.9571742	1	560 tags=12%, list=2%, signal=12%
KEGG_N_GLYCAN_ANTENNAE_ELONGATION_IN_THE_MEDIAL_TRANS_GOLGI	18	0.427161	0.914478	0.57699114	0.9571742	1	3133 tags=22%, list=12%, signal=25%
KEGG_SIGNALING_BY_FGFR_IN_DISEASE	114	0.324995	0.91253	0.62608695	0.9589143	1	4345 tags=17%, list=17%, signal=20%
KEGG_ACTIVATION_OF_KAINATE_RECEPTORS_UPON GLUTAMATE_BINDING	29	0.39865	0.908796	0.58132046	0.9649857	1	3010 tags=17%, list=12%, signal=20%
KEGG_METABOLISM_OF_CARBOHYDRATES	215	0.300002	0.903488	0.6744186	0.97487676	1	5758 tags=24%, list=23%, signal=30%
KEGG_ECRF_DOWNREGULATION	25	0.407342	0.901781	0.5721562	0.97594385	1	4032 tags=26%, list=20%, signal=31%
KEGG_CLEAVAGE_OF_GROWING_TRANSCRIPT_IN_THE_TERMINATION_REGION	42	0.369531	0.898961	0.59587955	0.97953606	1	5067 tags=24%, list=20%, signal=30%
KEGG_NKCELLS_PATHWAY	18	0.422056	0.898936	0.6016667	0.9762099	1	3223 tags=17%, list=13%, signal=19%
KEGG_CREB_PATHWAY	26	0.400396	0.897263	0.58949095	0.97718066	1	4756 tags=27%, list=19%, signal=33%
KEGG_MCALPAIN_PATHWAY	23	0.405298	0.89666	0.6044143	0.9747981	1	129 tags=4%, list=1%, signal=4%
KEGG_AMI_PATHWAY	17	0.427062	0.892331	0.57829183	0.98305625	1	6876 tags=53%, list=27%, signal=72%
KEGG_CREB_PHOSPHORYLATION_THROUGH_THE_ACTIVATION_OF_CAMKII	15	0.442303	0.891693	0.603321	0.9812917	1	3001 tags=20%, list=12%, signal=23%
KEGG_MELANOMA	64	0.347552	0.890275	0.6053812	0.9814557	1	1943 tags=13%, list=8%, signal=13%
KEGG_DOWNSTREAM_SIGNALING_OF_ACTIVATED_FGFR	88	0.330166	0.889066	0.63274336	0.9818006	1	1943 tags=8%, list=8%, signal=9%
KEGG_PATHWAYS_IN_CANCER	304	0.289375	0.888547	0.72073174	0.97910595	1	2481 tags=11%, list=10%, signal=12%
KEGG_HIV_LIFE_CYCLE	107	0.315885	0.887848	0.6589858	0.9773575	1	5397 tags=22%, list=21%, signal=28%
KEGG_APC_CDC20_MEDIATED_DEGRADATION_OF_NEK2A	22	0.406319	0.885405	0.6207483	0.9801927	1	4032 tags=26%, list=20%, signal=31%
KEGG_LATE_PHASE_OF_HIV_LIFE_CYCLE	94	0.325089	0.885023	0.66312593	0.9780901	1	5810 tags=24%, list=23%, signal=32%
KEGG_PDGF_PATHWAY	32	0.374941	0.882989	0.61833334	0.979926	1	4756 tags=22%, list=19%, signal=27%
KEGG_IGF1R_PATHWAY	22	0.396924	0.881202	0.6260575	0.98102975	1	4756 tags=27%, list=19%, signal=33%
KEGG_NO1_PATHWAY	28	0.391823	0.879905	0.6258741	0.98099935	1	4571 tags=21%, list=18%, signal=26%
KEGG_PURINE_METABOLISM	142	0.309216	0.879048	0.7053942	0.9797346	1	4169 tags=22%, list=16%, signal=26%
KEGG_FCER1_PATHWAY	36	0.371332	0.877034	0.64786327	0.981215	1	4756 tags=25%, list=19%, signal=31%
KEGG_GRB2_SOS_PROVIDES_LINKAGE_TO_MAPK_SIGNALING_FOR_INTERGRINS	15	0.438555	0.876101	0.6360544	0.9802957	1	6876 tags=60%, list=27%, signal=82%
KEGG_ALPHA_S_SIGNALING_EVENTS	82	0.329827	0.873133	0.6519757	0.9842461	1	1769 tags=11%, list=7%, signal=12%
KEGG_MHC_CLASS_II_ANTIGEN_PRESENTATION	77	0.32529	0.871913	0.675841	0.98400563	1	5346 tags=27%, list=21%, signal=34%
KEGG_PROSTACYCLIN_SIGNALING_THROUGH_PROSTACYCLIN_RECEPTOR	15	0.41237	0.871188	0.61565834	0.98262325	1	4894 tags=28%, list=19%, signal=34%
KEGG_MRNA_PROCESSING	151	0.300296	0.869791	0.7251521	0.9825969	1	7887 tags=35%, list=31%, signal=41%
KEGG_P130CAS_LINKAGE_TO_MAPK_SIGNALING_FOR_INTEGRINS	15	0.435331	0.869013	0.63783316	0.98127246	1	3948 tags=35%, list=31%, signal=39%
KEGG_PROSTATE_CANCER	84	0.324747	0.868399	0.6473827	0.97958845	1	1993 tags=13%, list=8%, signal=14%
KEGG_GPCR_DOWNSTREAM_SIGNALING	357	0.281552	0.86709	0.796319	0.97947335	1	2405 tags=10%, list=9%, signal=11%
KEGG_POST_NMDA_RECEPTOR_ACTIVATION_EVENTS	32	0.36967	0.862071	0.6247934	0.9881526	1	3972 tags=19%, list=16%, signal=22%
KEGG_RENAL_CELL_CARCINOMA	66	0.329005	0.861862	0.67771083	0.9854452	1	3223 tags=14%, list=13%, signal=16%
KEGG_HS_GAG_DEGRADATION	19	0.403421	0.858129	0.65180105	0.9911212	1	1034 tags=11%, list=4%, signal=11%
KEGG_SIGNALING_BY_NGF	206	0.288705	0.857243	0.7720685	0.99005795	1	4260 tags=15%, list=17%, signal=18%
KEGG_CASPASE_PATHWAY	23	0.387227	0.855904	0.67657346	0.9902075	1	3730 tags=17%, list=15%, signal=20%
KEGG_APC_C_CDC20_MEDIATED_DEGRADATION_OF_CYCLIN_B	20	0.394777	0.855312	0.6403509	0.9885222	1	410 tags=5%, list=2%, signal=5%
KEGG_G_PROTEIN_ACTIVATION	23	0.390369	0.85446	0.6565567	0.9873108	1	4937 tags=26%, list=19%, signal=32%
KEGG_PROGESTERONE_MEDIATED_OOCYTE_MATURATION	80	0.316155	0.851483	0.6927247	0.99134755	1	3326 tags=30%, list=25%, signal=40%
KEGG_INWARDLY_RECTIFYING_K_CHANNELS	29	0.36805	0.849027	0.6491525	0.9939637	1	1857 tags=14%, list=7%, signal=15%
KEGG_SRP_DEPENDENT_COTRANSLATIONAL_PROTEIN_TARGETING_TO_MEMBRANE	131	0.293028	0.845885	0.74110955	0.99817467	1	1959 tags=9%, list=8%, signal=10%
KEGG_FORMATION_OF_FIBRIN_CLOT_CLOTTING_CASCADE	20	0.397045	0.844449	0.6579407	0.9983575	1	3193 tags=25%, list=13%, signal=29%
KEGG_SIGNALING_BY_CONSTITUTIVELY_ACTIVE_EGFR	18	0.399531	0.843605	0.65591395	0.99716955	1	1927 tags=17%, list=8%, signal=18%
KEGG_PENTOSE_PHOSPHATE_PATHWAY	23	0.381611	0.842917	0.6627517	0.99577045	1	7082 tags=39%, list=28%, signal=54%
KEGG_INHIBITION_OF_VOLTAGE_GATED_CA2_CHANNELS_VIA_GBETA_GAMMA_SUBUNITS	23	0.380348	0.842746	0.66435987	0.99304473	1	458 tags=9%, list=2%, signal=9%
KEGG_RNA_POL_III_AND_MITOCHONDRIAL_TRANSCRIPTION	111	0.307818	0.842743	0.7573099	0.9899986	1	6099 tags=31%, list=24%, signal=40%
KEGG_DAG_AND_IP3_SIGNALING	28	0.364748	0.842039	0.6730769	0.98853767	1	125 tags=4%, list=0%, signal=4%
KEGG_ETHER_LIPID_METABOLISM	23	0.384826	0.84185	0.6730769	0.98859905	1	3608 tags=22%, list=14%, signal=25%
KEGG_ADP_SIGNALING_THROUGH_P2RY12	19	0.392729	0.84112	0.67911714	0.98438364	1	4894 tags=26%, list=21%, signal=33%
KEGG_L1CAM_INTERACTIONS	81	0.3127	0.840488	0.73417723	0.9830355	1	3595 tags=16%, list=14%, signal=19%
KEGG_NFKB_PATHWAY	23	0.386471	0.840144	0.68456376	0.9809637	1	67 tags=4%, list=0%, signal=4%
KEGG_DEADENYLATION_DEPENDENT_MRNA_DECAY	42	0.349118	0.839235	0.696875	0.9799033	1	4401 tags=17%, list=17%, signal=20%
KEGG_PREFOLDIN_MEDIATED_TRANSFER_OF_SUBSTRATE_TO_CCT_TRIC	26	0.375507	0.839232	0.6464471	0.9769777	1	5216 tags=31%, list=20%, signal=39%
KEGG_TOR_PATHWAY	43	0.336042	0.837426	0.6970684	0.9781385	1	4756 tags=23%, list=19%, signal=29%
KEGG_IL_RECEPTOR_SHC_SIGNALING	23	0.382502	0.837248	0.68576103	0.9756342	1	2431 tags=22%, list=10%, signal=24%
KEGG_METABOLISM_OF_MRNA	230	0.274984	0.836629	0.848745	0.97407556	1	7295 tags=29%, list=29%, signal=40%
KEGG_GLYCEROPHOSPHOLIPID_METABOLISM	64	0.326126	0.835972	0.71791047	0.9726612	1	4086 tags=20%, list=16%, signal=24%
KEGG_LIPOPROTEIN_METABOLISM	20	0.377266	0.83416	0.6828859	0.97379166	1	216 tags=4%, list=1%, signal=4%
KEGG_SYNTHESIS_SECRETION_AND_INACTIVATION_OF_GLP1	15	0.418548	0.834134	0.67591475	0.9709644	1	3010 tags=20%, list=12%, signal=23%
KEGG_HS_GAG_BIOSYNTHESIS	28	0.368518	0.831279	0.68770766	0.974		

REACTOME_GLYCOLYSIS	25	0.371162	0.814231	0.7111486	0.98997134	1	
KEGG_ALANINE_ASPARTATE_AND_GLUTAMATE_METABOLISM	30	0.346175	0.813167	0.7419355	0.98930585	1	4678 tags=28%, list=18%, signal=34%
KEGG_DILATED_CARDIOMYOPATHY	78	0.306368	0.806922	0.7848485	0.99923086	1	4649 tags=23%, list=18%, signal=28%
REACTOME_METABOLISM_OF_PROTEINS	430	0.253995	0.805984	0.93787336	0.9982001	1	3317 tags=15%, list=13%, signal=18%
KEGG_HYPERTROPHIC_CARDIOMYOPATHY_HCM	74	0.304273	0.805763	0.7807898	0.9953392	1	2244 tags=8%, list=9%, signal=9%
REACTOME_PHOSPHOLIPID_METABOLISM	176	0.275162	0.8049	0.8630319	0.9948158	1	3317 tags=15%, list=13%, signal=17%
REACTOME_INFLUENZA_LIFE_CYCLE	157	0.279685	0.803935	0.86052996	0.9938954	1	3906 tags=10%, list=15%, signal=33%
KEGG_FC_EPSILON_RI_SIGNALING_PATHWAY	66	0.308368	0.803192	0.7776097	0.992433	1	4167 tags=16%, list=16%, signal=19%
BIOCARTA_RARRXR_PATHWAY	15	0.389477	0.802852	0.68705034	0.9903209	1	4756 tags=26%, list=19%, signal=32%
BIOCARTA_CK1_PATHWAY	16	0.391346	0.801747	0.7101695	0.9896448	1	2579 tags=13%, list=10%, signal=15%
REACTOME_3_UTR_MEDIATED_TRANSLATIONAL_REGULATION	129	0.279422	0.797922	0.86609685	0.9946702	1	6447 tags=44%, list=25%, signal=59%
REACTOME_TRANSMEMBRANE_TRANSPORT_OF_SMALL_MOLECULES	350	0.256757	0.796416	0.9357231	0.9946787	1	4416 tags=16%, list=17%, signal=20%
REACTOME_GLUCCONEOGENESIS	30	0.346007	0.796333	0.7629382	0.99209505	1	4894 tags=20%, list=19%, signal=24%
REACTOME_ACTIVATED_NOTCH1_TRANSMITS_SIGNAL_TO_THE_NUCLEUS	26	0.349594	0.795941	0.7385965	0.9900732	1	4629 tags=30%, list=18%, signal=37%
REACTOME_ADP_SIGNALLING_THROUGH_P2RY1	24	0.380591	0.794235	0.74176776	0.9904164	1	4032 tags=23%, list=16%, signal=27%
REACTOME_NRF_SIGNALS_CELL_DEATH_FROM_THE_NUCLEUS	15	0.391797	0.793951	0.7241379	0.98826975	1	5467 tags=29%, list=21%, signal=37%
REACTOME_TRAFFICKING_OF_AMPA_RECEPTORS	25	0.353815	0.791745	0.72183098	0.9897952	1	410 tags=7%, list=2%, signal=7%
REACTOME_INNATE_IMMUNE_SYSTEM	199	0.262118	0.79169	0.90247077	0.9871895	1	4756 tags=24%, list=18%, signal=29%
REACTOME_PLATELET_ACTIVATION_SIGNALING_AND_AGGREGATION	183	0.27065	0.790907	0.8738502	0.9860624	1	4406 tags=14%, list=17%, signal=16%
REACTOME_TRANSCRIPTIONAL_REGULATION_OF_WHITE_ADIPOCYTE_DIFFERENTIATION	68	0.305295	0.786203	0.82182986	0.99220073	1	4756 tags=20%, list=19%, signal=24%
KEGG_CARDIAC_MUSCLE_CONTRACTION	59	0.305706	0.785053	0.82115084	0.99987906	1	6228 tags=32%, list=24%, signal=43%
REACTOME_METABOLISM_OF_RNA	274	0.256283	0.778546	0.94382024	1	1	6845 tags=31%, list=27%, signal=42%
KEGG_CHEMOKINE_SIGNALING_PATHWAY	155	0.26771	0.772236	0.8931909	1	1	7295 tags=29%, list=29%, signal=40%
REACTOME_GLYCEROPHOSPHOLIPID_BIOSYNTHESIS	74	0.296212	0.7718	0.83557546	1	1	3031 tags=12%, list=12%, signal=13%
KEGG_TIGHT_JUNCTION	117	0.274345	0.769347	0.8861314	1	1	4837 tags=22%, list=19%, signal=27%
REACTOME_SIGNALING_BY_FGFR1_FUSION_MUTANTS	18	0.367146	0.768394	0.76842105	1	1	1677 tags=5%, list=7%, signal=5%
REACTOME_CD28_CO_STIMULATION	30	0.337009	0.768171	0.7723577	1	1	7003 tags=44%, list=27%, signal=61%
REACTOME_PEPTIDE_CHAIN_ELONGATION	108	0.276174	0.767283	0.9101449	1	1	4756 tags=30%, list=15%, signal=33%
KEGG_TOLL_LIKE_RECEPTOR_SIGNALING_PATHWAY	85	0.284372	0.766152	0.8539493	1	1	1959 tags=9%, list=8%, signal=10%
REACTOME_ACTIVATION_OF_NMDA_RECEPTOR_UPON_GLUTAMATE_BINDING_AND_POSTSYNAPTIC_EVNTS	36	0.319211	0.76369	0.7971474	1	1	3972 tags=19%, list=16%, signal=23%
BIOCARTA_ACTIN_PATHWAY	20	0.354388	0.75125	0.79136693	1	1	1985 tags=10%, list=8%, signal=11%
KEGG_VASOPRESSIN_REGULATED_WATER_REABSORPTION	41	0.306725	0.746935	0.8398744	1	1	6131 tags=29%, list=24%, signal=38%
REACTOME_G1_PHASE	36	0.316415	0.746304	0.8424437	1	1	1444 tags=11%, list=6%, signal=12%
REACTOME_ACTIVATION_OF_ATR_IN_RESPONSE_TO_REPLICATION_STRESS	35	0.312086	0.744976	0.8338558	1	1	7671 tags=37%, list=30%, signal=53%
KEGG_BIOSYNTHESIS_OF_UNSATURATED_FATTY_ACIDS	20	0.345718	0.741844	0.81157072	1	1	2554 tags=20%, list=10%, signal=22%
REACTOME_DNA_STRAND_ELONGATION	30	0.321354	0.741428	0.81692004	1	1	4536 tags=27%, list=18%, signal=32%
REACTOME_NEGATIVE_REGULATORS_OF_RIG_I_MDA5_SIGNALING	31	0.321179	0.738558	0.8374793	1	1	4032 tags=16%, list=15%, signal=19%
REACTOME_PPARG_ACTIVATES_GENE_EXPRESSION	98	0.270821	0.736611	0.92539454	1	1	4726 tags=20%, list=19%, signal=25%
REACTOME_ENERGY_DEPENDENT_REGULATION_OF_MTOR_BY_LKB1_AMPK	17	0.352533	0.736191	0.8077634	1	1	4996 tags=24%, list=20%, signal=29%
REACTOME_UNBLOCKING_OF_NMDA_RECEPTOR_GLUTAMATE_BINDING_AND_ACTIVATION	15	0.366194	0.732353	0.81395346	1	1	3396 tags=27%, list=13%, signal=31%
REACTOME_INTEGRATION_OF_ENERGY_METABOLISM	104	0.263309	0.727346	0.9388972	1	1	3156 tags=13%, list=12%, signal=14%
REACTOME_MYD88_MAL_CASCADE_INITIATED_ON_PLASMA_MEMBRANE	81	0.274715	0.727344	0.89522344	1	1	4312 tags=15%, list=17%, signal=18%
KEGG_LONG_TERM_POTENTIATION	65	0.281273	0.723506	0.8773006	1	1	3811 tags=18%, list=15%, signal=22%
REACTOME_GLUCCAGON_SIGNALING_IN_METABOLIC_REGULATION	29	0.313815	0.722691	0.8241206	1	1	5544 tags=24%, list=22%, signal=31%
BIOCARTA_MPR_PATHWAY	33	0.305272	0.720274	0.8474026	1	1	4010 tags=15%, list=16%, signal=18%
REACTOME_NONSENSE_MEDIATED_DECAY_ENHANCED_BY_THE_EXON_JUNCTION_COMPLEX	129	0.258674	0.720192	0.94017094	1	1	4416 tags=16%, list=17%, signal=19%
REACTOME_TRANSCRIPTION_COUPLED_NER_TC_NER	44	0.294971	0.717555	0.8756278	1	1	4361 tags=18%, list=17%, signal=22%
REACTOME_NEF_MEDIATES_DOWN_MODULATION_OF_CELL_SURFACE_RECEPTORS_BY_RECRUITING_THEM_TO_CLATHRIN_ADAPTERS	18	0.339436	0.716812	0.8344827	1	1	3014 tags=11%, list=12%, signal=13%
KEGG_GAP_JUNCTION	82	0.266389	0.715417	0.93777776	1	1	5216 tags=24%, list=20%, signal=31%
REACTOME_SYNTHESIS_AND_INTERCONVERSION_OF_NUCLEOTIDE_DI_AND_TRIPHOSPHATES	17	0.343497	0.714292	0.8298611	1	1	7076 tags=47%, list=28%, signal=65%
KEGG_DNA_REPLICATION	36	0.300549	0.712964	0.87081337	1	1	5721 tags=25%, list=22%, signal=32%
REACTOME_AQUAPORIN_MEDIATED_TRANSPORT	43	0.295014	0.712322	0.8923328	1	1	5544 tags=23%, list=22%, signal=30%
REACTOME_G2_M_CHECKPOINTS	41	0.295785	0.711594	0.8901099	1	1	5860 tags=27%, list=23%, signal=35%
BIOCARTA_INTRINSIC_PATHWAY	18	0.33992	0.709666	0.8612521	1	1	3193 tags=28%, list=19%, signal=32%
BIOCARTA_INTEGRIN_PATHWAY	38	0.294555	0.709244	0.89621085	1	1	4943 tags=24%, list=13%, signal=29%
REACTOME_INHIBITION_OF_INSULIN_SECRETION_BY_ADRENALINE_NORADRENALINE	24	0.317919	0.709056	0.8545781	1	1	5120 tags=25%, list=20%, signal=31%
REACTOME_NUCLEOTIDE_BINDING_DOMAIN_LEUCINE_RICH_REPEAT_CONTAINING_RECEPTOR_NLR_SIGNALLING_PATHWAYS	44	0.285039	0.703516	0.9018692	1	1	3837 tags=16%, list=15%, signal=19%
KEGG_FATTY_ACID_METABOLISM	37	0.29585	0.703329	0.8659794	1	1	3976 tags=16%, list=16%, signal=19%
KEGG_ADIPOCYTOKINE_SIGNALING_PATHWAY	60	0.272976	0.703197	0.9178515	1	1	1682 tags=7%, list=7%, signal=7%
BIOCARTA_NOS1_PATHWAY	20	0.320737	0.702329	0.8583916	1	1	4010 tags=20%, list=16%, signal=24%
REACTOME_RNA_POL_III_CHAIN_ELONGATION	17	0.325353	0.697004	0.85561496	1	1	5620 tags=41%, list=22%, signal=53%
REACTOME_NFKB_AND_MAP_KINASES_ACTIVATION_MEDIATED_BY_TLR4_SIGNALING_REPERTOIRE	71	0.268627	0.696846	0.9411765	1	1	4312 tags=15%, list=17%, signal=19%
REACTOME_TRAFFICKING_OF_GLUR2_CONTAINING_AMPA_RECEPTORS	15	0.333374	0.696731	0.8531952	1	1	4602 tags=33%, list=18%, signal=41%
KEGG_CELL_CYCLE	123	0.248222	0.696488	0.97179127	1	1	6377 tags=28%, list=25%, signal=38%
REACTOME_G_ALPHA1213_SIGNALING_EVENTS	72	0.262559	0.696485	0.9425626	1	1	3239 tags=14%, list=13%, signal=16%
REACTOME_RNA_POL_III_TRANSCRIPTION_INITIATION_AMP_TYPE_3_PROMOTER	26	0.307167	0.692975	0.87261146	1	1	4696 tags=31%, list=18%, signal=38%
REACTOME_BASE_EXCISION_REPAIR	19	0.320773	0.692611	0.8544096	1	1	590 tags=5%, list=2%, signal=5%
REACTOME_LATENT_INFECTON_OF_HOMO_SAPIENS_WITH_MYCOBACTERIUM_TUBERCULOSIS	29	0.300828	0.691318	0.88566554	1	1	4014 tags=24%, list=16%, signal=25%
REACTOME_REGULATION_OF_INSULIN_SECRETION	79	0.25598	0.689401	0.9482014	1	1	3031 tags=11%, list=12%, signal=13%
REACTOME_THROMBOXANE_SIGNALING_THROUGH_TP_RECEPTOR	22	0.31396	0.688438	0.8836425	1	1	4894 tags=27%, list=19%, signal=34%
REACTOME_NUCLEOTIDE_EXCISION_REPAIR	49	0.277517	0.684542	0.9220986	1	1	4361 tags=16%, list=17%, signal=20%
KEGG_PROANOATE_METABOLISM	32	0.300051	0.682703	0.9086116	1	1	3497 tags=19%, list=14%, signal=22%
REACTOME_RESOLUTION_OF_AP_SITES_VIA_THE_MULTIPLE_NUCLEOTIDE_PATCH_REPLACEMENT_PATHWAY	17	0.331592	0.682479	0.86013985	1	1	590 tags=6%, list=2%, signal=6%
REACTOME_NOTCH1_INTRACELLULAR_DOMAIN_REGULATES_TRANSCRIPTION	45	0.281861	0.680661	0.9241706	1	1	5082 tags=22%, list=20%, signal=28%
REACTOME_THROMBIN_SIGNALING_THROUGH_PROTEINASE_ACTIVATED_RECEPTORS_PARS	30	0.291909	0.679698	0.9070946	1	1	4894 tags=23%, list=19%, signal=29%
REACTOME_LIPID_DIGESTION_MOBILIZATION_AND_TRANSPORT	35	0.282035	0.679328	0.91515892	1	1	216 tags=3%, list=1%, signal=3%
KEGG_LONG_TERM_DEPRESSION	59	0.268249	0.675805	0.9555921	1	1	3659 tags=19%, list=14%, signal=22%
REACTOME_NGF_SIGNALING_VIA_TRKA_FROM_THE_PLASMA_MEMBRANE	129	0.238959	0.674494	0.9869754	1	1	4260 tags=33%, list=17%, signal=19%
REACTOME_LOSS_OF_NLP_FROM_MITOTIC_CENTROSOMES	56	0.266325	0.671147	0.9344512	1	1	7430 tags=39%, list=29%, signal=55%
BIOCARTA_FAS_PATHWAY	29	0.287691	0.663761	0.9095652	1	1	586 tags=3%, list=2%, signal=4%
KEGG_VASCULAR_SMOOTH_MUSCLE_CONTRACTION	97	0.241399	0.662976	0.9851852	1	1	3811 tags=16%, list=15%, signal=19%
REACTOME_PROTEIN_FOLDING	50	0.26514	0.662704	0.95961225	1	1	5216 tags=26%, list=20%, signal=33%
KEGG_BASE_EXCISION_REPAIR	34	0.282527	0.662322	0.9325658	0.99992186	1	5611 tags=26%, list=26%, signal=34%
REACTOME_MITOTIC_G2_M_PHASES	78	0.244171	0.658318	0.98121387	1	1	6544 tags=31%, list=26%, signal=41%
REACTOME_RECRUITMENT_OF_MITOTIC_CENTROSOME_PROTEINS_AND_COMPLEXES	63	0.248583	0.648792	0.9727273	1	1	7430 tags=38%, list=29%, signal=54%
KEGG_ONE_CARBON_POOL_BY_FOLATE	17	0.312031	0.647882	0.899115	1	1	3780 tags=18%, list=15%, signal=21%
BIOCARTA_TNFR2_PATHWAY	17	0.300952	0.64111	0.9029982	1	1	2489 tags=12%, list=10%, signal=13%
REACTOME_CTNB1_PHOSPHORYLATION_CASCADE	15	0.314239	0.638467	0.90017515	1	1	6447 tags=33%, list=25%, signal=45%
KEGG_BETA_ALANINE_METABOLISM	20	0.295497	0.637264	0.9255499	1	1	4089 tags=20%, list=16%, signal=24%
REACTOME_REGULATION_OF_WATER_BALANCE_BY_RENAL_AQUAPORINS	38	0.264926	0.637239	0.93771046	1	1	5544 tags=24%, list=22%, signal=30%
BIOCARTA_GPCR_PATHWAY	33	0.276447	0.636476	0.93791944	1	1	4010 tags=18%, list=16%, signal=22%
REACTOME_MYOGENESIS	22	0.289066	0.631216	0.92691624	1	1	5380 tags=23%, list=21%, signal=29%
REACTOME_SIGNALING_BY_NOTCH1	68	0.237348	0.621752	0.9782271	1	1	4334 tags=18%, list=17%, signal=21%
REACTOME_CTLA4_INHIBITORY_SIGNALING	19	0.291152	0.620857	0.9201331	1	1	6447 tags=32%, list=25%, signal=42%
REACTOME_DOWNSTREAM_SIGNALING_EVENTS_OF_B_CELL_RECEPTOR_BCR	92	0.230357	0.619251	0.9884058	1	1	6059 tags=26%, list=24%, signal=34%
KEGG_TYROSINE_METABOLISM	37	0.295039	0.613437	0.9736842	1	1	4850 tags=30%, list=19%, signal=37%
REACTOME_SIGNAL_AMPLIFICATION	29	0.28354	0.607643	0.9378151	1	1	5467 tags=24%, list=21%, signal=31%
BIOCARTA_PSHYPOXIA_PATHWAY	22	0.274569	0.598838	0.94954956	1	1	4465 tags=23%, list=17%, signal=28%
BIOCARTA_IL2_PATHWAY	21	0.266801	0.572123	0.9052573	1	1	4756 tags=19%, list=19%, signal=23%
REACTOME_SEMA4D_INDUCED_CELL_MIGRATION_AND_GROWTH_CONE_COLLAPSE	25	0.255286	0.566477	0.96940416	1	1	1993 tags=8%, list=8%, signal=8%
REACTOME_CYCLIN_A_B1_ASSOCIATED_EVENTS_DURING_G2_M_TRANSITION	15	0.276371	0.562698	0.9422383	1	1	5695 tags=33%, list=22%, signal=43%
REACTOME_TRANSPORT_OF_MATURE_TRANSCRIPT_TO_CYTOPLASM	51	0.218359	0.546356	0.9953344	1	1	7857 tags=33%, list=31%, signal=48%
REACTOME_ACTIVATED_AMPK_STIMULATES_FATTY_ACID_OXIDATION_IN_MUSCLE	18	0.253547	0.534824	0.9770723	1	1	892 tags=6%, list=3%, signal=6%
REACTOME_METABOLISM_OF_VITAMINS_AND_COFACTORS	51	0.213589	0.53472	0.9921875	1	1	3830 tags=12%, list=15%, signal=14%
KEGG_BASAL_TRANSCRIPTION_FACTORS	33	0.230495	0.531035	0.992	1	1	5792 tags=18%, list=23%, signal=23%
REACTOME_A_TETRASACCHARIDE_LINKER_SEQUENCE_IS_REQUIRED_FOR_GAG_SYNTHESIS	25	0.238686	0.524326	0.99319726	1	1	6709 tags=36%, list=26%, signal=49%
KEGG_LYSOSOME	118	0.183579	0.511115	1	1	1	6416 tags=25%, list=25%, signal=34%
REACTOME_PKA_MEDIATED_PHOSPHORYLATION_OF_CREB	15	0.225	0.506549	0.98761064	1	1	5544 tags=25%, list=22%, signal=34%
BIOCARTA_P38MAPK_PATHWAY	39	0.210427	0.501706	1	1	1	4756 tags=13%, list=15%, signal=16%
BIOCARTA_MITOCHONDRIA_PATHWAY	21	0.234342	0.501085	0.9829642	1	1	3730 tags=14%, list=15%, signal=17%
KEGG_HOMOLOGOUS_RECOMBINATION	26	0.22136	0.498689	0.98694944	1	1	975 tags=4%, list=4%, signal=4%
BIOCARTA_CHREBP2_PATHWAY	30	0.204844	0.494083	0.99517685	1	1	2292 tags=8%, list=9%, signal=8%
REACTOME_SEMA4D_IN_SEMAPHORIN_SIGNALING	30	0.212383	0.490236	0.99169433	0.998529	1	1993 tags=7%, list=8%, signal=7%
KEGG_RNA_DEGRADATION	53	0.190189	0.484336	0.99841267	0.9969448	1	3943 tags=11%, list=15%, signal=13%
REACTOME_SIGNALING_BY_BMP	21	0.211124	0.45915	0.98967296	0.99678284	1	5637 tags=24%, list=22%, signal=31%

**Table S10**  
**GSEA Analysis on HNSC cancer cell lines comparing cell lines with or without 9p21.3 loss (arm or focal),**  
**Pathways Depleted**

NAME	SIZE	ES	NES	NOM p-Value	FDR q-Value	FWER p-Value	RANK AT MAX
SENESCENCE_ASSOCIATED_SECRETORY_PHENOTYPE	51	-0.78458	-2.17592	0	0	0	2818
KEGG_CYTOKINE_CYTOKINE_RECEPTOR_INTERACTION	192	-0.5017	-1.72496	0	0.64153993	0.697	3133
REACTOME_BILE_ACID_AND_BILE_SALT_METABOLISM	23	-0.71864	-1.68964	0.00952381	0.6409758	0.837	565
REACTOME_SIGNALING_BY_HIPPO	20	-0.71361	-1.66068	0.01946472	0.6629962	0.924	1698
REACTOME_CHEMOKINE_RECEPTORS_BIND_CHEMOKINES	35	-0.64063	-1.64026	0.007692308	0.6528666	0.96	1387
KEGG_GLYCOSPHINGOLIPID_BIOSYNTHESIS_GANGLIO_SERIES	15	-0.74765	-1.63676	0.027542373	0.5652866	0.963	2650
REACTOME_DEGRADATION_OF_THE_EXTRACELLULAR_MATRIX	26	-0.66388	-1.62693	0.018518519	0.53538847	0.974	3465
BIOCARTA_NTHI_PATHWAY	23	-0.68215	-1.6259	0.02173913	0.4731624	0.973	374
KEGG_PANTOTHENATE_AND_COA_BIOSYNTHESIS	15	-0.73479	-1.5942	0.027713627	0.5736192	0.999	2248
BIOCARTA_IL1R_PATHWAY	33	-0.62444	-1.58528	0.013850415	0.5587936	0.999	3128
BIOCARTA_IL10_PATHWAY	16	-0.69405	-1.56933	0.03640777	0.5820398	1	2803
KEGG_NOD LIKE_RECEPTOR_SIGNALING_PATHWAY	54	-0.5555	-1.5417	0.022160664	0.66784996	1	3213
REACTOME_UNFOLDED_PROTEIN_RESPONSE	76	-0.52139	-1.5358	0.002906977	0.64771	1	3682
REACTOME_ACTIVATION_OF_GENES_BY_ATF4	24	-0.65094	-1.52842	0.039443154	0.6385009	1	1843
REACTOME_IL1_SIGNALING	38	-0.57482	-1.51709	0.026455026	0.652598	1	3213
REACTOME_DESTABILIZATION_OF_MRNA_BY_TRISTETRAPROLIN_TTP	17	-0.69289	-1.51668	0.04090909	0.6142278	1	1843
REACTOME_DIABETES_PATHWAYS	121	-0.47113	-1.50756	0.003401361	0.61802757	1	3682
BIOCARTA_INFLAM_PATHWAY	19	-0.663	-1.50589	0.05263158	0.5900839	1	4562
REACTOME_GLYCOSPHINGOLIPID_METABOLISM	32	-0.57711	-1.49357	0.025943397	0.6133317	1	4028
REACTOME_PERK_REGULATED_GENE_EXPRESSION	27	-0.59888	-1.49041	0.04292929	0.5957531	1	1843
REACTOME_INSULIN_SYNTHESIS_AND_PROCESSING	18	-0.67034	-1.48716	0.05936073	0.5812557	1	3066
REACTOME_CYTOSOLIC_TRNA_AMINOACYLATION	24	-0.60789	-1.46884	0.047281325	0.63391376	1	5586
BIOCARTA_CARDIACEGF_PATHWAY	17	-0.66098	-1.46853	0.064665124	0.6077781	1	2049
KEGG_JAK_STAT_SIGNALING_PATHWAY	119	-0.45683	-1.46711	0.006644518	0.5883832	1	2986
BIOCARTA_CCR5_PATHWAY	16	-0.67326	-1.46374	0.08411215	0.5778716	1	3622
REACTOME_GROWTH_HORMONE_RECEPTOR_SIGNALING	20	-0.62341	-1.459	0.08056872	0.5746095	1	3843
REACTOME_GRB2_EVENTS_IN_ERBB2_SIGNALING	22	-0.62243	-1.45494	0.05140187	0.56986964	1	809
KEGG_STEROID_BIOSYNTHESIS	16	-0.65482	-1.43354	0.07042254	0.63690263	1	2164
REACTOME_SHC1_EVENTS_IN_ERBB4_SIGNALING	20	-0.60637	-1.42405	0.09046455	0.6541453	1	1545
REACTOME_ACTIVATION_OF_BH3_ONLY_PROTEINS	16	-0.61962	-1.41864	0.09134615	0.654754	1	3561
KEGG_CYTOSOLIC_DNA_SENSING_PATHWAY	42	-0.51974	-1.41837	0.038674034	0.63479376	1	383
REACTOME_ANTIGEN_PRESENTATION_FOLDING_ASSEMBLY_AND_PEPTIDE_LOADING_OF_CLASS_I_MHC	15	-0.6509	-1.41791	0.06823529	0.61653024	1	4863
REACTOME_DESTABILIZATION_OF_MRNA_BY_BRF1	17	-0.63866	-1.4121	0.107913665	0.621837	1	1843
REACTOME_SYNTHESIS_OF_BILE_ACIDS_AND_BILE_SALTS	16	-0.63288	-1.40151	0.07981221	0.64661723	1	565
REACTOME_SPHINGOLIPID_METABOLISM	58	-0.4828	-1.35851	0.07012987	0.81679744	1	4028
REACTOME_RAP1_SIGNALING	15	-0.61959	-1.35347	0.11111111	0.817296	1	1669
KEGG_BLADDER_CANCER	40	-0.49848	-1.35323	0.089058526	0.7965036	1	3640
REACTOME_AMINO_ACID_AND_OLIGOPEPTIDE_SLC_TRANSPORTERS	39	-0.51584	-1.34685	0.08478803	0.8051114	1	1078
BIOCARTA_TOB1_PATHWAY	15	-0.61235	-1.34295	0.11648352	0.8027014	1	6134
REACTOME_PRE_NOTCH_PROCESSING_IN_GOLGI	16	-0.60241	-1.3421	0.11111111	0.78618205	1	1457
REACTOME_BOTULINUM_NEUROTOXICITY	18	-0.58246	-1.3413	0.14186047	0.77120435	1	3392
REACTOME_SHC1_EVENTS_IN_EGFR_SIGNALING	15	-0.61863	-1.34109	0.12107623	0.7537293	1	3546
REACTOME_NUCLEAR_SIGNALING_BY_ERBB4	33	-0.52025	-1.33942	0.11764706	0.74291164	1	3100
BIOCARTA_G1_PATHWAY	28	-0.53841	-1.33444	0.10930233	0.7475818	1	3640
REACTOME_SIGNALING_BY_NODAL	15	-0.60018	-1.33109	0.13777778	0.7434885	1	3396
REACTOME_ACTIVATION_OF_CHAPERONE_GENES_BY_XBP1S	44	-0.4947	-1.31581	0.10962567	0.79034215	1	3585
REACTOME_PROTEOLYTIC_CLEAVAGE_OF_SNARE_COMPLEX_PROTEINS	16	-0.60328	-1.31301	0.1485849	0.7859284	1	3392
REACTOME_TRNA_AMINOACYLATION	42	-0.47725	-1.30805	0.08746356	0.78962204	1	7329
BIOCARTA_IGF1MOTOR_PATHWAY	20	-0.55706	-1.30408	0.14868106	0.79016745	1	1084
REACTOME_REGULATION_OF_BETA_CELL_DEVELOPMENT	20	-0.57063	-1.30304	0.12177986	0.7789526	1	101
BIOCARTA_BIOPEPTIDES_PATHWAY	39	-0.48886	-1.29675	0.11851852	0.789896	1	2779
REACTOME_ION_CHANNEL_TRANSPORT	40	-0.48697	-1.29588	0.11358025	0.778584	1	1519
KEGG_ADHERENS_JUNCTION	66	-0.44603	-1.28371	0.07058824	0.8153611	1	2422
BIOCARTA_IL22BP_PATHWAY	15	-0.58041	-1.28025	0.1670429	0.81481624	1	2474
KEGG_SNARE_INTERACTIONS_IN_VESICULAR_TRANSPORT	38	-0.48961	-1.27998	0.12958436	0.8010514	1	4941
BIOCARTA_MTOR_PATHWAY	23	-0.54278	-1.27733	0.15254237	0.7975162	1	10
KEGG_ABC_TRANSPORTERS	41	-0.4855	-1.27342	0.12953368	0.7986073	1	3184
REACTOME_PKB_MEDIATED_EVENTS	28	-0.50921	-1.27294	0.16504854	0.78696555	1	10
BIOCARTA_EIF_PATHWAY	16	-0.58704	-1.27179	0.19310345	0.778332	1	3149
REACTOME_GENERATION_OF_SECOND_MESSENGER_MOLECULES	18	-0.56213	-1.27159	0.1879518	0.7662122	1	5385
REACTOME_AMINE_COMPOUND_SLC_TRANSPORTERS	18	-0.54682	-1.26079	0.18203309	0.7974001	1	2181
KEGG_EPITHELIAL_CELL_SIGNALING_IN_HELICOBACTER_PYLORI_INFECTION	64	-0.42532	-1.25212	0.11171662	0.8188745	1	2779
REACTOME_INTRINSIC_PATHWAY_FOR_APOPTOSIS	29	-0.50293	-1.24816	0.17091836	0.82217526	1	4395
KEGG_VIRAL_MYOCARDITIS	41	-0.45657	-1.2462	0.15206185	0.8175235	1	4395
REACTOME_AMINO_ACID_TRANSPORT_ACROSS_THE_PLASMA_MEMBRANE	26	-0.50453	-1.24021	0.17848411	0.827238	1	996
REACTOME_Glutamate_NEUROTRANSMITTER_RELEASE_CYCLE	15	-0.57283	-1.23644	0.18485524	0.83017355	1	96
REACTOME_FORMATION_OF_INCISION_COMPLEX_IN_GG_NER	21	-0.52866	-1.23625	0.20179372	0.81872016	1	6499
BIOCARTA_AGR_PATHWAY	34	-0.47956	-1.23398	0.19900498	0.81527966	1	1127
KEGG_RIG_I LIKE_RECEPTOR_SIGNALING_PATHWAY	55	-0.43186	-1.22046	0.15789473	0.85688514	1	4953
REACTOME_SHC_MEDIATED_SIGNALING	15	-0.55442	-1.21907	0.2260274	0.85035044	1	3546
BIOCARTA_TEL_PATHWAY	18	-0.54131	-1.21745	0.22931442	0.8444314	1	4376
KEGG_UBIQUITIN_MEDIATED_PROTEOLYSIS	128	-0.37685	-1.21283	0.12014134	0.85079575	1	4109
REACTOME_GASTRIN_CREB_SIGNALING_PATHWAY_VIA_PKC_AND_MAPK	155	-0.36736	-1.20691	0.08802817	0.8638452	1	3777
REACTOME_Glutathione_CONJUGATION	19	-0.53192	-1.20373	0.27051	0.8637716	1	485
REACTOME_COSTIMULATION_BY_THE_CD28_FAMILY	51	-0.43897	-1.20298	0.21276596	0.8550459	1	4688
KEGG_COMPLEMENT_AND_COAGULATION_CASCADES	51	-0.424	-1.19436	0.17816092	0.8777522	1	752
REACTOME_ANTIGEN_ACTIVATES_B_CELL_RECEPTOR_LEADING_TO_GENERATION_OF_SECOND_MESSENGERS	29	-0.47411	-1.19196	0.200489	0.87619543	1	2049
REACTOME_CHOLESTEROL_BIOSYNTHESIS	20	-0.51398	-1.19057	0.25526932	0.87011504	1	5482
BIOCARTA_STATHMIN_PATHWAY	16	-0.54363	-1.18571	0.2665148	0.87849721	1	5405
REACTOME_SMOOTH_MUSCLE_CONTRACTION	23	-0.50655	-1.18159	0.23376623	0.8843391	1	2084
REACTOME_PTM_GAMMA_CARBOXYLATION_HYPUSINE_FORMATION_AND_ARYLSULFATASE_ACTIVATION	21	-0.50317	-1.18044	0.2451923	0.8779067	1	2204
KEGG_ALZHEIMERS_DISEASE	137	-0.3657	-1.17194	0.15309446	0.90151817	1	1282
REACTOME_PEPTIDE_LIGAND_BINDING_RECEPTORS	106	-0.36919	-1.15502	0.17610063	0.9593367	1	1554
REACTOME_CLASS_A1_RHODOPSIN LIKE_RECEPTORS	179	-0.34355	-1.15388	0.14457831	0.9528445	1	1949
REACTOME_TAK1_ACTIVATES_NFKB_BY_PHOSPHORYLATION_AND_ACTIVATION_OF_IKKS_COMPLEX	23	-0.47444	-1.1487	0.27525252	0.9622248	1	4870
REACTOME_PIP3_ACTIVATES_AKT_SIGNALING	27	-0.45835	-1.14853	0.2725061	0.9516227	1	5461
REACTOME_POST_TRANSLATIONAL_MODIFICATION_SYNTHESIS_OF_GPI_ANCHORED_PROTEINS	26	-0.4723	-1.14803	0.27272728	0.94270134	1	2960
REACTOME_SIGNALING_BY_ERBB4	83	-0.37438	-1.14219	0.19402985	0.9550951	1	4870
KEGG_TYPE_I_DIABETES_MELLITUS	17	-0.50106	-1.14111	0.2867647	0.9489478	1	374
KEGG_AMINOACYL_TRNA_BIOSYNTHESIS	41	-0.43631	-1.14099	0.25593668	0.9389376	1	5911
REACTOME_PEROXISOMAL_LIPID_METABOLISM	20	-0.49636	-1.13889	0.30904523	0.9375294	1	3090
REACTOME_ASPARAGINE_N_LINKED_GLYCOSYLATION	79	-0.38014	-1.13332	0.23964497	0.94997895	1	4901
KEGG_RIBOSOME	86	-0.37229	-1.13237	0.23493975	0.94339454	1	2730
BIOCARTA_PML_PATHWAY	16	-0.50987	-1.13196	0.30935252	0.935073	1	5039

REACTOME_NEUROTRANSMITTER_RELEASE_CYCLE	27	-0.45141	-1.12964	0.31026253	0.93379277	1	3468
KEGG_APOPTOSIS	82	-0.3707	-1.12718	0.24362606	0.93340075	1	4870
BIOCARTA_ARAP_PATHWAY	17	-0.50256	-1.12588	0.31381732	0.928381	1	2320
REACTOME_TRAF6_MEDIATED_NFKB_ACTIVATION	21	-0.48862	-1.12468	0.3101737	0.92327595	1	5414
REACTOME_PI3K_EVENTS_IN_ERBB4_SIGNALING	36	-0.42433	-1.12244	0.2543641	0.92342484	1	5034
KEGG_PEROXISOME	75	-0.3751	-1.11664	0.24852072	0.93679214	1	3793
REACTOME_SIGNALING_BY_GPCR	446	-0.30338	-1.11042	0.14569536	0.9510424	1	1949
KEGG_GNRH_SIGNALING_PATHWAY	90	-0.36524	-1.10516	0.26666668	0.9623404	1	3622
KEGG_ERBB_SIGNALING_PATHWAY	85	-0.36778	-1.10411	0.24293785	0.95717233	1	3318
BIOCARTA_RELA_PATHWAY	16	-0.50789	-1.10305	0.31506848	0.9518538	1	4870
REACTOME_BIOSYNTHESIS_OF_THE_N_GLYCAN_PRECURSOR_DOLICHOL_LIPID_LINKED_OLIGOSACCHARI DE_LLO_AND_TRANSFER_TO_A_NASCENT_PROTEIN	28	-0.44149	-1.10142	0.31042653	0.9490436	1	5280
REACTOME_SIGNALING_TO_RAS	27	-0.4637	-1.10075	0.33793104	0.94278616	1	4676
REACTOME_PURINE_METABOLISM	31	-0.43708	-1.09468	0.31782946	0.95706284	1	1953
BIOCARTA_CELLCYCLE_PATHWAY	23	-0.46085	-1.09169	0.33568075	0.9597506	1	4006
REACTOME_GLOBAL_GENOMIC_NER_GG_NER	33	-0.42752	-1.08948	0.32843137	0.95921445	1	6499
REACTOME_PI3K_EVENTS_IN_ERBB2_SIGNALING	42	-0.41481	-1.08707	0.31578946	0.95946663	1	809
KEGG_PPAR_SIGNALING_PATHWAY	59	-0.37115	-1.08186	0.31989247	0.9700675	1	835
BIOCARTA_SPRY_PATHWAY	18	-0.46819	-1.07968	0.3476298	0.9698046	1	4042
KEGG_LYSINE_DEGRADATION	39	-0.40624	-1.07847	0.32048193	0.96604973	1	1590
KEGG_GLYCINE_SERINE_AND_THREONINE_METABOLISM	28	-0.43346	-1.07693	0.3478261	0.9636791	1	2998
KEGG_WNT_SIGNALING_PATHWAY	139	-0.3304	-1.07518	0.27972028	0.9614057	1	1689
KEGG_GLIOMA	65	-0.36599	-1.07291	0.32777777	0.96178913	1	4376
REACTOME_AMINE_LIGAND_BINDING_RECEPTORS	21	-0.46299	-1.06601	0.3770115	0.97892004	1	1437
KEGG_PRION_DISEASES	28	-0.42456	-1.06286	0.39141414	0.9831543	1	4289
REACTOME_EXTRACELLULAR_MATRIX_ORGANIZATION	79	-0.36069	-1.05906	0.32173914	0.9891139	1	4547
KEGG_PYRIMIDINE_METABOLISM	91	-0.3448	-1.05738	0.32218844	0.9876187	1	1648
KEGG_MAPK_SIGNALING_PATHWAY	243	-0.30641	-1.05419	0.2764977	0.9915983	1	4212
REACTOME_SIGNALING_BY_ILS	101	-0.3385	-1.05342	0.33116883	0.9860404	1	3213
KEGG_MELANOGENESIS	94	-0.33279	-1.04841	0.36212623	0.9966328	1	1669
REACTOME_RIP_MEDIATED_NFKB_ACTIVATION_VIA_DAI	18	-0.45895	-1.04743	0.39240506	0.9923055	1	647
REACTOME_SHC_RELATED_EVENTS	16	-0.47886	-1.04598	0.39485982	0.9897641	1	3546
BIOCARTA_TGFB_PATHWAY	19	-0.45855	-1.04554	0.430622	0.9835973	1	162
KEGG_MATURITY_ONSET_DIABETES_OF_THE_YOUNG	16	-0.48511	-1.04209	0.4097222	0.98877114	1	12
REACTOME_SIGNALING_BY_FGFR_MUTANTS	37	-0.39738	-1.04067	0.39083558	0.986348	1	233
BIOCARTA_PGC1A_PATHWAY	22	-0.44047	-1.04046	0.4241706	0.97935855	1	5405
REACTOME_ABCA_TRANSPORTERS_IN_LIPID_HOMEOSTASIS	15	-0.4686	-1.03808	0.41025642	0.9803864	1	5450
REACTOME_GABA_RECEPTOR_ACTIVATION	42	-0.38625	-1.03646	0.36507937	0.97875273	1	808
KEGG_SPHINGOLIPID_METABOLISM	33	-0.40901	-1.03282	0.416	0.9846134	1	3988
REACTOME_TCR_SIGNALING	41	-0.38532	-1.03259	0.38659793	0.97808063	1	5385
REACTOME_SMAD2_SMAD3_SMAD4_HETEROTRIMER_REGULATES_TRANSCRIPTION	26	-0.41685	-1.02823	0.40048543	0.98703104	1	2949
REACTOME_METABOLISM_OF_AMINO_ACIDS_AND_DERIVATIVES	181	-0.30475	-1.02579	0.39694658	0.9886298	1	3281
KEGG_NATURAL_KILLER_CELL_MEDIATED_CYTOTOXICITY	95	-0.33036	-1.02325	0.38291138	0.9908038	1	3833
REACTOME_RNA_POL_III_TRANSCRIPTION_TERMINATION	19	-0.44031	-1.02299	0.43601894	0.9845582	1	518
BIOCARTA_AT1R_PATHWAY	31	-0.39812	-1.02215	0.40759495	0.98054165	1	5394
REACTOME_NETRIN1_SIGNALING	34	-0.39174	-1.02079	0.42964825	0.97848386	1	2377
BIOCARTA_IL6_PATHWAY	22	-0.42996	-1.01575	0.41411763	0.9892666	1	6108
BIOCARTA_IL12_PATHWAY	16	-0.46013	-1.01412	0.45971563	0.98792946	1	5394
REACTOME_NOD1_2_SIGNALING_PATHWAY	29	-0.41275	-1.01405	0.44533333	0.9811635	1	4870
REACTOME_SIGNALING_BY_SCF_KIT	74	-0.34595	-1.01383	0.4034091	0.97501534	1	5034
BIOCARTA_EPO_PATHWAY	19	-0.44963	-1.01359	0.44923857	0.9689287	1	5394
REACTOME_G_ALPHA_Q_SIGNALING_EVENTS	134	-0.31789	-1.01334	0.41744548	0.9630945	1	3777
KEGG_GLYCOSYLPHOSPHATIDYLINOSITOL_GPI_ANCHOR_BIOSYNTHESIS	24	-0.4216	-1.01321	0.4390244	0.95691824	1	2960
REACTOME_EFFECTS_OF_PIP2_HYDROLYSIS	21	-0.43413	-1.01264	0.44868734	0.9525308	1	2480
KEGG_GLYCOSAMINOGLYCAN_BIOSYNTHESIS_HEPARAN_SULFATE	24	-0.42255	-1.01215	0.44604316	0.94787043	1	4288
KEGG_THYROID_CANCER	29	-0.40631	-1.00895	0.45	0.9526414	1	2923
REACTOME_INTEGRIN_ALPHAIIIB_BETA3_SIGNALING	27	-0.40506	-1.00667	0.42892158	0.9538928	1	1545
REACTOME_TRIGLYCERIDE_BIOSYNTHESIS	36	-0.38336	-1.00466	0.4781491	0.9546423	1	4806
REACTOME_GPCR_LIGAND_BINDING	252	-0.2878	-1.0005	0.42156863	0.96210396	1	1949
REACTOME_TRANSPORT_OF_INORGANIC_CATIONS_ANIONS_AND_AMINO_ACIDS_OLIGOPEPTIDES	80	-0.33639	-1.00046	0.44508672	0.9559562	1	1078
REACTOME_POST_TRANSLATIONAL_PROTEIN_MODIFICATION	168	-0.29941	-0.99947	0.39922482	0.9528854	1	3077
KEGG_BASAL_CELL_CARCINOMA	51	-0.35938	-0.99389	0.46835443	0.9659308	1	1926
KEGG_NICOTINATE_AND_NICOTINAMIDE_METABOLISM	21	-0.40885	-0.99311	0.4608076	0.9623119	1	2703
REACTOME_SIGNALING_BY_FGFR1_MUTANTS	25	-0.40768	-0.99069	0.44963145	0.96421856	1	2979
KEGG_LEISHMANIA_INFECTION	51	-0.35281	-0.99047	0.44031832	0.95892656	1	374
REACTOME_REGULATION_OF_GLUKOKINASE_BY_GLUKOKINASE_REGULATORY_PROTEIN	26	-0.39971	-0.9877	0.46601942	0.96208173	1	4175
REACTOME_DARPP_32_EVENTS	23	-0.41147	-0.98363	0.47016707	0.9696435	1	1689
REACTOME_PI3K_CASCADE	61	-0.34048	-0.9751	0.52	0.9922334	1	233
REACTOME_MAP_KINASE_ACTIVATION_IN_TLR_CASCADE	49	-0.35355	-0.9724	0.4847561	0.99528515	1	5394
REACTOME_TRANSCRIPTIONAL_ACTIVITY_OF_SMAD2_SMAD3_SMAD4_HETEROTRIMER	37	-0.37037	-0.97216	0.51005024	0.99006045	1	2949
REACTOME_CYTOKINE_SIGNALING_IN_IMMUNE_SYSTEM	230	-0.28018	-0.97213	0.52100843	0.9841234	1	3843
REACTOME_SPHINGOLIPID_DE_NOVO_BIOSYNTHESIS	26	-0.3982	-0.9718	0.48566118	0.9792237	1	4762
REACTOME_PHASE1_FUNCTIONALIZATION_OF_COMPOUNDS	53	-0.34488	-0.96964	0.4903581	0.9810306	1	2946
KEGG_GLYCOSAMINOGLYCAN_BIOSYNTHESIS_CHONDROITIN_SULFATE	22	-0.40909	-0.96922	0.49427918	0.976411	1	3911
BIOCARTA_SHH_PATHWAY	15	-0.4326	-0.96512	0.49311927	0.98433006	1	1926
BIOCARTA_CSK_PATHWAY	18	-0.41884	-0.96411	0.48994976	0.98117641	1	5811
REACTOME_AMINO_ACID_SYNTHESIS_AND_INTERCONVERSION_TRANAMINATION	15	-0.44176	-0.95794	0.51746726	0.99680334	1	3026
KEGG_REGULATION_OF_AUTOPHAGY	20	-0.40775	-0.95616	0.5122549	0.9969625	1	3537
REACTOME_PRE_NOTCH_EXPRESSION_AND_PROCESSING	38	-0.36273	-0.95565	0.51344085	0.9929596	1	5562
KEGG_INSULIN_SIGNALING_PATHWAY	128	-0.29887	-0.95377	0.5628931	0.99384964	1	4134
BIOCARTA_ATM_PATHWAY	19	-0.41873	-0.95225	0.49408984	0.9931128	1	6299
BIOCARTA_NFAT_PATHWAY	48	-0.34847	-0.95101	0.55376345	0.9914395	1	1689
REACTOME_SIGNALING_BY_RHO_GTPASES	108	-0.30396	-0.9492	0.5765472	0.9914564	1	4100
KEGG_DORSO_VENTRAL_AXIS_FORMATION	23	-0.40375	-0.94809	0.52102804	0.989946506	1	1245
KEGG_ARRHYTHMOGENIC_RIGHT_VENTRICULAR_CARDIOMYOPATHY_ARVC	67	-0.33024	-0.94805	0.55588233	0.9839927	1	935
BIOCARTA_BCR_PATHWAY	34	-0.36103	-0.94191	0.53333336	0.99838036	1	2779
REACTOME_METABOLISM_OF_LIPIDS_AND_LIPOPROTEINS	422	-0.25658	-0.936	0.75	1	1	3445
KEGG_ENDOMETRIAL_CANCER	50	-0.3373	-0.93584	0.5380435	1	1	1408
REACTOME_TRANSPORT_TO_THE_GOLGI_AND_SUBSEQUENT_MODIFICATION	32	-0.36013	-0.93392	0.5364706	1	1	378
REACTOME_TRIF_MEDIATED_TLR3_SIGNALING	73	-0.30993	-0.93138	0.5770492	1	1	5034
BIOCARTA_WNT_PATHWAY	24	-0.3795	-0.91785	0.55504584	1	1	190
BIOCARTA_PYK2_PATHWAY	28	-0.36563	-0.91643	0.58780485	1	1	5957
REACTOME_NUCLEAR_EVENTS_KINASE_AND_TRANSCRIPTION_FACTOR_ACTIVATION	24	-0.38021	-0.91589	0.56222224	1	1	5034
KEGG_CYSSTEINE_AND_METHIONINE_METABOLISM	33	-0.35948	-0.91459	0.57462686	1	1	1277
KEGG_T_CELL_RECEPTOR_SIGNALING_PATHWAY	95	-0.29628	-0.91452	0.64576805	1	1	3425
REACTOME_INSULIN_RECEPTOR_SIGNALING_CASCADE	77	-0.30828	-0.9131	0.6126126	1	1	723
REACTOME_NRAGE_SIGNALS_DEATH_THROUGH_JNK	43	-0.33946	-0.91232	0.58679706	1	1	5920
REACTOME_METABOLISM_OF_NUCLEOTIDES	64	-0.31793	-0.91204	0.59375	1	1	1953
REACTOME_SIGNALING_BY_ROBO_RECEPTOR	27	-0.37038	-0.90807	0.58542717	1	1	5110
BIOCARTA_VIP_PATHWAY	25	-0.37879	-0.90586	0.614486	1	1	4953
REACTOME_ASSOCIATION_OF_TRIC_CCT_WITH_TARGET_PROTEINS_DURING_BIOSYNTHESIS	26	-0.36696	-0.90556	0.6167076	1	1	1095

REACTOME_SIGNALLING_TO_ERKS	35	-0.34729	-0.90439	0.6	1	1	3823
REACTOME_ARMS_MEDIATED_ACTIVATION	17	-0.39948	-0.89962	0.5970516	1	1	3823
BIOCARTA_ERK_PATHWAY	28	-0.36533	-0.89914	0.615942	1	1	4376
KEGG_COLORECTAL_CANCER	62	-0.30849	-0.89908	0.65591395	1	1	1408
REACTOME_JNK_C_JUN_KINASES_PHOSPHORYLATION_AND_ACTIVATION_MEDIATED_BY_ACTIVATED_HU MAN_TAK1	16	-0.40099	-0.89869	0.57798165	1	1	3318
REACTOME_CYTOCHROME_P450_ARRANGED_BY_SUBSTRATE_TYPE	39	-0.33575	-0.89788	0.6393443	1	1	2946
REACTOME_SYNTHESIS_OF_PIP3_AT_THE_GOLGI_MEMBRANE	16	-0.4099	-0.89657	0.6	1	1	5749
REACTOME_GAB1_SIGNALOSOME	36	-0.33854	-0.89513	0.6315789	1	1	5461
BIOCARTA_NDKDYNAMIN_PATHWAY	18	-0.39241	-0.89184	0.5788235	1	1	812
KEGG_PANCREATIC_CANCER	69	-0.30684	-0.89136	0.6571429	1	1	4870
REACTOME_ADAPTIVE_IMMUNE_SYSTEM	458	-0.24302	-0.88942	0.9440559	1	1	5075
REACTOME_ABC_FAMILY_PROTEINS_MEDIATED_TRANSPORT	31	-0.35065	-0.88891	0.62857145	1	1	5450
BIOCARTA_CDMAC_PATHWAY	16	-0.40406	-0.88695	0.60807604	1	1	374
REACTOME_ERK_MAPK_TARGETS	21	-0.38032	-0.88567	0.6518847	1	1	4676
KEGG_GLUTATHIONE_METABOLISM	43	-0.32352	-0.88413	0.6666667	1	1	485
REACTOME_G_ALPHA_I_SIGNALING_EVENTS	128	-0.27591	-0.88106	0.75767916	1	1	1949
REACTOME_MAPK_TARGETS_NUCLEAR_EVENTS_MEDIATED_BY_MAP_KINASES	30	-0.34566	-0.88103	0.6627635	1	1	5394
REACTOME_FORMATION_OF_THE_TERNARY_COMPLEX_AND_SUBSEQUENTLY_THE_43S_COMPLEX	58	-0.31524	-0.88041	0.67639256	1	1	1084
BIOCARTA_EGF_PATHWAY	31	-0.3464	-0.87992	0.64871794	1	1	2813
REACTOME_CARMA1_ER_PATHWAY	34	-0.34286	-0.87976	0.68190475	1	1	2156
REACTOME_RNA_POL_III_TRANSCRIPTION	33	-0.34797	-0.87559	0.6967419	1	1	938
REACTOME_INTERFERON_ALPHA_BETA_SIGNALING	46	-0.3221	-0.87521	0.6717949	1	1	9073
REACTOME_SIGNALING_BY_TGF_BETA_RECEPTOR_COMPLEX	61	-0.30603	-0.87468	0.6857143	1	1	4432
REACTOME_ION_TRANSPORT_BY_P_TYPE_ATPASES	30	-0.34774	-0.87274	0.6244019	1	1	2670
KEGG_MTOR_SIGNALING_PATHWAY	49	-0.31416	-0.87266	0.6666667	1	1	4543
REACTOME_SIGNALING_BY_INSULIN_RECEPTOR	97	-0.27702	-0.87216	0.77627116	0.99968946	1	723
REACTOME_ACTIVATION_OF_THE_MRNA_UPON_BINDING_OF_THE_CAP_BINDING_COMPLEX_AND_EIF5A ND_SUBSEQUENT_BINDING_TO_43S	66	-0.29703	-0.8635	0.7318436	1	1	10
REACTOME_PLATELET_AGGREGATION_PLUG_FORMATION	33	-0.34183	-0.86321	0.6466165	1	1	1545
REACTOME_TRAF6_MEDIATED_INDUCION_OF_NFKB_AND_MAP_KINASES_UPON_TLR7_8_OR_9_ACTIVATI ON	73	-0.2921	-0.86192	0.71387285	1	1	5105
REACTOME_INTERACTION_BETWEEN_L1_AND_ANKYRINS	20	-0.37615	-0.85429	0.64568764	1	1	1910
REACTOME_CHONDROITIN_SULFATE_DERMATAN_SULFATE_METABOLISM	47	-0.31503	-0.851	0.69529086	1	1	3911
BIOCARTA_NKT_PATHWAY	21	-0.35455	-0.84152	0.702765	1	1	7183
REACTOME_SIGNALING_BY_NOTCH	96	-0.27373	-0.84135	0.8262195	1	1	2860
REACTOME_ACTIVATED_TLR4_SIGNALING	91	-0.28211	-0.84056	0.82729805	1	1	5034
REACTOME_SULFUR_AMINO_ACID_METABOLISM	23	-0.35543	-0.83682	0.692494	1	1	1527
REACTOME_TOLL_RECEPTOR_CASCADES	108	-0.26752	-0.83583	0.85119045	1	1	5105
KEGG_CHRONIC_MYELOID_LEUKEMIA	73	-0.28447	-0.83284	0.78571427	1	1	4198
REACTOME_G_ALPHA_Z_SIGNALING_EVENTS	42	-0.30621	-0.83002	0.7350649	1	1	3769
KEGG_OOCYTE_MEIOSIS	102	-0.26411	-0.82904	0.85755813	1	1	2174
REACTOME_PLATELET_SENSITIZATION_BY_LDL	16	-0.36631	-0.82527	0.70159453	1	1	2129
KEGG_ARGININE_AND_PROLINE_METABOLISM	48	-0.29806	-0.82358	0.78370786	1	1	3519
REACTOME_CHONDROITIN_SULFATE_BIOSYNTHESIS	19	-0.35666	-0.82318	0.74125874	1	1	4710
KEGG_LINOLEIC_ACID_METABOLISM	20	-0.3465	-0.82202	0.6944444	1	1	520
KEGG_RIBOFLAVIN_METABOLISM	15	-0.37095	-0.82124	0.6723716	1	1	7594
REACTOME_SIGNALING_BY_PDGF	114	-0.25992	-0.82092	0.89320385	1	1	5034
REACTOME_PROLONGED_ERK_ACTIVATION_EVENTS	19	-0.35006	-0.81445	0.71566266	1	1	3823
BIOCARTA_MAPK_PATHWAY	86	-0.26426	-0.81277	0.8628049	1	1	5034
KEGG_OTHER_GLYCAN_DEGRADATION	15	-0.37517	-0.8127	0.7024608	1	1	5304
REACTOME_BMAL1_CLOCK_NPAS2_ACTIVATES_CIRCADIAN_EXPRESSION	32	-0.32016	-0.81153	0.79	1	1	4297
KEGG_VIBRIO_CHOLERAE_INFECTION	51	-0.29173	-0.81041	0.8161209	1	1	2080
REACTOME_REGULATION_OF_KIT_SIGNALING	16	-0.36385	-0.80992	0.7334852	1	1	1104
REACTOME_CLASS_I_MHC_MEDIATED_ANTIGEN_PROCESSING_PRESENTATION	220	-0.23357	-0.80947	0.9823009	1	1	4109
REACTOME_DOWNSTREAM_SIGNAL_TRANSDUCTION	88	-0.26681	-0.8031	0.87261146	1	1	5034
KEGG_TRYPTOPHAN_METABOLISM	37	-0.30639	-0.80124	0.786385	1	1	5006
REACTOME_PROCESSIVE_SYNTHESIS_ON_THE_LAGGING_STRAND	15	-0.35583	-0.80059	0.7414188	1	1	3467
KEGG_GLYCEROLIPID_METABOLISM	37	-0.30099	-0.79991	0.8025641	1	1	3714
REACTOME_IL_2_SIGNALING	37	-0.30467	-0.79455	0.80548626	1	1	3622
REACTOME_MITOCHONDRIAL_TRNA_AMINOACYLATION	21	-0.33956	-0.79434	0.7651163	1	1	7329
REACTOME_SIGNALING_BY_EGFR_IN_CANCER	103	-0.25296	-0.79148	0.9297125	1	1	5034
REACTOME_DOWNSTREAM_TCR_SIGNALING	25	-0.32258	-0.78891	0.7570755	1	1	5385
REACTOME_PI3K_AKT_ACTIVATION	36	-0.30825	-0.78808	0.80100757	1	1	5461
KEGG_PYRUVATE_METABOLISM	36	-0.30706	-0.78766	0.8230769	1	1	5006
BIOCARTA_KERATINOCYTE_PATHWAY	45	-0.29103	-0.78757	0.83715016	1	1	5961
REACTOME_INTERFERON_SIGNALING	129	-0.24288	-0.7861	0.94055945	1	1	5451
REACTOME_INTERFERON_GAMMA_SIGNALING	46	-0.28457	-0.78583	0.8314917	1	1	6107
REACTOME_TRANSPORT_OF_RIBONUCLEOPROTEINS_INTO_THE_HOST_NUCLEUS	26	-0.32581	-0.78332	0.76960784	1	1	4626
REACTOME_FATTY_ACYL_COA_BIOSYNTHESIS	18	-0.34914	-0.78163	0.74647886	1	1	4806
KEGG_PRIMARY_IMMUNODEFICIENCY	29	-0.30775	-0.77593	0.80100757	1	1	6756
REACTOME_HOMOLOGOUS_RECOMBINATION_REPAIR_OF_REPLICATION_INDEPENDENT_DOUBLE_STRAN D_BREAKS	15	-0.35425	-0.77278	0.7529412	1	1	6774
REACTOME_RESPONSE_TO_ELEVATED_PLATELET_CYTOSOLIC_CA2	75	-0.25835	-0.76891	0.91354465	1	1	5343
REACTOME_INTERACTIONS_OF_VPR_WITH_HOST_CELLULAR_PROTEINS	31	-0.30054	-0.76809	0.8230769	1	1	6114
REACTOME_DOWNREGULATION_OF_SMAD2_3_SMAD4_TRANSCRIPTIONAL_ACTIVITY	20	-0.3326	-0.76527	0.7975	1	1	2484
BIOCARTA_DEATH_PATHWAY	33	-0.29956	-0.76417	0.80987656	1	1	677
REACTOME_PRE_NOTCH_TRANSCRIPTION_AND_TRANSLATION	23	-0.31524	-0.76246	0.7943925	1	1	5562
BIOCARTA_CALCINEURIN_PATHWAY	18	-0.34525	-0.76199	0.7708831	1	1	3715
REACTOME_SIGNALING_BY_THE_B_CELL_RECEPTOR_BCR	121	-0.23761	-0.76117	0.97077924	1	1	5461
KEGG_NEUROTROPHIN_SIGNALING_PATHWAY	124	-0.23524	-0.75659	0.9685315	1	1	5405
REACTOME_CELL_DEATH_SIGNALING_VIA_NFkB_IRF1_AND_NADE	58	-0.2644	-0.7564	0.9017341	1	1	3823
BIOCARTA_ETS_PATHWAY	18	-0.33422	-0.7498	0.82678986	1	1	5964
REACTOME_PHOSPHORYLATION_OF_THE_APC_C	17	-0.33041	-0.74948	0.79586565	1	1	3936
REACTOME_BRANCHED_CHAIN_AMINO_ACID_CATABOLISM	17	-0.33051	-0.74918	0.8252427	1	1	1481
REACTOME_GLUCOSE_TRANSPORT	33	-0.28789	-0.74814	0.89637303	1	1	4175
REACTOME_ANTIGEN_PROCESSING_UBIQUITINATION_PROTEASOME_DEGRADATION	189	-0.21976	-0.74806	0.9920949	1	1	2977
REACTOME_TRANSPORT_OF_VITAMINS_NUCLEOSIDES_AND_RELATED_MOLECULES	29	-0.30017	-0.74654	0.8440594	1	1	2295
REACTOME_DOUBLE_STRAND_BREAK_REPAIR	21	-0.3276	-0.74494	0.7849224	1	1	6774
KEGG_NUCLEOTIDE_EXCISION_REPAIR	44	-0.27268	-0.74458	0.8680739	1	1	6499
REACTOME_TRAF6_MEDIATED_IRF1_ACTIVATION	19	-0.32744	-0.73987	0.795045	1	1	8696
BIOCARTA_CHEMICAL_PATHWAY	22	-0.32053	-0.73927	0.8202765	1	1	4395
REACTOME_CIRCADIAN_CLOCK	49	-0.26779	-0.73866	0.8981723	1	1	4428
BIOCARTA_G2_PATHWAY	24	-0.30449	-0.7303	0.8633257	1	1	6980
REACTOME_EXTENSION_OF_TELOMERES	27	-0.29517	-0.73003	0.84782606	1	1	3467
BIOCARTA_HIF_PATHWAY	15	-0.32845	-0.72503	0.8315098	1	1	6303
REACTOME_FATTY_ACID_TRIACYLGLYCEROL_AND_KETONE_BODY_METABOLISM	160	-0.21672	-0.72134	0.99622643	1	1	3845
BIOCARTA_MYOSIN_PATHWAY	30	-0.28501	-0.72128	0.8912037	1	1	1126
KEGG_AMYOTROPHIC_LATERAL_SCLEROSIS_ALS	51	-0.2585	-0.71529	0.92268044	1	1	4676
REACTOME_YAP1_AND_WWTR1_TAZ_STIMULATED_GENE_EXPRESSION	22	-0.30523	-0.71408	0.875	1	1	4621
BIOCARTA_PTDINS_PATHWAY	23	-0.29339	-0.71269	0.89638555	1	1	2049



REACTOME_SYNTHESIS_OF_GLYCOSYLPHOSPHATIDYLINOSITOL_GPI	17	-0.31683	-0.7114	0.8538283	1	1	7712
REACTOME_DESTABILIZATION_OF_MRNA_BY_KSRP	17	-0.31788	-0.71009	0.8294931	1	1	4676
KEGG_NITROGEN_METABOLISM	18	-0.3065	-0.70693	0.8413793	1	1	1646
REACTOME_NEP_NS2_INTERACTS_WITH_THE_CELLULAR_EXPORT_MACHINERY	26	-0.28525	-0.70485	0.8829517	1	1	4175
KEGG_HISTIDINE_METABOLISM	26	-0.28976	-0.70409	0.9253012	1	1	5006
REACTOME_DOWNREGULATION_OF_TGF_BETA_RECEPTOR_SIGNALING	22	-0.30076	-0.69762	0.8628429	1	1	162
REACTOME_REGULATION_OF_INSULIN_SECRETION_BY_GLUCAGON_LIKE_PEPTIDE1	37	-0.26501	-0.69403	0.91161615	1	1	2514
REACTOME_RIG_I_MDA5_MEDIATED_INDUCION_OF_IFN_ALPHA_BETA_PATHWAYS	61	-0.23847	-0.69007	0.9833795	1	1	5414
KEGG_P53_SIGNALING_PATHWAY	65	-0.23988	-0.68973	0.9769452	1	1	4571
REACTOME_CONVERSION_FROM_APC_C_CDC20_TO_APC_C_CDH1_IN_LATE_ANAPHASE	16	-0.30359	-0.68733	0.8591224	1	1	3936
REACTOME_TGF_BETA_RECEPTOR_SIGNALING_ACTIVATES_SMADS	25	-0.2883	-0.6871	0.8973747	0.99728656	1	162
KEGG_GLYCOLYSIS_GLUconeogenesis	52	-0.24121	-0.67471	0.97493035	1	1	2173
KEGG_SELENOAMINO_ACID_METABOLISM	25	-0.27707	-0.67118	0.9123223	1	1	4971
BIOCARTA_ATRBRCA_PATHWAY	20	-0.2893	-0.67043	0.8905908	1	1	4320
KEGG_AMINO_SUGAR_AND_NUCLEOTIDE_SUGAR_METABOLISM	41	-0.24886	-0.66913	0.9678284	0.99861455	1	4739
KEGG_NOTCH_SIGNALING_PATHWAY	45	-0.24723	-0.66434	0.9680851	0.998819	1	4782
BIOCARTA_STRESS_PATHWAY	25	-0.27321	-0.66347	0.94089836	0.9962066	1	5394
REACTOME_ANTIVIRAL_MECHANISM_BY_IFN_STIMULATED_GENES	65	-0.22592	-0.66099	0.982906	0.9947969	1	4626
KEGG_PHENYLALANINE_METABOLISM	17	-0.28562	-0.64004	0.9022727	1	1	6019
REACTOME_INHIBITION_OF_THE_PROTEOLYTIC_ACTIVITY_OF_APC_C_REQUIRED_FOR_THE_ONSET_OF_A	18	-0.28349	-0.63916	0.9375	1	1	5568
NAPHASE_BY_MITOTIC_SPINDLE_CHECKPOINT_COMPONENTS	17	-0.27737	-0.63632	0.9236111	1	1	4676
REACTOME_ACTIVATED_TAK1_MEDIATES_P38_MAPK_ACTIVATION	19	-0.2727	-0.63083	0.91484183	0.9997657	1	3467
REACTOME_LAGGING_STRAND_SYNTHESIS	57	-0.21901	-0.61826	0.9945355	1	1	4953
BIOCARTA_HIVNEF_PATHWAY	22	-0.261	-0.61313	0.9291139	1	1	4428
REACTOME_CIRCADIAN_REPRESSION_OF_EXPRESSION_BY_REV_ERBA	20	-0.24995	-0.59132	0.95486933	1	1	6499
REACTOME_RNA_POL_I_TRANSCRIPTION_TERMINATION	31	-0.23107	-0.58688	0.98288506	1	1	4175
REACTOME_TRANSPORT_OF_MATURE_MRNA_DERIVED_FROM_AN_INTRONLESS_TRANSCRIPT	23	-0.24234	-0.57592	0.97932816	1	1	3778
REACTOME_RORA_ACTIVATES_CIRCADIAN_EXPRESSION	24	-0.23945	-0.56971	0.9683377	1	1	7540
KEGG_VALINE_LEUCINE_AND_ISOLEUCINE_DEGRADATION	44	-0.20788	-0.55669	0.9839142	1	1	5318
KEGG_N_GLYCAN_BIOSYNTHESIS	46	-0.19773	-0.54484	0.9948052	1	1	7592
BIOCARTA_TNFR1_PATHWAY	29	-0.21167	-0.54224	0.9832134	1	1	5394
KEGG_MISMATCH_REPAIR	23	-0.21676	-0.51991	0.99012345	1	1	5634
BIOCARTA_CERAMIDE_PATHWAY	22	-0.19858	-0.47425	0.99766356	1	1	4953
REACTOME_ENOS_ACTIVATION_AND_REGULATION	20	-0.20465	-0.4731	0.9928058	0.9995718	1	5892
REACTOME_METABOLISM_OF_NON_CODING_RNA	47	-0.15849	-0.43849	1	0.9984103	1	4801

















REACTOME_FACTORS_INVOLVED_IN_MEGAKARYOCYTE_DEVELOPMENT_AND_PLATELET_PRODUCTION	112	-0.25412	-0.85658	0.7708738	0.94791764	1	5674
KEGG_APOPTOSIS	82	-0.26318	-0.85528	0.7218814	0.9464275	1	5747
REACTOME_GENERIC_TRANSCRIPTION_PATHWAY	325	-0.22455	-0.85527	0.8950495	0.9420661	1	6272
REACTOME_GLYCOGEN_BREAKDOWN_GLYCOGENOLYSIS	17	-0.36086	-0.85347	0.6496063	0.94201744	1	3363
KEGG_TASTE_TRANSDUCTION	35	-0.31112	-0.85327	0.66927594	0.9382261	1	6435
KEGG_RIBOFLAVIN_METABOLISM	15	-0.36268	-0.85295	0.6461825	0.9364226	1	2907
REACTOME_PHOSPHOLIPID_METABOLISM	177	-0.23716	-0.84951	0.8241966	0.93847656	1	4420
REACTOME_RESOLUTION_OF_AP_SITES_VIA_THE_MULTIPLE_NUCLEOTIDE_PATCH_REPLACEMENT_PATCHWAY	17	-0.35263	-0.84945	0.6420233	0.9343616	1	7366
REACTOME_RNA_POL_III_TRANSCRIPTION	33	-0.3046	-0.84919	0.71009177	0.9306715	1	9379
KEGG_BUTANOATE_METABOLISM	29	-0.3198	-0.84247	0.6673077	0.9416033	1	4810
BIOCARTA_IGF1MOTOR_PATHWAY	20	-0.33935	-0.83758	0.68473893	0.94836736	1	4009
REACTOME_SYNTHESIS_OF_GLYCOSYLPHOSPHATIDYLINOSITOL_GPI	17	-0.35409	-0.83626	0.6952191	0.9470011	1	4943
REACTOME_METABOLISM_OF_PROTEINS	437	-0.21484	-0.83555	0.95229006	0.94445914	1	5540
REACTOME_APC_C_CDC20_MEDIATED_DEGRADATION_OF_MITOTIC_PROTEINS	65	-0.26891	-0.83404	0.751503	0.9437442	1	5321
REACTOME_G_BETA_GAMMA_SIGNALING_THROUGH_PL_C_BETA	19	-0.34351	-0.82924	0.69719625	0.9499042	1	4359
REACTOME_P53_INDEPENDENT_G1_S_DNA_DAMAGE_CHECKPOINT	48	-0.27931	-0.82337	0.7713718	0.9582862	1	5321
REACTOME_ASSEMBLY_OF_THE_PRE_REPLICATIVE_COMPLEX	63	-0.26889	-0.82255	0.7943396	0.9558644	1	5783
KEGG_PHOSPHATIDYLINOSITOL_SIGNALING_SYSTEM	75	-0.26277	-0.82141	0.78557116	0.9540864	1	3294
REACTOME_PROSTACYCLIN_SIGNALING_THROUGH_PROSTACYCLIN_RECEPTOR	18	-0.33655	-0.82139	0.71	0.9499842	1	4359
KEGG_SMALL_CELL_LUNG_CANCER	84	-0.25914	-0.82027	0.8004115	0.94816387	1	4009
BIOCARTA_ATM_PATHWAY	19	-0.33641	-0.81114	0.7061144	0.9628532	1	5214
KEGG_PROSTATE_CANCER	86	-0.24925	-0.8058	0.86564296	0.9691689	1	4009
REACTOME_ARMS_MEDIATED_ACTIVATION	17	-0.33721	-0.80424	0.71929824	0.96821976	1	1177
REACTOME_THROMBIN_SIGNALING_THROUGH_PROTEINASE_ACTIVATED_RECEPTORS_PARS	31	-0.29753	-0.80186	0.7740668	0.9687531	1	4643
REACTOME_RNA_POL_III_TRANSCRIPTION_INITIATION_FROM_TYPE_3_PROMOTER	26	-0.29963	-0.79334	0.748538	0.9808601	1	6451
KEGG_BIOSYNTHESIS_OF_UNSATURATED_FATTY_ACIDS	20	-0.31823	-0.79329	0.75435203	0.9768265	1	2176
REACTOME_DEGRADATION_OF_THE_EXTRACELLULAR_MATRIX	26	-0.30759	-0.79301	0.7810651	0.9732097	1	2390
REACTOME_RNA_POL_I_PROMOTER_OPENING	55	-0.26379	-0.79205	0.81431335	0.970916	1	7958
REACTOME_DESTABILIZATION_OF_MRNA_BY_KSRP	17	-0.33299	-0.791	0.7348178	0.96888906	1	2296
REACTOME_MRNA_SPLICING_MINOR_PATHWAY	40	-0.27535	-0.78904	0.82778865	0.9684718	1	3619
REACTOME_PROTEOLYTIC_CLEAVAGE_OF_SNARE_COMPLEX_PROTEINS	16	-0.32716	-0.78227	0.76982594	0.97639394	1	2737
REACTOME_TRANSPORT_OF_VITAMINS_NUCLEOSIDES_AND_RELATED_MOLECULES	30	-0.2915	-0.78178	0.77757007	0.97322243	1	5551
REACTOME_PACKAGING_OF_TELOMERE_ENDS	43	-0.27077	-0.77546	0.822736	0.98003745	1	7958
REACTOME_PROLONGED_ERK_ACTIVATION_EVENTS	19	-0.3169	-0.77454	0.77238804	0.97762376	1	1177
REACTOME_FORMATION_OF_RNA_POL_II_ELONGATION_COMPLEX	36	-0.27322	-0.75724	0.8246628	1	1	4411
REACTOME_ADP_SIGNALING_THROUGH_P2RY12	20	-0.30588	-0.75612	0.8062016	0.99857086	1	4359
REACTOME_THROMBOXANE_SIGNALING_THROUGH_TP_RECEPTOR	22	-0.29497	-0.74976	0.8233083	1	1	4359
REACTOME_IL_RECEPTOR_SHC_SIGNALING	23	-0.29722	-0.74619	0.825188	1	1	4009
BIOCARTA_P53_PATHWAY	16	-0.32146	-0.74428	0.8187023	1	1	1164
REACTOME_ORC1_REMOVAL_FROM_CHROMATIN	65	-0.23918	-0.74381	0.9080675	1	1	5321
REACTOME_INWARDLY_RECTIFYING_K_CHANNELS	30	-0.27282	-0.743	0.8446602	0.99746615	1	4750
REACTOME_SYNTHESIS_OF_PIP3_AT_THE_GOLGI_MEMBRANE	17	-0.31243	-0.74191	0.81409	0.995004	1	5177
REACTOME_ENDOSOMAL_SORTING_COMPLEX_REQUIRED_FOR_TRANSPORT_ESCRT	27	-0.28283	-0.74147	0.84063745	0.99172986	1	467
BIOCARTA_CSK_PATHWAY	19	-0.29855	-0.74107	0.78515625	0.98837787	1	7351
REACTOME_BOTULINUM_NEUROTOXICITY	18	-0.30763	-0.73622	0.819802	0.9909563	1	2737
REACTOME_OPIOID_SIGNALING	71	-0.23454	-0.73211	0.93385214	0.99236876	1	3787
REACTOME_RNA_POL_III_TRANSCRIPTION_INITIATION_FROM_TYPE_2_PROMOTER	23	-0.28766	-0.73164	0.8241107	0.9891374	1	9379
REACTOME_DOWNREGULATION_OF_TGF_BETA_RECEPTOR_SIGNALING	22	-0.28594	-0.72511	0.8678862	0.9933764	1	992
REACTOME_IRON_UPTAKE_AND_TRANSPORT	35	-0.26092	-0.72476	0.8790036	0.9899676	1	2834
REACTOME_APC_C_CDH1_MEDIATED_DEGRADATION_OF_CDC20_AND_OTHER_APC_C_CDH1_TARGET_ED_PROTEINS_IN_LATE_MITOSIS_EARLY_G1	64	-0.23498	-0.72397	0.9201597	0.98724705	1	5321
REACTOME_PRE_NOTCH_TRANSCRIPTION_AND_TRANSLATION	23	-0.2834	-0.71637	0.8466135	0.99244124	1	5712
REACTOME_GLUconeogenesis	30	-0.26578	-0.71443	0.85626286	0.9907701	1	8178
REACTOME_G_PROTEIN_ACTIVATION	24	-0.26902	-0.71068	0.8698885	0.99109393	1	4359
REACTOME_AUTODEGRADATION_OF_CDH1_BY_CDH1_APC_C	57	-0.23698	-0.70912	0.92734224	0.9890383	1	5321
REACTOME_P53_DEPENDENT_G1_DNA_DAMAGE_RESPONSE	52	-0.23725	-0.7077	0.9390244	0.9868264	1	5321
REACTOME_INHIBITION_OF_INSULIN_SECRETION_BY_ADRENALINE_NORADRENALINE	24	-0.27689	-0.69319	0.88323915	0.9976971	1	4359
KEGG_PENTOSE_PHOSPHATE_PATHWAY	24	-0.27207	-0.68799	0.8787276	0.99867594	1	2522
REACTOME_HOST_INTERACTIONS_OF_HIV_FACTORS	116	-0.20425	-0.68796	0.98998	0.99500364	1	5321
REACTOME_BILE_ACID_AND_BILE_SALT_METABOLISM	23	-0.2652	-0.68652	0.89366055	1	1	4118
REACTOME_GLUcose_Metabolism	62	-0.21953	-0.6655	0.9701789	1	1	6249
REACTOME_NCAM1_INTERACTIONS	36	-0.24121	-0.66008	0.9217221	1	1	1121
REACTOME_REGULATORY_RNA_PATHWAYS	21	-0.26054	-0.6534	0.90818363	1	1	6451
REACTOME_STRIATED_MUSCLE_CONTRACTION	22	-0.25804	-0.65254	0.92738587	1	1	3491
REACTOME_APOPTOTIC_EXECUTION_PHASE	51	-0.21899	-0.65222	0.9526749	1	1	3899
REACTOME_PKA_MEDIATED_PHOSPHORYLATION_OF_CREB	15	-0.28293	-0.649	0.925636	0.9994366	1	2287
REACTOME_AUTODEGRADATION_OF_THE_E3_UBIQUITIN_LIGASE_COP1	46	-0.21974	-0.64531	0.96	0.9981019	1	423
REACTOME_GLYCOLYSIS	26	-0.24966	-0.64092	0.9419729	0.9971357	1	5142
REACTOME_PLATELET_CALCIIUM_HOMEOSTASIS	15	-0.27471	-0.64038	0.9158513	0.99388343	1	6783
REACTOME_CYCLIN_E_ASSOCIATED_EVENTS_DURING_G1_S_TRANSITION	63	-0.20425	-0.63596	0.9831461	0.9928616	1	5321
REACTOME_MYOGEnESIS	22	-0.25107	-0.6327	0.94497156	0.9910975	1	2785
REACTOME_SYNTHESIS_AND_INTERCONVERSION_OF_NUCLEOTIDE_DI_AND_TRIPHOSPHATES	17	-0.26377	-0.63034	0.9291667	0.98885316	1	4967
KEGG_PROXIMAL_TUBULE_BICARBONATE_RECLAMATION	20	-0.24691	-0.61606	0.93737376	0.99204016	1	3733
REACTOME_CGMP_EFFECTS	18	-0.25093	-0.6092	0.93907565	0.9914725	1	1289
REACTOME_CDT1_ASSOCIATION_WITH_THE_CDC6_ORC_ORIGIN_COMPLEX	54	-0.20706	-0.60814	0.99206346	0.98845905	1	5321
REACTOME_NOTCH1_INTRACELLULAR_DOMAIN_REGULATES_TRANSCRIPTION	45	-0.18741	-0.56148	0.99019605	0.99935603	1	4174
REACTOME_NITRIC_OXIDE_STIMULATES_GUANYLATE_CYCLASE	22	-0.21918	-0.54869	0.9881188	0.9986603	1	3882
BIOCARTA_SHH_PATHWAY	15	-0.23905	-0.54429	0.9705882	0.9960576	1	5560
KEGG_PROTEIN_EXPORT	23	-0.20266	-0.51983	0.982659	0.996304	1	3673
BIOCARTA_CHREBP2_PATHWAY	40	-0.17642	-0.50042	0.9980732	0.995005	1	967







REACTOME_TRANS_GOLGI_NETWORK_VESICLE_BUDDING	57	0.224579	0.717003	0.9476584	1	1	4577
REACTOME_JNK_C_JUN_KINASES_PHOSPHORYLATION_AND_ACTIVATION_MEDIATED_BY_ACTIVATED_HUMAN_TAK1	16	0.29738	0.715557	0.8639618	1	1	5033
BIOCARTA_ACH_PATHWAY	15	0.304614	0.71059	0.85560346	1	1	2701
KEGG_BETA_ALANINE_METABOLISM	20	0.275958	0.708319	0.8824885	1	1	3192
KEGG_BASAL_CELL_CARCINOMA	51	0.230112	0.707152	0.9435484	1	1	4296
REACTOME_GLUCAGON_TYPE_LIGAND_RECEPTORS	26	0.282805	0.706071	0.89	1	1	4837
REACTOME_DESTABILIZATION_OF_MRNA_BY_BRF1	17	0.282723	0.702595	0.8517588	1	1	10039
REACTOME_PRE_NOTCH_TRANSCRIPTION_AND_TRANSLATION	23	0.266009	0.701646	0.8915663	1	1	1968
REACTOME_SIGNALLING_TO_RAS	27	0.260808	0.701602	0.91022444	1	1	1771
BIOCARTA_RACCYCD_PATHWAY	26	0.258186	0.696851	0.875	1	1	5033
REACTOME_TIGHT_JUNCTION_INTERACTIONS	28	0.252525	0.694508	0.91022444	1	1	899
BIOCARTA_INTEGRIN_PATHWAY	38	0.232565	0.693842	0.9276486	0.9976979	1	1776
REACTOME_AQUAPORIN_MEDIATED_TRANSPORT	44	0.233614	0.693446	0.9661017	0.99492216	1	5877
REACTOME_P75_NTR_RECEPTOR_MEDIATED_SIGNALLING	79	0.210563	0.692214	0.9844237	0.9928695	1	2885
REACTOME_SIGNALLING_BY_BMP	21	0.263774	0.69077	0.87616825	0.9910225	1	4471
REACTOME_CTLA4_INHIBITORY_SIGNALLING	19	0.27077	0.685635	0.88941175	0.9921806	1	4017
BIOCARTA_ECM_PATHWAY	24	0.258711	0.684961	0.913486	0.9896728	1	6151
BIOCARTA_AKT_PATHWAY	20	0.26825	0.678527	0.89320385	0.9915761	1	5033
BIOCARTA_IGF1R_PATHWAY	22	0.25784	0.66813	0.90951276	0.9959315	1	8870
REACTOME_CIRCADIAN_CLOCK	49	0.220549	0.667369	0.97680414	0.99338967	1	5796
BIOCARTA_HDAC_PATHWAY	26	0.244853	0.660639	0.92957747	0.9945235	1	7203
REACTOME_LATENT_INFECTION_OF_HOMO_SAPIENS_WITH_MYCOBACTERIUM_TUBERCULOSIS	30	0.24224	0.660095	0.92561984	0.9918345	1	7127
REACTOME_CLASS_B_2_SECRETIN_FAMILY_RECEPTORS	67	0.20182	0.657849	0.994429	0.99029386	1	3572
BIOCARTA_TEL_PATHWAY	18	0.268798	0.654044	0.9178744	0.9897232	1	7032
KEGG_FATTY_ACID_METABOLISM	38	0.21791	0.648345	0.9614396	0.9899922	1	2710
REACTOME_REGULATION_OF_INSULIN_SECRETION_BY_GLUCAGON_LIKE_PEPTIDE1	37	0.221832	0.642486	0.9514563	0.9902519	1	5154
BIOCARTA_FCER1_PATHWAY	36	0.215791	0.637713	0.9748111	0.9897374	1	2831
REACTOME_REGULATION_OF_WATER_BALANCE_BY_RENAL_AQUAPORINS	38	0.214891	0.624516	0.9691517	0.9930952	1	5877
REACTOME_TRANSFERRIN_ENDOCYTOSIS_AND_RECYCLING	24	0.230602	0.612281	0.9625293	0.9952525	1	6375
REACTOME_ENERGY_DEPENDENT_REGULATION_OF_MTOR_BY_LKB1_AMPK	17	0.247289	0.606279	0.94549763	0.9945977	1	4116
REACTOME_FATTY_ACYL_COA_BIOSYNTHESIS	18	0.23974	0.605789	0.95591646	0.99180514	1	712
KEGG_RIBOSOME	87	0.174154	0.588277	0.99681526	0.9943779	1	5220
REACTOME_NRF1_SIGNALS_CELL_DEATH_FROM_THE_NUCLEUS	15	0.220933	0.5307	0.96511626	1	1	1046
BIOCARTA_CERAMIDE_PATHWAY	22	0.20748	0.530025	0.990099	1	1	6921
REACTOME_TGF_BETA_RECEPTOR_SIGNALLING_IN_EMT_EPITHELIAL_TO_MESENCHYMAL_TRANSITION	15	0.219892	0.522174	0.9744186	0.9987877	1	1046
KEGG_PORPHYRIN_AND_CHLOROPHYLL_METABOLISM	34	0.175859	0.507369	0.9974619	0.9974923	1	2731
REACTOME_GLUCAGON_SIGNALLING_IN_METABOLIC_REGULATION	30	0.168902	0.469727	0.9972826	0.99754775	1	5877











## Table S15

### List of Aneuploidy-associated SASP genes and IFNA gene set

<b>Aneuploidy-associated SASP</b>	<b>IFNA gene set</b>
AREG	IFNA6
CCL2	IFNA8
CCL20	IFNA21
CCL3	IFNA5
CSF1	IFNA16
CSF2	IFNA10
CXCL1	IFNA2
CXCL2	IFNA1
EREG	IFNA7
FAS	IFNA14
FGF2	IFNA13
ICAM1	IFNA17
IGFBP2	IFNA4
IL1A	
IL1B	
IL6	
LIF	
MMP1	
MMP2	
CXCL8	





KEGG_BASAL_TRANSCRIPTION_FACTORS	34	0.325361	0.903558	0.6112532	0.8989622	1	6119
REACTOME_SIGNALING_BY_ROBO_RECEPTOR	29	0.340909	0.89683	0.6340326	0.9136431	1	3995
REACTOME_G1_PHASE	35	0.323864	0.896035	0.64028776	0.9114048	1	6312
REACTOME_MITOCHONDRIAL_TRNA_AMINOACYLATION	21	0.369118	0.895043	0.60954446	0.9094593	1	3562
KEGG_PROXIMAL_TUBULE_BICARBONATE_RECLAMATION	23	0.359846	0.89421	0.6270023	0.9073314	1	3827
BIOCARTA_P53HYPOXIA_PATHWAY	22	0.368836	0.893575	0.6273148	0.9045066	1	1501
REACTOME_INTERACTION_BETWEEN_L1_AND_ANKYRINS	21	0.365477	0.892616	0.61777776	0.90262	1	583
REACTOME_KINESINS	23	0.358895	0.888883	0.6218679	0.90824825	1	9101
REACTOME_METABOLISM_OF_POLYAMINES	15	0.395075	0.883043	0.6231884	0.9194484	1	688
KEGG_PHENYLALANINE_METABOLISM	18	0.379926	0.881748	0.63053095	0.9186142	1	4676
REACTOME_METABOLISM_OF_PROTEINS	421	0.226706	0.88063	0.94074076	0.9170738	1	4530
REACTOME_STEROID_HORMONES	28	0.338296	0.878596	0.62690353	0.91781265	1	567
REACTOME_RNA_POL_III_TRANSCRIPTION_TERMINATION	19	0.360596	0.877485	0.64444447	0.91631633	1	6458
BIOCARTA_MITOCHONDRIA_PATHWAY	21	0.353299	0.877229	0.6396396	0.9127416	1	2470
REACTOME_SULFUR_AMINO_ACID_METABOLISM	24	0.352228	0.876941	0.63752663	0.9092441	1	795
REACTOME_SHC1_EVENTS_IN_EGFR_SIGNALING	15	0.387488	0.875552	0.6272727	0.9087133	1	5036
KEGG_TASTE_TRANSDUCTION	44	0.299893	0.874578	0.6968912	0.90697443	1	3726
REACTOME_REGULATION_OF_INSULIN_LIKE_GROWTH_FACTOR_IGF_ACTIVITY_BY_INSULIN_LIKE_GROWTH_FACTOR_BINDING_PROTEINS_IGFBPS	16	0.375159	0.873693	0.6332623	0.9049986	1	1572
REACTOME_RORA_ACTIVATES_CIRCADIAN_EXPRESSION	24	0.345304	0.871394	0.6595289	0.9063157	1	5049
REACTOME_HIV_LIFE_CYCLE	114	0.259519	0.871377	0.81528664	0.90222454	1	4103
REACTOME_PLATELET_SENSITIZATION_BY_LDL	16	0.386782	0.869662	0.6260504	0.9021305	1	1916
KEGG_PANTOTHENATE_AND_COA_BIOSYNTHESIS	16	0.384878	0.864637	0.6515151	0.91033673	1	57
REACTOME_HOMOLOGOUS_RECOMBINATION_REPAIR_OF_REPLICATION_INDEPENDENT_DOUBLE_STRAND_BREAKS	16	0.372275	0.862205	0.66317993	0.91178536	1	4366
REACTOME_CHYLOMICRON_MEDIATED_LIPID_TRANSPORT	16	0.380346	0.862128	0.6292373	0.9079215	1	2587
REACTOME_SHC1_EVENTS_IN_ERBB4_SIGNALING	20	0.360113	0.860327	0.67264575	0.9080713	1	5111
REACTOME_INFLUENZA_LIFE_CYCLE	136	0.250668	0.860059	0.8722628	0.9046037	1	4103
REACTOME_SYNTHESIS_AND_INTERCONVERSION_OF_NUCLEOTIDE_DI_AND_TRIPHOSPHATES	18	0.362619	0.850298	0.6731602	0.9231615	1	4189
BIOCARTA_CELLCYCLE_PATHWAY	23	0.338512	0.848326	0.6989011	0.92342734	1	930
REACTOME_PRE_NOTCH_TRANSCRIPTION_AND_TRANSLATION	27	0.323538	0.83762	0.7083333	0.9434212	1	1753
KEGG_MELANOMA	71	0.271067	0.83679	0.82058823	0.9411162	1	3820
BIOCARTA_ATM_PATHWAY	20	0.348762	0.836148	0.7256637	0.9382481	1	663
KEGG_SNARE_INTERACTIONS_IN_VESICULAR_TRANSPORT	38	0.302018	0.83443	0.7582697	0.93781126	1	2611
REACTOME_NCAM_SIGNALING_FOR_NEURITE_OUT_GROWTH	64	0.272018	0.830339	0.8060109	0.9422419	1	320
REACTOME_RNA_POL_I_TRANSCRIPTION_TERMINATION	21	0.332772	0.823584	0.72789115	0.9522546	1	3370
KEGG_MISMATCH_REPAIR	23	0.328809	0.820438	0.7256637	0.95464194	1	3384
KEGG_THYROID_CANCER	29	0.311783	0.816313	0.7791262	0.9586997	1	5177
REACTOME_PREFOLDIN_MEDIATED_TRANSFER_OF_SUBSTRATE_TO_CCT_TRIC	25	0.322651	0.810479	0.7710843	0.96577865	1	2271
BIOCARTA_ACTIN_PATHWAY	20	0.339542	0.809163	0.75838923	0.9641299	1	3294
REACTOME_SIGNALING_BY_TGF_BETA_RECEPTOR_COMPLEX	60	0.261314	0.805983	0.8518519	0.9662671	1	3029
REACTOME_SIGNALING_BY_CONSTITUTIVELY_ACTIVE_EGFR	17	0.344139	0.798326	0.75789475	0.976252	1	2531
REACTOME_ZINC_TRANSPORTERS	15	0.345745	0.7953	0.7694013	0.97761196	1	3133
REACTOME_Glutamate_NEUROTRANSMITTER_RELEASE_CYCLE	15	0.350117	0.790896	0.76626015	0.9812927	1	1089
BIOCARTA_ERK_PATHWAY	28	0.304815	0.78599	0.82988507	0.9856851	1	5036
REACTOME_POST_TRANSLATIONAL_PROTEIN_MODIFICATION	179	0.21791	0.782628	0.99615383	0.98714775	1	4324
KEGG_PROSTATE_CANCER	88	0.238026	0.768428	0.9478528	1	1	3034
BIOCARTA_AML_PATHWAY	20	0.313301	0.767067	0.8198198	1	1	4906
REACTOME_DOUBLE_STRAND_BREAK_REPAIR	22	0.309711	0.763524	0.8249453	1	1	4366
REACTOME_PROCESSING_OF_CAPPED_INTRONLESS_PRE_MRNA	23	0.317277	0.763391	0.8149883	1	1	6132
BIOCARTA_PITX2_PATHWAY	15	0.343267	0.758531	0.8097448	1	1	6152
REACTOME_RNA_POL_III_CHAIN_ELONGATION	17	0.329405	0.754798	0.8314351	1	1	6458
REACTOME_BIOSYNTHESIS_OF_THE_N_GLYCAN_PRECURSOR_DOLICHOL_LIPID_LINKED_OLIGOSACCHARIDE_LLO_AND_TRANSFER_TO_A_NASCENT_PROTEIN	28	0.288774	0.751642	0.85131896	1	1	1530
REACTOME_APC_CDC20_MEDIATED_DEGRADATION_OF_NEK2A	21	0.302184	0.739707	0.86206895	1	1	2333
REACTOME_PI_3K_CASCADE	54	0.247967	0.732334	0.9587912	1	1	3488
REACTOME_SIGNALING_BY_INSULIN_RECEPTOR	104	0.214653	0.72562	0.9755245	1	1	3268
REACTOME_SYNTHESIS_OF_GLYCOSYLPHOSPHATIDYLINOSITOL_GPI	17	0.317487	0.718085	0.8532495	1	1	5578
REACTOME_PURINE_METABOLISM	33	0.265501	0.711552	0.9110577	1	1	3467
REACTOME_SMAD2_SMAD3_SMAD4_HETEROTRIMER_REGULATES_TRANSCRIPTION	25	0.281972	0.707454	0.8727273	1	1	6239
BIOCARTA_HIF_PATHWAY	15	0.318605	0.70286	0.87142855	1	1	6268
BIOCARTA_G1_PATHWAY	28	0.266252	0.702377	0.91079813	1	1	5574
REACTOME_A_TETRASACCHARIDE_LINKER_SEQUENCE_IS_REQUIRED_FOR_GAG_SYNTHESIS	25	0.279409	0.698494	0.9166667	1	1	994
REACTOME_HS_GAG_DEGRADATION	20	0.287705	0.693345	0.9031532	1	1	3526
REACTOME_CIRCADIAN_CLOCK	51	0.237343	0.69305	0.9506493	1	1	6362
REACTOME_BMAL1_CLOCK_NPAS2_ACTIVATES_CIRCADIAN_EXPRESSION	35	0.252101	0.690605	0.9514563	1	1	4899
REACTOME_RNA_POL_III_TRANSCRIPTION_INITIATION_FROM_TYPE_3_PROMOTER	26	0.26938	0.686316	0.9320843	1	1	6458
REACTOME_P13K_EVENTS_IN_ERBB2_SIGNALING	42	0.242959	0.68472	0.97783935	1	1	2531
REACTOME_DEADENYLATION_OF_MRNA	19	0.281857	0.671377	0.9273128	1	1	4664
KEGG_O_GLYCAN_BIOSYNTHESIS	29	0.253753	0.668192	0.9649123	1	1	3404
REACTOME_INSULIN_RECEPTOR_SIGNALING_CASCADE	84	0.207176	0.667062	0.99680513	1	1	3268
REACTOME_TRANSLATION	147	0.187013	0.652252	1	1	1	3509
REACTOME_NUCLEAR_RECEPTOR_TRANSCRIPTION_PATHWAY	47	0.228047	0.650082	0.984252	1	1	1168
KEGG_NUCLEOTIDE_EXCISION_REPAIR	44	0.220619	0.642355	0.9727723	1	1	6900
KEGG_ONE_CARBON_POOL_BY_FOLATE	17	0.275636	0.638603	0.9252137	1	1	7894
REACTOME_CIRCADIAN_REPRESSION_OF_EXPRESSION_BY_REV_ERBA	23	0.255637	0.634617	0.95681816	1	1	4899
BIOCARTA_SHH_PATHWAY	16	0.273708	0.629782	0.9413043	1	1	4751
REACTOME_TRANSFERRIN_ENDOCYTOSIS_AND_RECYCLING	24	0.248904	0.621073	0.96803653	1	1	4666
REACTOME_SHC_MEDIATED_SIGNALING	15	0.271423	0.611833	0.9527027	1	1	1655
REACTOME_TRANSCRIPTIONAL_ACTIVITY_OF_SMAD2_SMAD3_SMAD4_HETEROTRIMER	36	0.218394	0.603626	0.99731183	1	1	6239
REACTOME_SRP_DEPENDENT_COTRANSLATIONAL_PROTEIN_TARGETING_TO_MEMBRANE	110	0.175991	0.589149	1	1	1	2081
REACTOME_INFLUENZA_VIRAL_RNA_TRANSCRIPTION_AND_REPLICATION	102	0.170044	0.568726	1	1	1	2081
REACTOME_SHC_RELATED_EVENTS	17	0.245577	0.565353	0.9774775	1	1	1655
BIOCARTA_BARRESTIN_SRC_PATHWAY	15	0.243879	0.54886	0.98004436	1	1	6303
REACTOME_INHIBITION_OF_THE_PROTEOLYTIC_ACTIVITY_OF_APC_C_REQUIRED_FOR_THE_ONSET_OF_ANAPHASE_BY_MITOTIC_SPINDLE_CHECKPOINT_COMPONENTS	18	0.222638	0.51956	0.9912088	1	1	2333
REACTOME_CTNNB1_PHOSPHORYLATION_CASCADE	16	0.210932	0.484911	0.9843049	1	1	6152
BIOCARTA_CERAMIDE_PATHWAY	22	0.194343	0.4739	0.9977064	1	1	5983
KEGG_TERPENOID_BACKBONE_BIOSYNTHESIS	15	0.204606	0.455568	0.9958592	1	1	6952
REACTOME_ENERGY_DEPENDENT_REGULATION_OF_MTOR_BY_LKB1_AMPK	17	0.154424	0.362149	1	0.9999491	1	7332

















REACTOME_A_TETRASACCHARIDE_LINKER_SEQUENCE_IS_REQUIRED_FOR_GAG_SYNTHESIS	25	0.32839	0.838496	0.7311321	0.974537	1	1151
REACTOME_GLYCOSE_METABOLISM	64	0.269366	0.83769	0.81556195	0.9713127	1	3497
KEGG_PURINE_METABOLISM	156	0.232621	0.834497	0.9366516	0.9738739	1	4431
KEGG_PANTOTHENATE_AND_COA_BIOSYNTHESIS	16	0.367397	0.833408	0.6859504	0.9713969	1	1211
KEGG_GLYCOGEN_PATHWAY	28	0.31768	0.832433	0.73965937	0.9688097	1	3052
REACTOME_GLYCERATE_NEUROTRANSMITTER_RELEASE_CYCLE	15	0.366501	0.822135	0.7120879	0.9857624	1	754
REACTOME_KINESINS	23	0.324903	0.821806	0.72596157	0.98155564	1	8375
REACTOME_DOUBLE_STRAND_BREAK_REPAIR	22	0.327565	0.821786	0.7278761	0.9768117	1	59
KEGG_SPHINGOLIPID_METABOLISM	39	0.291055	0.821786	0.8109589	0.9720699	1	3709
REACTOME_SHC1_EVENTS_IN_EGFR_SIGNALING	15	0.356468	0.821719	0.7	0.96753186	1	4473
KEGG_PORPHYRIN_AND_CHLOROPHYLL_METABOLISM	39	0.285283	0.816964	0.78446114	0.97232	1	3223
REACTOME_DARPP32_EVENTS	24	0.318266	0.811709	0.77261615	0.97792643	1	949
KEGG_SMALL_CELL_LUNG_CANCER	84	0.248463	0.810873	0.88387096	0.97491497	1	3664
REACTOME_INHIBITION_OF_THE_PROTEOLYTIC_ACTIVITY_OF_APC_C_REQUIRED_FOR_THE_ONSET_OF_ANAPHASE_BY_MITOTIC_SPINDLE_CHECKPOINT_COMPONENTS	18	0.338813	0.810336	0.7201835	0.97126454	1	5433
REACTOME_DOWNREGULATION_OF_TGF_BETA_RECEPTOR_SIGNALING	21	0.32006	0.798857	0.7644445	0.9878821	1	4774
KEGG_MISMATCH_REPAIR	23	0.308993	0.794459	0.7701422	0.9909085	1	4758
REACTOME_MITOCHONDRIAL_TRNA_AMINOACYLATION	21	0.325317	0.793601	0.75296915	0.98770875	1	2998
REACTOME_GLYCATION_CONJUGATION	22	0.315715	0.788675	0.8053528	0.9916118	1	5216
REACTOME_G1_PHASE	35	0.282498	0.787875	0.83937824	0.98849857	1	3163
REACTOME_RNA_POL_III_TRANSCRIPTION_TERMINATION	19	0.328696	0.787057	0.78483605	0.9853419	1	4406
REACTOME_ZINC_TRANSPORTERS	15	0.343266	0.780698	0.7827051	0.9911039	1	4637
REACTOME_PTM_GAMMA_CARBOXYLATION_HYPUISINE_FORMATION_AND_ARYLSULFATASE_ACTIVATION	26	0.304187	0.779905	0.81113803	0.9878738	1	1559
REACTOME_FATTY_ACID_TRIACYLGLYCEROL_AND_KETONE_BODY_METABOLISM	167	0.215497	0.776877	0.9834025	0.9880686	1	3371
KEGG_PITX2_PATHWAY	15	0.338221	0.771901	0.77102804	0.9913178	1	1633
REACTOME_RNA_POL_III_CHAIN_ELONGATION	17	0.326992	0.768899	0.81100476	0.9911907	1	4406
REACTOME_METABOLISM_OF_STEROID_HORMONES_AND_VITAMINS_A_AND_D	34	0.273971	0.764574	0.8682927	0.9930346	1	1822
KEGG_ATRBRA_PATHWAY	21	0.309393	0.760355	0.79334915	0.99437445	1	2328
KEGG_PRIMARY_BILE_ACID_BIOSYNTHESIS	16	0.322802	0.750778	0.81400967	1	1	5074
KEGG_BETA_ALANINE_METABOLISM	22	0.299269	0.745157	0.85091746	1	1	2261
REACTOME_AMINE_LIGAND_BINDING_RECEPTORS	30	0.271046	0.734404	0.90076333	1	1	901
KEGG_OOCYTE_MEIOSIS	111	0.215373	0.728819	0.9895105	1	1	5205
REACTOME_PREFOLDIN_MEDIATED_TRANSFER_OF_SUBSTRATE_TO_CCT_TRIC	25	0.278434	0.7208	0.89772725	1	1	3296
KEGG_PROSTATE_CANCER	88	0.221018	0.718948	0.990625	1	1	4208
REACTOME_NCAM_SIGNALING_FOR_NEURITE_OUT_GROWTH	64	0.227021	0.71584	0.96438354	1	1	3886
REACTOME_GLOBAL_GENOMIC_NER_GG_NER	33	0.259129	0.711103	0.89646465	1	1	4834
REACTOME_BIOSYNTHESIS_OF_THE_N_GLYCAN_PRECURSOR_DOLICHOL_LIPID_LINKED_O_LIGOSACCHARIDE_LLO_AND_TRANSFER_TO_A_NASCENT_PROTEIN	28	0.271005	0.701739	0.9147465	1	1	3001
REACTOME_CONVERSION_FROM_APC_C_CDC20_TO_APC_C_CDH1_IN_LATE_ANAPHASE	16	0.301917	0.701196	0.86946905	1	1	5433
REACTOME_ACYL_CHAIN_REMODELLING_OF_PG	15	0.301446	0.688813	0.87782806	1	1	1410
REACTOME_TGF_BETA_RECEPTOR_SIGNALING_ACTIVATES_SMADS	24	0.266147	0.686114	0.94183445	1	1	4774
KEGG_CARM_ER_PATHWAY	35	0.243743	0.67777	0.95595855	1	1	4511
REACTOME_PYRUVATE_METABOLISM	18	0.283381	0.674789	0.9057971	1	1	4520
REACTOME_STEROID_HORMONES	28	0.258219	0.671929	0.9443038	1	1	386
REACTOME_GRB2_EVENTS_IN_ERBB2_SIGNALING	22	0.263886	0.663835	0.9413093	1	1	6560
KEGG_OTHER_GLYCAN_DEGRADATION	16	0.286161	0.660193	0.8975501	1	1	1205
KEGG_EIF_PATHWAY	16	0.28344	0.656585	0.93453723	1	1	1474
KEGG_BLADDER_CANCER	42	0.229964	0.651932	0.97461927	1	1	3770
KEGG_DRUG_METABOLISM_OTHER_ENZYMES	49	0.222539	0.649809	0.9848101	1	1	2834
REACTOME_PHOSPHORYLATION_OF_THE_APC_C	17	0.279755	0.647967	0.92410713	1	1	5433
REACTOME_PI3K_CASCADE	54	0.213189	0.645941	0.98559076	1	1	5381
KEGG_AGR_PATHWAY	36	0.229651	0.635679	0.97105265	1	1	3135
REACTOME_SYNTHESIS_OF_BILE_ACIDS_AND_BILE_SALTS_VIA_7ALPHA_HYDROXYCHOLESTEROL	15	0.278441	0.630066	0.9263158	1	1	5600
REACTOME_APC_C_CDC20_MEDIATED_DEGRADATION_OF_CYCLIN_B	19	0.262629	0.629567	0.947619	0.99813354	1	5433
KEGG_NDKDYNAMIN_PATHWAY	18	0.269743	0.625561	0.94725275	0.9957655	1	3132
REACTOME_PPARA_ACTIVATES_GENE_EXPRESSION	104	0.187198	0.625293	1	0.99188656	1	3371
REACTOME_INFLUENZA_LIFE_CYCLE	136	0.175907	0.621058	1	0.98961276	1	4617
REACTOME_SYNTHESIS_OF_BILE_ACIDS_AND_BILE_SALTS	19	0.253764	0.617989	0.9675174	0.9868294	1	5600
REACTOME_SHC_MEDIATED_SIGNALING	15	0.262253	0.584576	0.9622222	0.992697	1	4473
KEGG_SHH_PATHWAY	16	0.25386	0.584095	0.96351933	0.9888904	1	3455
REACTOME_METABOLISM_OF_VITAMINS_AND_COFACTORS	50	0.18014	0.540497	0.99710983	0.9927477	1	3207













REACTOME_INSULIN_SYNTHESIS_AND_PROCESSING	20	-0.320024	-0.715567	0.8460177	0.9760173	1	4503 tags=30%, list=23%, signal=39%
KEGG_ALPHA_LINOLENIC_ACID_METABOLISM	15	-0.335895	-0.714253	0.83302754	0.9755561	1	2148 tags=33%, list=11%, signal=37%
REACTOME_METAL_ION_SLC_TRANSPORTERS	22	-0.309791	-0.71005	0.8894831	0.9782005	1	1683 tags=14%, list=9%, signal=15%
REACTOME_PI3K_CASCADE	68	-0.249406	-0.706686	0.9582043	0.9797577	1	3970 tags=24%, list=21%, signal=30%
REACTOME_L1CAM_INTERACTIONS	84	-0.24142	-0.705869	0.9636099	0.97878844	1	3352 tags=19%, list=17%, signal=23%
REACTOME_SIGNALING_BY_BMP	22	-0.30503	-0.703371	0.8705674	0.9793487	1	3409 tags=27%, list=18%, signal=33%
REACTOME_DEADENYLATION_OF_MRNA	19	-0.312823	-0.699452	0.8938849	0.98124206	1	3622 tags=32%, list=19%, signal=39%
REACTOME_SIGNALING_BY_INSULIN_RECEPTOR	104	-0.232768	-0.698298	0.9818689	0.98050326	1	4344 tags=27%, list=22%, signal=35%
REACTOME_FORMATION_OF_INCISION_COMPLEX_IN_GG_NER	21	-0.301442	-0.692932	0.9027778	0.9836121	1	2407 tags=19%, list=12%, signal=22%
KEGG_VIBRIO_CHOLERAE_INFECTION	53	-0.254406	-0.690984	0.9330065	0.9835881	1	1852 tags=13%, list=10%, signal=15%
KEGG_GLYCOSAMINOGLYCAN_BIOSYNTHESIS_CHONDROITIN_SULFATE	22	-0.297505	-0.684483	0.91071427	0.9872328	1	1999 tags=18%, list=10%, signal=20%
REACTOME_ENOS_ACTIVATION_AND_REGULATION	19	-0.302111	-0.679006	0.90575916	0.9898656	1	269 tags=5%, list=1%, signal=5%
KEGG_PROXIMAL_TUBULE_BICARBONATE_RECLAMATION	23	-0.284239	-0.663994	0.902439	0.9963672	1	2875 tags=30%, list=15%, signal=36%
REACTOME_TRANSLATION	147	-0.21329	-0.663994	0.9945726	0.9971091	1	3977 tags=16%, list=21%, signal=20%
REACTOME_RNA_POL_III_TRANSCRIPTION_INITIATION_FROM_TYPE_3_PROMOTER	26	-0.278229	-0.661865	0.9394464	0.9966464	1	171 tags=4%, list=1%, signal=4%
REACTOME_SRP_DEPENDENT_COTRANSLATIONAL_PROTEIN_TARGETING_TO_MEMBRANE	110	-0.217884	-0.65727	0.9958449	0.9978254	1	3977 tags=16%, list=21%, signal=20%
REACTOME_PURINE_METABOLISM	33	-0.262993	-0.656635	0.950764	0.9964178	1	3856 tags=30%, list=20%, signal=38%
REACTOME_INSULIN_RECEPTOR_SIGNALING_CASCADE	84	-0.226203	-0.655465	0.99277455	0.99537104	1	4344 tags=26%, list=22%, signal=34%
BIOCARTA_RACCYCD_PATHWAY	26	-0.2737	-0.65368	0.9324547	0.9946653	1	2656 tags=15%, list=14%, signal=18%
BIOCARTA_ACTINY_PATHWAY	20	-0.295755	-0.649893	0.91943955	0.99524635	1	3621 tags=30%, list=19%, signal=37%
REACTOME_CHONDROITIN_SULFATE_BIOSYNTHESIS	19	-0.289207	-0.645917	0.94727594	0.99582535	1	4786 tags=42%, list=25%, signal=56%
REACTOME_ACTIVATED_AMPK_STIMULATES_FATTY_ACID_OXIDATION_IN_MUSCLE	18	-0.28986	-0.638158	0.9381818	0.99837476	1	3070 tags=28%, list=16%, signal=33%
REACTOME_INSULIN_RECEPTOR_RECYCLING	22	-0.275272	-0.634939	0.9300341	0.99821424	1	5227 tags=45%, list=27%, signal=62%
REACTOME_PI3K_EVENTS_IN_ERBB2_SIGNALING	42	-0.241929	-0.632374	0.9549249	0.9977341	1	3733 tags=17%, list=19%, signal=21%
REACTOME_METABOLISM_OF_PROTEINS	421	-0.185197	-0.630972	1	0.99663234	1	3701 tags=16%, list=19%, signal=19%
BIOCARTA_CK1_PATHWAY	17	-0.288032	-0.623582	0.914611	0.998367	1	5505 tags=47%, list=28%, signal=66%
REACTOME_ENERGY_DEPENDENT_REGULATION_OF_MTOR_BY_LKB1_AMPK	17	-0.282806	-0.61727	0.9310987	0.9994191	1	3070 tags=29%, list=16%, signal=35%
REACTOME_CITRIC_ACID_CYCLE_TCA_CYCLE	19	-0.267336	-0.599544	0.9607843	1	1	5253 tags=32%, list=27%, signal=43%
REACTOME_SIGNALING_BY_CONSTITUTIVELY_ACTIVE_EGFR	17	-0.265338	-0.588285	0.9634146	1	1	4276 tags=29%, list=22%, signal=38%
BIOCARTA_BARRESTIN_SRC_PATHWAY	15	-0.276828	-0.584767	0.9669725	1	1	2656 tags=27%, list=14%, signal=31%
REACTOME_TRANSFERRIN_ENDOCYTOSIS_AND_RECYCLING	24	-0.246405	-0.57551	0.97727275	1	1	5227 tags=46%, list=27%, signal=63%
REACTOME_CYCLIN_A_B1_ASSOCIATED_EVENTS_DURING_G2_M_TRANSITION	15	-0.265094	-0.568964	0.9715808	1	1	2081 tags=13%, list=11%, signal=15%
KEGG_OLFACTORY_TRANSDUCTION	118	-0.183274	-0.563515	1	1	1	5428 tags=21%, list=28%, signal=29%
REACTOME_SYNTHESIS_SECRETION_AND_INACTIVATION_OF_GLP1	17	-0.253845	-0.544989	0.96892136	1	1	3220 tags=18%, list=17%, signal=21%
REACTOME_PYRUVATE_METABOLISM_AND_CITRIC_ACID_TCA_CYCLE	40	-0.204317	-0.534722	0.996748	1	1	3887 tags=18%, list=20%, signal=22%
REACTOME_SHC_RELATED_EVENTS	17	-0.242006	-0.532551	0.97806215	1	1	4344 tags=41%, list=22%, signal=53%
REACTOME_CREB_PHOSPHORYLATION_THROUGH_THE_ACTIVATION_OF_CAMKII	15	-0.24108	-0.519183	0.9842209	1	1	4957 tags=47%, list=26%, signal=63%
REACTOME_RECYCLING_PATHWAY_OF_L1	27	-0.210367	-0.504187	0.9935065	1	1	5710 tags=37%, list=30%, signal=52%
REACTOME_INCRETIN_SYNTHESIS_SECRETION_AND_INACTIVATION	20	-0.221099	-0.497781	0.9894921	1	1	3220 tags=15%, list=17%, signal=18%
REACTOME_PIP3_ACTIVATES_AKT_SIGNALING	27	-0.203992	-0.485553	0.99823636	1	1	5180 tags=26%, list=27%, signal=35%
REACTOME_SHC1_EVENTS_IN_ERBB4_SIGNALING	20	-0.214823	-0.479978	0.9893617	1	1	4344 tags=30%, list=22%, signal=39%
BIOCARTA_P53HYPOXIA_PATHWAY	22	-0.208517	-0.476881	0.9929453	0.99877846	1	4807 tags=27%, list=25%, signal=36%
REACTOME_OLFACTORY_SIGNALING_PATHWAY	80	-0.150169	-0.427563	1	0.99907035	1	4055 tags=11%, list=21%, signal=14%

**Table S20**  
**Association between SASP signature pathway and copy number alterations in HPV-negative HNSC cell lines.**

**S20A**

**Logistic Regression for the prediction of SASP enrichment in HNSC cell lines (CCLE) - after separating arm-level and focal-level loss at 9p21.3**

Distinction between tumors showing arm-only, focal-only events and a combination of both.

**SASP enrichment**

Top and bottom 35% of the distributions were considered.

	$\beta$ coefficient	z value	Pr(> z )	FDR	OR
9p21.3 Loss: ARM	-3.465736	-2.619891	0.008796	0.017592	0.03125 binary
9p21.3 Loss: FOCAL	-2.772589	-1.711297	0.087026	0.087026	0.0625 binary

For each copy number event, we used copy number values after standardization.

	$\beta$ coefficient	z value	Pr(> z )	FDR	OR
9p21.3 copy number ARM Level	0.7924514	1.646595	0.099641	0.199283	2.208804 continuous
9p21.3 copy number FOCAL Level	-34.3869968	-0.006174	0.995074	0.995074	1.16E-15 continuous

**SASP enrichment**

Top and bottom 50% of the distributions were considered.

	$\beta$ coefficient	z value	Pr(> z )	FDR	OR
9p21.3 Loss: ARM	-1.856298	-2.155478	0.031124	0.062249	0.15625 binary
9p21.3 Loss: FOCAL	-1.974081	-1.552584	0.120523	0.120523	0.138889 binary

For each copy number event, we used copy number values after standardization.

	$\beta$ coefficient	z value	Pr(> z )	FDR	OR
9p21.3 copy number ARM Level	0.4695842	1.186006	0.23562	0.47124	1.599329 continuous
9p21.3 copy number FOCAL Level	-33.6715041	-0.006905	0.994491	0.994491	2.38E-15 continuous

**SASP enrichment**

Top and bottom 35% of the distributions were considered.

	$\beta$ coefficient	z value	Pr(> z )	FDR	OR
9p21.3 Loss: ARM	-4.852692	-2.509997	0.012073	0.03622	0.007807 binary
9p21.3 Loss: FOCAL	-4.884157	-2.112046	0.034663	0.052024	0.007565 binary
SCNA level	-1.531852	-1.718469	0.085711	0.085711	0.216135 continuous

For each copy number event, we used copy number values after standardization.

	$\beta$ coefficient	z value	Pr(> z )	FDR	OR
9p21.3 copy number ARM Level	0.8971552	1.763381	0.077836	0.233509	2.452616 continuous
9p21.3 copy number FOCAL Level	-34.017447	-0.005999	0.995214	0.995214	1.68E-15 continuous
SCNA level	-0.6681904	-1.22247	0.22153	0.332295	0.512635 continuous

**S20B**

**Logistic Regression for the prediction of SASP enrichment in HNSC cell lines (CCLE) - after separating arm-level and focal-level loss at 3p14.**

Distinction between tumors showing arm-only, focal-only events and a combination of both.

**SASP enrichment**

Top and bottom 35% of the distributions were considered.

	$\beta$ coefficient	z value	Pr(> z )	FDR	OR
3p14 Loss: ARM	-0.5596158	-0.420888	0.673837	0.673837	0.571429 binary
3p14 Loss: FOCAL	-1.7917595	-1.064464	0.287118	0.574237	0.166667 binary

For each copy number event, we used copy number values after standardization.

	$\beta$ coefficient	z value	Pr(> z )	FDR	OR
3p14 copy number ARM Level	-0.3296374	-0.64421	0.519439	0.519439	0.719184 continuous
3p14 copy number FOCAL Level	0.9255492	1.015226	0.309998	0.519439	2.523254 continuous

**SASP enrichment**

Top and bottom 50% of the distributions were considered.

	$\beta$ coefficient	z value	Pr(> z )	FDR	OR
3p14 Loss: ARM	-0.2231436	-0.221307	0.824853	0.824853	0.8 binary
3p14 Loss: FOCAL	-1.7917595	-1.241368	0.21447	0.42894	0.166667 binary

For each copy number event, we used copy number values after standardization.

	$\beta$ coefficient	z value	Pr(> z )	FDR	OR
3p14 copy number ARM Level	-0.4207858	-0.964783	0.334654	0.334654	0.656531 continuous
3p14 copy number FOCAL Level	0.9358364	1.08422	0.278267	0.334654	2.549345 continuous

**SASP enrichment**

Top and bottom 35% of the distributions were considered.

	$\beta$ coefficient	z value	Pr(> z )	FDR	OR
3p14 Loss: ARM	-0.5015306	-0.373447	0.708816	0.708816	0.605603 binary
3p14 Loss: FOCAL	-1.733305	-1.017104	0.309104	0.563351	0.176699 binary
SCNA level	-0.4339868	-0.886093	0.375568	0.563351	0.647921 continuous

For each copy number event, we used copy number values after standardization.

	$\beta$ coefficient	z value	Pr(> z )	FDR	OR
3p14 copy number ARM Level	-0.1552262	-0.287761	0.77353	0.77353	0.856221 continuous
3p14 copy number FOCAL Level	1.2632036	1.188531	0.234624	0.383854	3.536734 continuous
SCNA level	-0.6588838	-1.136447	0.255769	0.383854	0.517439 continuous











REACTOME_APC_C_CDC20_MEDIATED_DEGRADATION_OF_CYCLIN_B	19	-0.41498	-0.909393	0.58894646	0.7684364	1	109
BIOCARTA_ARF_PATHWAY	17	-0.428125	-0.908937	0.6299484	0.76785415	1	2990
REACTOME_METABOLISM_OF_PROTEINS	422	-0.285477	-0.907225	0.7312296	0.76974905	1	3044
KEGG_TASTE_TRANSDUCTION	51	-0.348326	-0.904195	0.63338304	0.774478	1	2098
REACTOME_BIOSYNTHESIS_OF_THE_N_GLYCAN_PRECURSOR_DOLICHOH_LIPID_LINKED_OLIGOSACCHARIDE_LL	28	-0.394092	-0.901959	0.6196513	0.777535	1	3344
REACTOME_PRE_NOTCH_PROCESSING_IN_GOLGI	16	-0.438637	-0.900337	0.62432915	0.7793128	1	3431
REACTOME_SYNTHESIS_OF_BILE_ACIDS_AND_BILE_SALTS	19	-0.413569	-0.898448	0.6211382	0.78149563	1	3661
REACTOME_UNFOLDED_PROTEIN_RESPONSE	76	-0.330674	-0.894229	0.6526459	0.78860307	1	2440
REACTOME_ACTIVATION_OF_NF_KAPPAB_IN_B_CELLS	61	-0.343775	-0.893682	0.6495957	0.7881682	1	2223
KEGG_GLYCOLYTIC_SIGNALING_PATHWAY	67	-0.320263	-0.89146	0.6592479	0.791114	1	2345
REACTOME_PHASEI_FUNCTIONALIZATION_OF_COMPOUNDS	69	-0.33116473	-0.891285	0.6676301	0.7988373	1	3661
REACTOME_PROSTACYCLIN_SIGNALING_THROUGH_PROSTACYCLIN_RECEPTOR	19	-0.413617	-0.889327	0.6471572	0.7922459	1	897
REACTOME_KERATAN_SULFATE_BIOSYNTHESIS	26	-0.385801	-0.889512	0.6286201	0.79226935	1	3431
REACTOME_ADP_SIGNALING_THROUGH_P2RY1	25	-0.394867	-0.888414	0.62222224	0.79085326	1	1117
KEGG_WNT_SIGNALING_PATHWAY	150	-0.300921	-0.887246	0.72095805	0.79167455	1	2949
REACTOME_DOWNSTREAM_SIGNALING_EVENTS_OF_B_CELL_RECEPTOR_BCR	92	-0.31852	-0.886073	0.65539664	0.7922254	1	2223
REACTOME_AMYLOIDS	76	-0.326171	-0.884749	0.66944444	0.7933415	1	2394
REACTOME_BOTULINUM_NEUROTOXICITY	18	-0.420018	-0.884047	0.62051284	0.79310703	1	2065
KEGG_NICOTINATE_AND_NICOTINAMIDE_METABOLISM	24	-0.392834	-0.882619	0.6628478	0.7942912	1	3368
REACTOME_ACTIVATION_OF_THE_MRNA_UPON_BINDING_OF_THE_CAP_BINDING_COMPLEX_AND_EIF5_AND_SUE	57	-0.336226	-0.877202	0.66248256	0.8036385	1	5815
REACTOME_PHOSPHORYLATION_OF_THE_APC_C	17	-0.409407	-0.876864	0.63468015	0.8026842	1	109
KEGG_BETA_ALANINE_METABOLISM	22	-0.393923	-0.87537	0.65139115	0.80404234	1	3821
KEGG_GLYCOSAMINOGLYCAN_BIOSYNTHESIS_HEPARAN_SULFATE	26	-0.38109	-0.875035	0.63857377	0.8030728	1	3235
REACTOME_MAPK_TARGETS_NUCLEAR_EVENTS_MEDIATED_BY_MAP_KINASES	30	-0.369852	-0.872363	0.64162755	0.8066701	1	5935
REACTOME_TRANS_GOLGI_NETWORK_VESICLE_BUDDING	59	-0.329536	-0.868586	0.68265164	0.812729	1	4072
KEGG_BUTANOATE_METABOLISM	34	-0.359569	-0.864747	0.68621236	0.81886595	1	1896
REACTOME_ENDOGENOUS_STEROLS	15	-0.408557	-0.860498	0.66972476	0.8254858	1	4340
KEGG_AMINOACYL_TRNA_BIOSYNTHESIS	41	-0.345852	-0.859603	0.7016743	0.82561976	1	659
KEGG_NOTCH_SIGNALING_PATHWAY	47	-0.33395	-0.859478	0.69777775	0.8242276	1	988
KEGG_ADIPOLYTIC_SIGNALING_PATHWAY	67	-0.322748	-0.859392	0.7590249	0.82774824	1	1716
KEGG_SPHINGOLIPID_METABOLISM	39	-0.342416	-0.851348	0.70750386	0.8364014	1	2626
REACTOME_TRNA_AMINOACYLATION	42	-0.340455	-0.847261	0.71080667	0.84269583	1	659
BIOCARTA_IGF1MTOX_PATHWAY	20	-0.391613	-0.845424	0.68585527	0.84451026	1	2825
REACTOME_REGULATION_OF_MRNA_STABILITY_BY_PROTEINS_THAT_BIND_AU_RICH_ELEMENTS	81	-0.30738	-0.845097	0.7455296	0.843501	1	2223
REACTOME_TRANSPORT_OF_GLUCOSE_AND_OTHER_SUGARS_BILE_SALTS_AND_ORGANIC_ACIDS_METAL_IONS	89	-0.304972	-0.844614	0.7520107	0.84270555	1	3349
KEGG_PHENYLALANINE_METABOLISM	18	-0.390474	-0.843251	0.679868	0.8438651	1	2344
REACTOME_SLC_MEDIATED_TRANSMEMBRANE_TRANSPORT	240	-0.271032	-0.833869	0.837963	0.8594955	1	2512
KEGG_P53_SIGNALING_PATHWAY	67	-0.308986	-0.833002	0.7479893	0.8593835	1	1892
KEGG_VIBRIO_CHOLERAE_INFECTION	54	-0.319407	-0.828957	0.754173	0.8653242	1	1626
REACTOME_GOLGI_ASSOCIATED_VESICLE_BIOSYNTHESIS	52	-0.323384	-0.82626	0.7684515	0.868613	1	4072
REACTOME_INWARDLY_RECTIFYING_K_CHANNELS	31	-0.345383	-0.826066	0.74615383	0.8672585	1	2135
REACTOME_CELL_JUNCTION_ORGANIZATION	77	-0.299217	-0.826025	0.79727894	0.865639	1	3265
KEGG_SMALL_CELL_LUNG_CANCER	84	-0.299082	-0.821688	0.7911051	0.87196344	1	3594
REACTOME_GABA_SYNTHESIS_RELEASE_REUPTAKE_AND_DEGRADATION	17	-0.394891	-0.821045	0.71428573	0.8713924	1	3753
REACTOME_DESTABILIZATION_OF_MRNA_BY_BRF1	17	-0.382653	-0.819127	0.714527	0.8729923	1	3717
KEGG_INOSITOL_PHOSPHATE_METABOLISM	54	-0.310626	-0.810317	0.80780345	0.88664806	1	2523
REACTOME_ANTIVIRAL_MECHANISM_BY_IFN_STIMULATED_GENES	65	-0.303413	-0.808838	0.8175389	0.8874882	1	1577
KEGG_STARCH_AND_SUCROSE_METABOLISM	49	-0.319043	-0.808484	0.7796374	0.8864626	1	3408
REACTOME_INHIBITION_OF_VOLTAGE_GATED_CA2_CHANNELS_VIA_GBETA_GAMMA_SUBUNITS	25	-0.35546	-0.807793	0.7451613	0.8859923	1	2135
REACTOME_DARPP_32_EVENTS	24	-0.349992	-0.80476	0.7590249	0.8859926	1	5094
REACTOME_GLUCAAGON_TYPE_LIGAND_RECEPTORS	33	-0.330969	-0.803665	0.7816265	0.88978523	1	1475
REACTOME_INHIBITION_OF_THE_PROTEOLYTIC_ACTIVITY_OF_APC_C_REQUIRED_FOR_THE_ONSET_OF_ANAPHAS	18	-0.376164	-0.803664	0.7361111	0.88808715	1	109
REACTOME_SIGNALING_BY_NOTCH	99	-0.284701	-0.802705	0.85128206	0.8880725	1	3515
REACTOME_SIGNALING_BY_FGFR1_MUTANTS	28	-0.342527	-0.801833	0.7755102	0.887816	1	3053
REACTOME_NEPHRIN_INTERACTIONS	19	-0.369823	-0.798597	0.7350877	0.89163345	1	5792
BIOCARTA_AML_PATHWAY	20	-0.374604	-0.794875	0.7615894	0.8960689	1	4830
REACTOME_INSULIN_SYNTHESIS_AND_PROCESSING	20	-0.361479	-0.79047	0.7436333	0.9015925	1	2955
REACTOME_PRE_NOTCH_TRANSCRIPTION_AND_TRANSLATION	27	-0.339037	-0.788273	0.7752066	0.9033928	1	89
REACTOME_FORMATION_OF_INCISION_COMPLEX_IN_GG_NER	21	-0.353711	-0.787033	0.7561779	0.9037108	1	14
REACTOME_CTNNB1_PHOSPHORYLATION_CASCADE	16	-0.376249	-0.78695	0.76584506	0.90215254	1	602
BIOCARTA_MTA3_PATHWAY	19	-0.359245	-0.784736	0.7740303	0.90410954	1	4105
REACTOME_XENOBIOTICS	15	-0.375519	-0.784479	0.7474403	0.90286434	1	4760
KEGG_SELENOAMINO_ACID_METABOLISM	26	-0.340402	-0.784298	0.79375	0.90146804	1	1889
BIOCARTA_MPR_PATHWAY	34	-0.326529	-0.784008	0.7893916	0.90026	1	4320
KEGG_GLYCOSAMINOGLYCAN_BIOSYNTHESIS_CHONDROITIN_SULFATE	22	-0.341931	-0.776564	0.779661	0.91003215	1	3498
REACTOME_GLYCOGEN_BREAKDOWN_GLYCOGENOLYSIS	16	-0.373035	-0.774704	0.7804878	0.9113505	1	1197
REACTOME_ABCA_TRANSPORTERS_IN_LIPID_HOMEOSTASIS	17	-0.365823	-0.77086	0.8044218	0.91568774	1	5158
REACTOME_METAL_ION_SLC_TRANSPORTERS	22	-0.343155	-0.770264	0.8039867	0.9148409	1	2378
REACTOME_PURINE_METABOLISM	33	-0.319243	-0.768295	0.796875	0.9161606	1	1796
REACTOME_COX2_TRANSMITTER_RESPIRATORY_ELECTRON_TRANSPORT	20	-0.326931	-0.7652	0.8076076	0.9169076	1	220
REACTOME_NEUROTRANSMITTER_RELEASE_CYCLE	34	-0.319367	-0.764318	0.84326017	0.91844934	1	3753
REACTOME_SIGNALING_BY_ROBO_RECEPTOR	29	-0.318613	-0.757674	0.83548385	0.926346	1	4671
REACTOME_GLUCAAGON_SIGNALING_IN_METABOLIC_REGULATION	33	-0.315015	-0.755597	0.8539157	0.92767715	1	1681
REACTOME_REGULATION_OF_APOPTOSIS	56	-0.289258	-0.755315	0.8809182	0.92639977	1	2223
REACTOME_SIGNAL_TRANSDUCTION_BY_L1	34	-0.311378	-0.75415	0.84076434	0.92633367	1	4685
REACTOME_VOLTAGE_GATED_POTASSIUM_CHANNELS	43	-0.301416	-0.750408	0.8781575	0.92968476	1	1606
REACTOME_INFLUENZA_LIFE_CYCLE	136	-0.255666	-0.742948	0.9520295	0.93770105	1	718
REACTOME_GAB1_SIGNALOSOME	36	-0.300756	-0.739129	0.8556391	0.9408471	1	3307
KEGG_UBIQUITIN_MEDIATED_PROTEOLYSIS	134	-0.252953	-0.733906	0.9455006	0.94553185	1	1927
BIOCARTA_TNFR1_PATHWAY	29	-0.308342	-0.730797	0.86846274	0.94763726	1	4095
REACTOME_DOWNREGULATION_OF_TGF_BETA_RECEPTOR_SIGNALING	21	-0.326935	-0.724071	0.8598616	0.95381194	1	268
REACTOME_DEADENYLATION_DEPENDENT_MRNA_DECAY	44	-0.284287	-0.718413	0.9138973	0.9584092	1	1997
REACTOME_REGULATION_OF_INSULIN_LIKE_GROWTH_FACTOR_IGF_ACTIVITY_BY_INSULIN_LIKE_GROWTH_FACT	16	-0.341021	-0.718235	0.83779263	0.95690286	1	2729
KEGG_ALPHA_LINOLENIC_ACID_METABOLISM	17	-0.344082	-0.718169	0.840604	0.95527446	1	3098
REACTOME_BMAL1_CLOCK_NPAS2_ACTIVATES_CIRCADIAN_EXPRESSION	36	-0.290552	-0.714093	0.9050536	0.95800055	1	3598
REACTOME_GLUCOSE_METABOLISM	64	-0.268994	-0.713682	0.9374131	0.95675236	1	1197
REACTOME_ACYL_CHAIN_REMODELLING_OF_PG	16	-0.345389	-0.713307	0.82807016	0.95545001	1	2063
KEGG_OLFACTORY_TRANSDUCTION	346	-0.225016	-0.708377	1	0.95884	1	5777
REACTOME_TGF_BETA_RECEPTOR_SIGNALING_ACTIVATES_SMADS	24	-0.307222	-0.707935	0.8982512	0.95757596	1	268
REACTOME_LIGAND_GATED_ION_CHANNEL_TRANSPORT	21	-0.316712	-0.701207	0.86551726	0.96255654	1	2898
REACTOME_A_TETRASACCHARIDE_LINKER_SEQUENCE_IS_REQUIRED_FOR_GAG_SYNTHESIS	25	-0.301313	-0.69909	0.88611543	0.96281976	1	4068
KEGG_ALZHEIMERS_DISEASE	157	-0.232236	-0.69564	0.9891957	0.96431965	1	2680
REACTOME_OLFACTORY_SIGNALING_PATHWAY	284	-0.220622	-0.687443	1	0.96970683	1	6781
REACTOME_L1CAM_INTERACTIONS	84	-0.247201	-0.683925	0.9699864	0.97100705	1	4184
KEGG_LINOLEIC_ACID_METABOLISM	27	-0.292624	-0.682039	0.9052133	0.97083235	1	4812
REACTOME_INTRINSIC_PATHWAY_FOR_APOPTOSIS	29	-0.28749	-0.67827	0.92948717	0.9721099	1	5157
REACTOME_JNK_C_JUN_KINASES_PHOSPHORYLATION_AND_ACTIVATION_MEDIATED_BY_ACTIVATED_HUMAN_TA	16	-0.32721	-0.674352	0.8863262	0.9732686	1	4095
KEGG_RNA_DEGRADATION	57	-0.25107	-0.664339	0.9739508	0.9784989	1	3822
REACTOME_BILE_ACID_AND_BILE_SALT_METABOLISM	27	-0.286761	-0.663613	0.9411765	0.9772409	1	3661
REACTOME_SPHINGOLIPID_DE_NOVO_BIOSYNTHESIS	25	-0.293277	-0.660608	0.928115	0.97747743	1	5607
REACTOME_PRE_NOTCH_EXPRESSION_AND_PROCESSING	41	-0.258487	-0.657469	0.96879643	0.9778058	1	2980
REACTOME_NOTCH1_INTRACELLULAR_DOMAIN_REGULATES_TRANSCRIPTION	44	-0.263583	-0.654998	0.9571865	0.9776515	1	89
REACTOME_CIRCADIAN_CLOCK	52	-0.24377	-0.64542	0.98107713	0.9816033	1	3961
REACTOME_ENERGY_DEPENDENT_REGULATION_OF_MTOR_BY_LKB1_AMPK	17	-0.301432	-0.643621	0.93085104	0.98083603	1	539
REACTOME_REGULATION_OF_BETA_CELL_DEVELOPMENT	28	-0.277462	-0.642456	0.94548285	0.9797443	1	4440
KEGG_PYRUVATE_METABOLISM	40	-0.257954	-0.64213	0.9618768	0.9781831	1	2249
REACTOME_STEROID_HORMONES	29	-0.260786	-0.606871	0.9649123	0.9915026	1	3302
KEGG_DORSO_VENTRAL_AXIS_FORMATION	24	-0.26424	-0.598832	0.966129	0.99247366	1	3148
REACTOME_SYNTHESIS_OF_BILE_ACIDS_AND_BILE_SALTS_VIA_7ALPHA_HYDROXYCHOLESTEROL	15	-0.286393	-0.583332	0.95614034	0.99505985	1	3661
REACTOME_METABOLISM_OF_STEROID_HORMONES_AND_VITAMINS_A_AND_D	35	-0.228453	-0.55668	0.9985251	0.9989997	1	3302
REACTOME_TRIGLYCERIDE_BIOSYNTHESIS	38	-0.22488	-0.554937	0.9939302	0.99748184	1	4177
KEGG_MATURITY_ONSET_DIABETES_OF_THE_YOUNG	23	-0.249986	-0.554803	0.98489934	0.9957926	1	2499
REACTOME_SYNTHESIS_AND_INTERCONVERSION_OF_NUCLEOTIDE_DI_AND_TRIPHOSPHATES	18	-0.245262	-0.518613	0.989547	0.9985278	1	3405
BIOCARTA_MTOR_PATHWAY	23	-0.231662	-0.518345	0.9967051	0.99685454	1	2825
REACTOME_CREB_PHOSPHORYLATION_THROUGH_THE_ACTIVATION_OF_CAMKII	15	-0.248614	-0.512436	0.9876543	0.9956517	1	2511

Table S22

GSEA Analysis on HNSC cancer cell lines comparing cell lines with or without 9p21.3 focal loss, Pathways Depleted

NAME	SIZE	ES	NES	NOM p-value	FDR q-value	FWER p-value	RANK AT MAX
KEGG_OLFACTORY_TRANSDUCTION	384	-0.966582	-1.570215	0	0	0	1460
REACTOME_OLFACTORY_SIGNALING_PATHWAY	322	-0.966583	-1.519536	0	0.00181627	0.003	1460
REACTOME_METABOLISM_OF_RNA	282	-0.958056	-1.501448	0	0.002426551	0.007	1565
REACTOME_METABOLISM_OF_MRNA	237	-0.958109	-1.486494	0	0.003849077	0.016	1553
REACTOME_NONSENSE_MEDIATED_DECAY_ENHANCED_BY_THE_EXON_JUNCTION_COMPLEX	135	-0.969243	-1.411333	0.010224949	0.065579645	0.295	1352
REACTOME_3_UTR_MEDIATED_TRANSLATIONAL_REGULATION	135	-0.971784	-1.38709	0.015151516	0.11254018	0.529	1242
REACTOME_INFLUENZA_LIFE_CYCLE	163	-0.947652	-1.377813	0.02504817	0.12453453	0.62	1394
REACTOME_PEPTIDE_CHAIN_ELONGATION	114	-0.979871	-1.351344	0.017408123	0.21148005	0.842	886
REACTOME_CELL_CYCLE_CHECKPOINTS	112	-0.954638	-1.338975	0.063432835	0.255265	0.917	1498
REACTOME_MEIOSIS	109	-0.968374	-1.336612	0.03018868	0.2445686	0.929	1326
REACTOME_TRANSLATION	178	-0.895932	-1.3313	0.065298505	0.25445583	0.945	1315
KEGG_OXIDATIVE_PHOSPHORYLATION	101	-0.96227	-1.319854	0.068716094	0.30401286	0.975	1656
REACTOME_INFLUENZA_VIRAL_RNA_TRANSCRIPTION_AND_REPLICATION	130	-0.954472	-1.318634	0.06212425	0.28751013	0.977	886
REACTOME_MRNA_PROCESSING	153	-0.902436	-1.303765	0.09665427	0.35262087	0.992	1444
KEGG_LYSOSOME	119	-0.933274	-1.289031	0.09811321	0.43243542	0.997	745
REACTOME_MEIOTIC_RECOMBINATION	82	-0.97877	-1.282584	0.033771105	0.45758796	0.999	858
REACTOME_PROCESSING_OF_CAPPED_INTRON_CONTAINING_PRE_MRNA	133	-0.902451	-1.279398	0.106343284	0.4559873	0.999	1444
KEGG_RIBOSOME	88	-0.962032	-1.276651	0.12723657	0.4363941	0.999	886
REACTOME_SRP_DEPENDENT_COTRANSLATIONAL_PROTEIN_TARGETING_TO_MEMBRANE	137	-0.891906	-1.277578	0.11005693	0.42162213	0.999	1315
REACTOME_M_G1_TRANSITION	79	-0.966037	-1.271325	0.123809524	0.44989657	1	1498
KEGG_RIG_I_LIKE_RECEPTOR_SIGNALING_PATHWAY	69	-0.987022	-1.264915	0.024029575	0.48383516	1	343
KEGG_PARKINSONS_DISEASE	100	-0.946655	-1.261275	0.1302682	0.4932273	1	1611
REACTOME_TCA_CYCLE_AND_RESPIRATORY_ELECTRON_TRANSPORT	106	-0.917339	-1.25705	0.12660551	0.5055512	1	1167
REACTOME_RNA_POL_I_RNA_POL_III_AND_MITOCHONDRIAL_TRANSCRIPTION	117	-0.880353	-1.242042	0.16666667	0.62274367	1	1416
REACTOME_MEIOTIC_SYNAPSIS	70	-0.969883	-1.240017	0.12641509	0.61825067	1	1326
REACTOME_ACTIVATION_OF_THE_MRNA_UPON_BINDING_OF_THE_CAP_BINDING_COMPLEX_AND_EIFS_AND_SUBSEQUENT_BINDING_TO_43S	68	-0.971781	-1.237979	0.13518198	0.61422616	1	1242
REACTOME_REGULATION_OF_MRNA_STABILITY_BY_PROTEINS_THAT_BIND_AU_RICH_ELEMENTS	82	-0.940749	-1.233865	0.18410853	0.63091195	1	1498
REACTOME_ORC1_REMOVAL_FROM_CHROMATIN	68	-0.966025	-1.233612	0.16759777	0.61072023	1	1498
REACTOME_REGULATION_OF_MITOTIC_CELL_CYCLE	76	-0.950323	-1.230189	0.18878505	0.6243817	1	1498
REACTOME_TRANSCRIPTION	195	-0.829107	-1.229017	0.15313654	0.6146667	1	1444
REACTOME_HOST_INTERACTIONS_OF_HIV_FACTORS	117	-0.886442	-1.227058	0.18426104	0.6130133	1	1498
REACTOME_CYCLIN_E_ASSOCIATED_EVENTS_DURING_G1_S_TRANSITION	63	-0.966004	-1.22657	0.21003717	0.59813327	1	1498
REACTOME_ASSEMBLY_OF_THE_PRE_REPLICATIVE_COMPLEX	64	-0.966026	-1.226354	0.2021858	0.5818355	1	1498
REACTOME_SLC_MEDIATED_TRANSMEMBRANE_TRANSPORT	235	-0.8086	-1.226095	0.14314516	0.5669874	1	1655
KEGG_PPARG_SIGNALING_PATHWAY	67	-0.962528	-1.222725	0.25703564	0.577399	1	1644
REACTOME_RNA_POL_I_PROMOTER_OPENING	61	-0.980558	-1.219392	0.10159363	0.587706	1	858
REACTOME_RESPIRATORY_ELECTRON_TRANSPORT	66	-0.963283	-1.21815	0.2326923	0.58088434	1	1611
REACTOME_APC_C_CDC20_MEDIATED_DEGRADATION_OF_MITOTIC_PROTEINS	66	-0.949807	-1.213854	0.24770643	0.5996209	1	1498
REACTOME_ACTIVATION_OF_NF_KAPPAB_IN_B_CELLS	62	-0.965959	-1.212812	0.23597679	0.591823	1	1498
REACTOME_FORMATION_OF_THE_TERNARY_COMPLEX_AND_SUBSEQUENTLY_THE_43S_COMPLEX	60	-0.979851	-1.211938	0.1009009	0.5826653	1	886
REACTOME_ANTIVIRAL_MECHANISM_BY_IFN_STIMULATED_GENES	65	-0.966484	-1.209872	0.20907298	0.5825583	1	1256
KEGG_NOD_LIKE_RECEPTOR_SIGNALING_PATHWAY	59	-0.975384	-1.209434	0.14857143	0.5715719	1	536
REACTOME_PHASE1_FUNCTIONALIZATION_OF_COMPOUNDS	64	-0.964541	-1.206815	0.24452555	0.57914436	1	1555
REACTOME_DEPOSITION_OF_NEW_CENPA_CONTAINING_NUCLEOSOMES_AT_THE_CENTROMERE	61	-0.965275	-1.202766	0.24904214	0.59427947	1	1532
REACTOME_CHROMOSOME_MAINTENANCE	116	-0.869715	-1.19787	0.2041237	0.61800783	1	1532
KEGG_P53_SIGNALING_PATHWAY	65	-0.932707	-1.196858	0.2818533	0.61229575	1	1509
KEGG_RNA_DEGRADATION	56	-0.962447	-1.19032	0.30952382	0.64977884	1	1553
KEGG_P53_SIGNALING_PATHWAY	57	-0.967859	-1.18836	0.23782772	0.6511815	1	1413
KEGG_CYTOSOLIC_DNA_SENSING_PATHWAY	55	-0.978574	-1.185622	0.14492753	0.6624674	1	946
REACTOME_CDT1_ASSOCIATION_WITH_THE_CDC6_ORC_ORIGIN_COMPLEX	55	-0.96601	-1.180831	0.27376425	0.6880872	1	1498
REACTOME_APC_C_CDH1_MEDIATED_DEGRADATION_OF_CDC20_AND_OTHER_APC_C_CDH1_TARGETED_PROTEIN	65	-0.940632	-1.178563	0.3012939	0.69476273	1	1498
REACTOME_HIV_INFECTION	185	-0.794107	-1.177431	0.19361277	0.6912577	1	1498
REACTOME_REGULATION_OF_APOPTOSIS	57	-0.96363	-1.176976	0.3126177	0.68258864	1	1498
REACTOME_SCSKP2_MEDIATED_DEGRADATION_OF_P27_P21	54	-0.965988	-1.176359	0.30215827	0.67477626	1	1498
REACTOME_TRANSPORT_OF_MATURE_TRANSCRIPT_TO_CYTOPLASM	51	-0.964266	-1.173971	0.36452243	0.68148255	1	1352
REACTOME_IMMUNOREGULATORY_INTERACTIONS_BETWEEN_A_LYMPHOID_AND_A_NON_LYMPHOID_CELL	52	-0.962495	-1.172961	0.3339383	0.67901456	1	1647
REACTOME_DESTABILIZATION_OF_MRNA_BY_AUF1_HNRNP_D0	51	-0.966013	-1.172326	0.29009008	0.6724569	1	1498
REACTOME_SIGNALING_BY_WNT	63	-0.942804	-1.171382	0.330855	0.6681148	1	1498
REACTOME_ER_PHAGOSOME_PATHWAY	54	-0.966011	-1.169294	0.3	0.6743329	1	1498
REACTOME_PACKAGING_OF_TELOMERE_ENDS	48	-0.984584	-1.169184	0.11615245	0.66402787	1	680
REACTOME_P53_DEPENDENT_G1_DNA_DAMAGE_RESPONSE	54	-0.965965	-1.164918	0.3134058	0.6877373	1	1498
REACTOME_RNA_POL_I_TRANSCRIPTION	85	-0.886983	-1.161842	0.29704797	0.7029846	1	858
REACTOME_REGULATION_OF_ORNITHINE_DECARBOXYLASE_ODC	48	-0.96597	-1.161087	0.36050725	0.6975247	1	1498
KEGG_STEROID_HORMONE_BIOSYNTHESIS	52	-0.966241	-1.159654	0.32688588	0.69901687	1	1482
REACTOME_P53_INDEPENDENT_G1_S_DNA_DAMAGE_CHECKPOINT	49	-0.966015	-1.159284	0.30922243	0.6908135	1	1498
REACTOME_CDK_MEDIATED_PHOSPHORYLATION_AND_REMOVAL_OF_CDC6	47	-0.965971	-1.1577	0.35728157	0.6944802	1	1498
REACTOME_SCF_BETA_TRCP_MEDIATED_DEGRADATION_OF_EMI1	50	-0.965991	-1.157087	0.33716476	0.68804353	1	1498
REACTOME_TRANSMEMBRANE_TRANSPORT_OF_SMALL_MOLECULES	402	-0.709214	-1.155713	0.17669903	0.68793213	1	1510
SENESCENCE_ASSOCIATED_SECRETORY_PHENOTYPE	56	-0.939241	-1.155076	0.36753732	0.68371826	1	712
REACTOME_AUTODEGRADATION_OF_THE_E3_UBIQUITIN_LIGASE_COP1	48	-0.96597	-1.153195	0.35365853	0.68906426	1	1498
REACTOME_MRNA_SPLICING	105	-0.834715	-1.152429	0.2919132	0.6864178	1	1444
REACTOME_CYTOCHROME_P450_ARRANGED_BY_SUBSTRATE_TYPE	48	-0.964531	-1.150882	0.33273703	0.6906865	1	1555
KEGG_N_GLYCAN_BIOSYNTHESIS	46	-0.969603	-1.150278	0.30072463	0.6858194	1	1336
REACTOME_VIF_MEDIATED_DEGRADATION_OF_APOBEC3G	45	-0.965993	-1.150106	0.3631068	0.67773026	1	1498
REACTOME_G2_M_CHECKPOINTS	41	-0.967095	-1.149411	0.3697632	0.67409104	1	1452
REACTOME_CELL_CELL_JUNCTION_ORGANIZATION	69	-0.899918	-1.144182	0.34593573	0.7033701	1	1100
KEGG_ABC_TRANSPORTERS	42	-0.969446	-1.143148	0.34649912	0.7028204	1	1342
REACTOME_CHEMOKINE_RECEPTORS_BIND_CHEMOKINES	47	-0.958232	-1.14198	0.46494466	0.7062116	1	1396
REACTOME_AUTODEGRADATION_OF_CDH1_BY_CDH1_APC_C	57	-0.927637	-1.141967	0.36635515	0.69736284	1	1498
KEGG_PROTEASOME	45	-0.965972	-1.140106	0.36555362	0.7064526	1	1498
REACTOME_AMYLOIDS	79	-0.861283	-1.139864	0.34541985	0.6993203	1	1272
REACTOME_TRNA_AMINOACYLATION	42	-0.972255	-1.1327	0.30601093	0.746862	1	1218
REACTOME_METABOLISM_OF_NON_CODING_RNA	48	-0.963298	-1.132823	0.41340783	0.7382546	1	1617
KEGG_HEMATOPOIETIC_CELL_LINEAGE	78	-0.868287	-1.131879	0.3463687	0.73699206	1	545
REACTOME_PYRUVATE_METABOLISM_AND_CITRIC_ACID_TCA_CYCLE	41	-0.964632	-1.131211	0.45403376	0.7329017	1	1036
KEGG_CYTOKINE_CYTOKINE_RECEPTOR_INTERACTION	246	-0.73071	-1.127931	0.25824177	0.75280493	1	1413
REACTOME_CELL_CELL_COMMUNICATION	109	-0.82682	-1.127834	0.30518234	0.7447584	1	1100
REACTOME_SIGNALING_TO_ERKS	36	-0.983743	-1.125363	0.25252524	0.7576674	1	714
REACTOME_DEADENYLATION_DEPENDENT_MRNA_DECAY	42	-0.964719	-1.124994	0.4342857	0.7517295	1	1553
REACTOME_GLYCOSPHINGOLIPID_METABOLISM	37	-0.983058	-1.122821	0.26713532	0.7657651	1	745
KEGG_INTESTINAL_IMMUNE_NETWORK_FOR_IGA_PRODUCTION	33	-0.984612	-1.122326	0.23498233	0.7610311	1	677
KEGG_GLYCEROLIPID_METABOLISM	41	-0.967145	-1.118327	0.42537314	0.78770375	1	715
KEGG_AMINOACYL_TRNA_BIOSYNTHESIS	41	-0.972255	-1.117561	0.37275985	0.7854432	1	1218
KEGG_CELL_CYCLE	124	-0.799369	-1.116212	0.3001912	0.7875411	1	1509
KEGG_TRYPTOPHAN_METABOLISM	39	-0.962483	-1.115341	0.49816176	0.78837	1	1648
REACTOME_POST_NMDA_RECEPTOR_ACTIVATION_EVENTS	33	-0.984087	-1.113232	0.23304348	0.7983367	1	700
KEGG_PORPHYRIN_AND_CHLOROPHYLL_METABOLISM	39	-0.966228	-1.111907	0.43327555	0.8009853	1	1482
REACTOME_ACTIVATION_OF_NMDA_RECEPTOR_UPON_GLUTAMATE_BINDING_AND_POSTSYNAPTIC_EVENTS	36	-0.984086	-1.111842	0.26056337	0.7931834	1	700
REACTOME_CLEAVAGE_OF_GROWING_TRANSCRIPT_IN_THE_TERMINATION_REGION	42	-0.967162	-1.111176	0.41981983	0.7918292	1	1444
REACTOME_MITOCHONDRIAL_PROTEIN_IMPORT	45	-0.961588	-1.107272	0.49371633	0.8221689	1	1690
REACTOME_CELL_CELL_JUNCTION_ORGANIZATION	48	-0.938817	-1.106988	0.4954792	0.8160397	1	939
KEGG_CELL_CYCLE	32	-0.992215	-1.106923	0.20274915	0.8084987	1	343
REACTOME_GLUCAGON_TYPE_LIGAND_RECEPTORS	32	-0.986051	-1.105766	0.28	0.8106108	1	613
REACTOME_DEFENSINS	36	-0.968217	-1.104642	0.45251396	0.81199893	1	1396
KEGG_SYSTEMIC_LUPUS_ERYTHEMATOSUS	122	-0.783547	-1.104452	0.33641404	0.8057548	1	858
REACTOME_CYTOKINE_SIGNALING_IN_IMMUNE_SYSTEM	250	-0.715721	-1.103731	0.2746615	0.80453926	1	1286

REACTOME_GLUCOSE_TRANSPORT	37	-0.965589	-1.103421	0.4731369	0.8001916	1	1256
KEGG_PRIMARY_IMMUNODEFICIENCY	34	-0.968903	-1.101413	0.45025295	0.81821275	1	1367
KEGG_Cysteine_and_Methionine_Metabolism	34	-0.964565	-1.100488	0.5365854	0.8195437	1	1558
REACTOME_S_PHASE	107	-0.805954	-1.096186	0.35897437	0.8623263	1	1498
REACTOME_G_ALPHA_I_SIGNALLING_EVENTS	174	-0.745644	-1.091785	0.33730158	0.9058555	1	1522
KEGG_FRUCTOSE_AND_MANNANOSE_METABOLISM	34	-0.970593	-1.09155	0.46785715	0.9008367	1	1292
REACTOME_RNA_POL_III_TRANSCRIPTION	33	-0.967763	-1.09044	0.5170068	0.90405005	1	1416
REACTOME_ACTIVATION_OF_ATR_IN_RESPONSE_TO_REPLICATION_STRESS	35	-0.967053	-1.090246	0.5218914	0.8977201	1	1452
REACTOME_SYNTHESIS_OF_DNA	91	-0.813556	-1.089626	0.35907337	0.89848727	1	1498
REACTOME_ABC_FAMILY_PROTEINS_MEDIATED_TRANSPORT	32	-0.96943	-1.08782	0.48951048	0.91378504	1	1342
REACTOME_MRNA_3_END_PROCESSING	33	-0.967169	-1.086088	0.50359714	0.9292356	1	1444
REACTOME_G_ALPHA_S_SIGNALLING_EVENTS	113	-0.784283	-1.086046	0.3683206	0.922657	1	1542
KEGG_LINOLEIC_ACID_METABOLISM	24	-0.999976	-1.086037	0.001652893	0.91612875	1	1
REACTOME_SIGNAL_AMPLIFICATION	30	-0.986051	-1.08528	0.30533117	0.92117226	1	613
REACTOME_CREB_PHOSPHORYLATION_THROUGH_THE_ACTIVATION_OF_RAS	27	-0.984089	-1.083765	0.33275864	0.92992747	1	700
KEGG_PRION_DISEASES	35	-0.961286	-1.082933	0.6013986	0.9336537	1	78
REACTOME_GLUCCONEOGENESIS	32	-0.972192	-1.081887	0.45172414	0.9412339	1	1222
REACTOME_BILE_ACID_AND_BILE_SALT_METABOLISM	26	-0.990801	-1.080974	0.3136289	0.9433922	1	405
KEGG_APOPTOSIS	81	-0.836968	-1.078628	0.43065694	0.9721876	1	449
BIOCARTA_PGC1A_PATHWAY	23	-0.999977	-1.078219	0	0.9726739	1	1
REACTOME_PURINE_METABOLISM	33	-0.965776	-1.076782	0.54905034	0.98427653	1	1505
REACTOME_TRANSPORT_OF_VITAMINS_NUCLEOSIDES_AND_RELATED_MOLECULES	30	-0.978723	-1.076692	0.41237113	0.9773498	1	934
REACTOME_SIGNALLING_TO_RAS	27	-0.983746	-1.075618	0.36482084	0.9818135	1	714
REACTOME_INTERACTIONS_OF_VPR_WITH_HOST_CELLULAR_PROTEINS	31	-0.963289	-1.073815	0.61204016	1	1	1617
REACTOME_G_PROTEIN_ACTIVATION	27	-0.986052	-1.073664	0.33840948	0.9957269	1	613
REACTOME_TRANSPORT_OF_MATURE_MRNA_DERIVED_FROM_AN_INTRONLESS_TRANSCRIPT	31	-0.963289	-1.071684	0.60267115	1	1	1617
REACTOME_G_PROTEIN_BETA_GAMMA_SIGNALLING	26	-0.986052	-1.071183	0.3747927	1	1	613
REACTOME_CELL_CYCLE	394	-0.662591	-1.070904	0.32447818	1	1	1532
REACTOME_BIOSYNTHESIS_OF_THE_N_GLYCAN_PRECURSOR_DOLICHOL_LIPID_LINKED_OLIGOSACCHARIDE_LLO_AND_TRANSFER_TO_A_NASCENT_PROTEIN	28	-0.985801	-1.069572	0.36243823	1	1	625
REACTOME_TRANSPORT_OF_GLUCOSE_AND_OTHER_SUGARS_BILE_SALTS_AND_ORGANIC_ACIDS_METAL_IONS_AND_AMINE_COMPOUNDS	88	-0.808334	-1.067033	0.4090909	1	1	959
REACTOME_INHIBITION_OF_INSULIN_SECRETION_BY_ADRENALINE_NORADRENALINE	25	-0.986053	-1.066994	0.37886178	1	1	613
KEGG_CITRATE_CYCLE_TCA_CYCLE	30	-0.966234	-1.066525	0.5711864	1	1	609
BIOCARTA_NKT_PATHWAY	29	-0.964364	-1.064254	0.61157024	1	1	1566
REACTOME_LATENT_INFECTION_OF_HOMO_SAPIENS_WITH_MYCOBACTERIUM_TUBERCULOSIS	31	-0.962079	-1.064028	0.6424682	1	1	1664
BIOCARTA_CASPASE_PATHWAY	22	-0.983474	-1.062878	0.49675325	1	1	727
KEGG_DORSO_VENTRAL_AXIS_FORMATION	23	-0.983748	-1.062527	0.44301766	1	1	714
KEGG_THYROID_CANCER	29	-0.966048	-1.062426	0.6026059	1	1	714
KEGG_ETHER_LIPID_METABOLISM	26	-0.975164	-1.060816	0.5135135	1	1	1090
REACTOME_BETA_DEFENSINS	28	-0.968223	-1.060689	0.59	1	1	1396
REACTOME_TRAF6_MEDIATED_NFKB_ACTIVATION	20	-0.992217	-1.060566	0.40552995	1	1	343
REACTOME_FORMATION_OF_INCISION_COMPLEX_IN_GG_NER	21	-0.999979	-1.059947	0	1	1	1
REACTOME_ADP_SIGNALLING_THROUGH_P2RY12	21	-0.986054	-1.059938	0.4542536	1	1	613
REACTOME_G_BETA_GAMMA_SIGNALLING_THROUGH_PI3K_GAMMA	23	-0.986053	-1.059349	0.43086818	1	1	613
REACTOME_MITOTIC_G2_M_PHASES	78	-0.820858	-1.058504	0.44444445	1	1	1372
REACTOME_LIGAND_GATED_ION_CHANNEL_TRANSPORT	20	-0.998927	-1.057787	0.3494705	1	1	49
REACTOME_THROMBOXANE_SIGNALLING_THROUGH_TP_RECEPTOR	22	-0.986054	-1.057781	0.4667747	1	1	613
REACTOME_RNA_POL_III_TRANSCRIPTION_INITIATION_FROM_TYPE_3_PROMOTER	26	-0.967745	-1.056775	0.59126365	1	1	1416
REACTOME_ADP_SIGNALLING_THROUGH_P2RY11	24	-0.986053	-1.057481	0.45768026	1	1	613
REACTOME_RNA_POL_I_TRANSCRIPTION_TERMINATION	20	-0.99998	-1.056357	0	1	1	1
BIOCARTA_NFKB_PATHWAY	23	-0.980154	-1.056259	0.4511628	1	1	412
BIOCARTA_CERAMIDE_PATHWAY	22	-0.992217	-1.056101	0.40758294	1	1	343
REACTOME_ACYL_CHAIN_REMODELLING_OF_PC	18	-0.999982	-1.055476	0.001512859	1	1	1
BIOCARTA_G2_PATHWAY	24	-0.969869	-1.055357	0.59253246	1	1	1326
KEGG_PENTOSE_AND_GLUCCURONATE_INTERCONVERSIONS	25	-0.966216	-1.055334	0.6337308	1	1	1482
REACTOME_GENERATION_OF_SECOND_MESSENGER_MOLECULES	19	-0.998605	-1.055137	0.3903577	1	1	47
REACTOME_ACTIVATION_OF_THE_PRE_REPLICATIVE_COMPLEX	30	-0.966943	-1.054513	0.6094771	1	1	1452
REACTOME_DOWNSTREAM_SIGNALING_EVENTS_OF_B_CELL_RECEPTOR_BCR	93	-0.797486	-1.053391	0.44212523	1	1	1498
REACTOME_RNA_POL_III_TRANSCRIPTION_TERMINATION	19	-0.999981	-1.052278	0	1	1	1
REACTOME_MITOTIC_G1_G1_S_PHASES	133	-0.731177	-1.051835	0.41016334	1	1	1509
REACTOME_ACYL_CHAIN_REMODELLING_OF_PE	17	-0.999983	-1.051024	0	1	1	1
REACTOME_CTLA4_INHIBITORY_SIGNALING	21	-0.984611	-1.050167	0.48387095	1	1	615
REACTOME_SYNTHESIS_OF_BILE_ACIDS_AND_BILE_SALTS	19	-0.999981	-1.050047	0	1	1	1
REACTOME_TIGHT_JUNCTION_INTERACTIONS	27	-0.948684	-1.047947	0.687389	1	1	178
REACTOME_ABCA_TRANSPORTERS_IN_LIPID_HOMEOSTASIS	17	-0.999983	-1.047845	0	1	1	1
REACTOME_TRANSPORT_OF_RIBONUCLEOPROTEINS_INTO_THE_HOST_NUCLEUS	26	-0.965166	-1.047724	0.6672384	1	1	1266
REACTOME_NEP_NS2_INTERACTS_WITH_THE_CELLULAR_EXPORT_MACHINERY	26	-0.963271	-1.045913	0.7019231	1	1	1617
REACTOME_G_BETA_GAMMA_SIGNALLING_THROUGH_PLC_BETA	20	-0.986054	-1.044326	0.45625	1	1	613
REACTOME_PROLONGED_ERK_ACTIVATION_EVENTS	19	-0.98375	-1.043765	0.51309705	1	1	714
KEGG_TYPE_I_DIABETES_MELLITUS	21	-0.977745	-1.043627	0.5496063	1	1	32
REACTOME_SYNTHESIS_OF_PIP3_AT_THE_GOLGI_MEMBRANE	17	-0.999983	-1.043517	0	1	1	1
REACTOME_CYTOSOLIC_TRNA_AMINOACYLATION	24	-0.972243	-1.043431	0.60720134	1	1	1218
REACTOME_REGULATION_OF_GLUCCOKINASE_BY_GLUCCOKINASE_REGULATORY_PROTEIN	26	-0.964302	-1.043394	0.6834171	1	1	1256
BIOCARTA_MITOCHONDRIA_PATHWAY	20	-0.989638	-1.043326	0.43661973	1	1	456
BIOCARTA_P53_HYPOXIA_PATHWAY	22	-0.983817	-1.043197	0.47351524	1	1	712
KEGG_ALZHEIMERS_DISEASE	140	-0.73382	-1.042833	0.41040462	1	1	1474
REACTOME_APOPTOSIS	142	-0.725695	-1.042557	0.4035433	1	1	1498
KEGG_ALPHA_LINOLENIC_ACID_METABOLISM	15	-0.999985	-1.042109	0	1	1	1
REACTOME_DOUBLE_STRAND_BREAK_REPAIR	21	-0.979235	-1.042025	0.5489891	1	1	680
REACTOME_ENDOGENOUS_STEROLS	15	-0.999985	-1.041597	0	1	1	1
REACTOME_RNA_POL_III_TRANSCRIPTION_INITIATION_FROM_TYPE_2_PROMOTER	23	-0.971673	-1.041541	0.6309148	1	1	1243
REACTOME_RNA_POL_III_CHAIN_ELONGATION	17	-0.999983	-1.04087	0	1	1	1
REACTOME_SYNTHESIS_OF_BILE_ACIDS_AND_BILE_SALTS_VIA_7ALPHA_HYDROXYCHOLESTEROL	15	-0.999985	-1.040817	0.001428571	1	1	1
KEGG_PRIMARY_BILE_ACID_BIOSYNTHESIS	16	-0.999984	-1.039786	0	1	1	1
REACTOME_PROCESSING_OF_CAPPED_INTRONLESS_PRE_MRNA	23	-0.967131	-1.039332	0.66169155	1	1	1444
BIOCARTA_CYTOKINE_PATHWAY	20	-0.976968	-1.038409	0.6	1	1	536
REACTOME_ADHERENS_JUNCTIONS_INTERACTIONS	21	-0.978613	-1.0381	0.55254775	1	1	939
BIOCARTA_TNFR2_PATHWAY	17	-0.992217	-1.037875	0.48765433	1	1	343
REACTOME_METAL_ION_SLC_TRANSPORTERS	21	-0.978933	-1.037564	0.56414217	1	1	927
REACTOME_RIP_MEDIATED_NFKB_ACTIVATION_VIA_DAI	17	-0.994865	-1.037467	0.45679012	1	1	227
REACTOME_SHC1_EVENTS_IN_ERBB4_SIGNALING	19	-0.983772	-1.037409	0.53015876	1	1	714
REACTOME_SULFUR_AMINO_ACID_METABOLISM	23	-0.964529	-1.036187	0.71770334	1	1	1558
REACTOME_RAP1_SIGNALLING	16	-0.999984	-1.035918	0	1	1	1
KEGG_ASCORBATE_AND_ALDARATE_METABOLISM	23	-0.965556	-1.035145	0.7069243	1	1	1512
KEGG_GRAFT_VERSUS_HOST_DISEASE	19	-0.976847	-1.034532	0.61001515	1	1	32
REACTOME_MITOCHONDRIAL_TRNA_AMINOACYLATION	21	-0.972405	-1.034424	0.6201923	1	1	1211
REACTOME_PROSTACYCLIN_SIGNALLING_THROUGH_PROSTACYCLIN_RECEPTOR	19	-0.986055	-1.034201	0.51339287	1	1	613
REACTOME_ENOS_ACTIVATION_AND_REGULATION	20	-0.972474	-1.033679	0.6527778	1	1	1210
REACTOME_RESPIRATORY_ELECTRON_TRANSPORT_ATP_SYNTHESIS_BY_CHEMIOSMOTIC_COUPLING_AND_HEAT_PRODUCTION_BY_UNCOUPLING_PROTEINS	69	-0.812886	-1.032643	0.48653847	1	1	1611
BIOCARTA_PROTEASOME_PATHWAY	28	-0.937308	-1.032542	0.7016129	1	1	1346
KEGG_REGULATION_OF_AUTOPHAGY	33	-0.913516	-1.032481	0.64735943	1	1	1341
REACTOME_INSULIN_RECEPTOR_RECYCLING	22	-0.962247	-1.032336	0.7693548	1	1	1656
REACTOME_METABOLISM_OF_PROTEINS	442	-0.630142	-1.03086	0.37662336	1	1	1336
REACTOME_SHC_RELATED_EVENTS	16	-0.983751	-1.03072	0.5854015	1	1	714
REACTOME_ACETYLCHOLINE_BINDING_AND_DOWNSTREAM_EVENTS	15	-0.998813	-1.030455	0.48579547	1	1	54
REACTOME_PYRUVATE_METABOLISM	18	-0.976469	-1.029666	0.6346749	1	1	1036
BIOCARTA_IL10_PATHWAY	17	-0.987567	-1.029613	0.5319813	1	1	23
REACTOME_NUCLEAR_EVENTS_KINASE_AND_TRANSCRIPTION_FACTOR_ACTIVATION	24	-0.961538	-1.027937	0.7696	1	1	1687
REACTOME_ARMS_MEDIATED_ACTIVATION	17	-0.98375	-1.027245	0.5461422	1	1	714
REACTOME_PRE_NOTCH_PROCESSING_IN_GOLGI	16	-0.991328	-1.026855	0.5386819	1	1	382

REACTOME_ERK_MAPK_TARGETS	21	-0.96154	-1.02657	0.78971964	1	1	1687
BIOCARTA_CTLA4_PATHWAY	17	-0.98423	-1.02651	0.5762463	1	1	47
REACTOME_KINESINS	24	-0.963843	-1.026382	0.7447833	1	1	1591
REACTOME_FANCONI_ANEMIA_PATHWAY	20	-0.969803	-1.026107	0.70542634	1	1	1326
REACTOME_AMINO_ACID_TRANSPORT_ACROSS_THE_PLASMA_MEMBRANE	31	-0.913424	-1.025802	0.6566164	1	1	453
KEGG_NICOTINATE_AND_NICOTINAMIDE_METABOLISM	22	-0.967497	-1.02556	0.7092308	1	1	1427
REACTOME_RAS_ACTIVATION_UOPN_CA2_INFUX_THROUGH_NMDA_RECEPTOR	17	-0.98407	-1.025525	0.5802469	1	1	700
BIOCARTA_ATRBRCA_PATHWAY	20	-0.969872	-1.025331	0.70253164	1	1	1326
REACTOME_CREB_PHOSPHORYLATION_THROUGH_THE_ACTIVATION_OF_CAMKII	15	-0.984071	-1.024459	0.60795456	1	1	700
BIOCARTA_SPRY_PATHWAY	18	-0.973731	-1.023779	0.67261904	1	1	1153
REACTOME_SIGNALING_TO_P38_VIA_RIT_AND_RIN	15	-0.983751	-1.023338	0.6172662	1	1	714
BIOCARTA_MCM_PATHWAY	18	-0.966929	-1.023303	0.74558824	1	1	1452
KEGG_ADIPOCYTOKINE_SIGNALING_PATHWAY	66	-0.806931	-1.022785	0.51459855	1	1	1644
REACTOME_NUCLEOTIDE_BINDING_DOMAIN_LEUCINE_RICH_REPEAT_CONTAINING_RECEPTOR_NLR_SIGNALING_PATHWAYS	43	-0.876039	-1.020906	0.5934066	1	1	946
REACTOME_TELOMERE_MAINTENANCE	75	-0.802698	-1.020484	0.51498127	1	1	862
BIOCARTA_TALL1_PATHWAY	15	-0.984618	-1.020458	0.6091954	1	1	677
REACTOME_DEADENYLATION_OF_MRNA	17	-0.971746	-1.020093	0.7023644	1	1	1242
REACTOME_SHC_MEDIATED_SIGNALING	15	-0.983751	-1.01933	0.62154293	1	1	714
BIOCARTA_LAIR_PATHWAY	16	-0.977898	-1.019262	0.67127496	1	1	23
REACTOME_INFLAMMASOMES	16	-0.978524	-1.019186	0.6622807	1	1	946
REACTOME_INCRETIN_SYNTHESIS_SECRETION_AND_INACTIVATION	18	-0.970079	-1.017264	0.73590505	1	1	1315
REACTOME_SHC1_EVENTS_IN_EGFR_SIGNALING	15	-0.983751	-1.017121	0.615942	1	1	714
BIOCARTA_TH1TH2_PATHWAY	17	-0.964328	-1.015358	0.7966616	1	1	1566
REACTOME_DESTABILIZATION_OF_MRNA_BY_KSRP	17	-0.967706	-1.014581	0.7695652	1	1	1418
KEGG_ASTHMA	16	-0.967798	-1.013773	0.77286136	1	1	1413
BIOCARTA_EIF_PATHWAY	16	-0.971746	-1.01372	0.729927	1	1	1242
REACTOME_HOMOLOGOUS_RECOMBINATION_REPAIR_OF_REPLICATION_INDEPENDENT_DOUBLE_STRAND_BREAKS	15	-0.979237	-1.013661	0.6897038	1	1	680
REACTOME_CGMP_EFFECTS	17	-0.964853	-1.013659	0.7886677	1	1	1542
REACTOME_N_GLYCAN_ANTENNAE_ELONGATION_IN_THE_MEDIAL_TRANS_GOLGI	17	-0.969555	-1.013495	0.7394469	1	1	1336
BIOCARTA_CELLCYCLE_PATHWAY	23	-0.944974	-1.013446	0.7941176	1	1	1509
KEGG_ALLOGRAFT_REJECTION	17	-0.96782	-1.013414	0.7732733	1	1	1413
KEGG_OOCYTE_MEIOSIS	108	-0.739103	-1.01303	0.45383105	1	1	1299
REACTOME_PEPTIDE_LIGAND_BINDING_RECEPTORS	162	-0.690757	-1.011808	0.44636014	1	1	1522
KEGG_TERPENOID_BACKBONE_BIOSYNTHESIS	15	-0.974988	-1.011419	0.73938507	1	1	1098
REACTOME_GLUCURONIDATION	18	-0.966222	-1.011107	0.809593	1	1	1482
REACTOME_EARLY_PHASE_OF_HIV_LIFE_CYCLE	15	-0.971633	-1.010759	0.7373737	1	1	1245
KEGG_RIBOFLAVIN_METABOLISM	15	-0.97056	-1.009219	0.75637394	1	1	1292
REACTOME_TRANSPORT_OF_INORGANIC_CATIONS_ANIONS_AND_AMINO_ACIDS_OLIGOPEPTIDES	91	-0.744322	-1.008175	0.4716312	1	1	1585
REACTOME_CYCLIN_A_B1_ASSOCIATED_EVENTS_DURING_G2_M_TRANSITION	15	-0.975878	-1.00785	0.7221418	1	1	1062
REACTOME_DESTABILIZATION_OF_MRNA_BY_TRISTETRAPROLIN_TTP	17	-0.967706	-1.007474	0.78549385	1	1	1418
REACTOME_SYNTHESIS_OF_PC	18	-0.957618	-1.007428	0.851227	1	1	553
REACTOME_DESTABILIZATION_OF_MRNA_BY_BRF1	17	-0.967706	-1.007047	0.7912913	1	1	1418
REACTOME_G0_AND_EARLY_G1	24	-0.931521	-1.006398	0.78405315	1	1	1247
BIOCARTA_NOZIL12_PATHWAY	17	-0.964305	-1.006025	0.8192956	1	1	1566
REACTOME_PLATELET_SENSITIZATION_BY_LDL	16	-0.961545	-1.004381	0.8684211	1	1	1687
REACTOME_SYNTHESIS_SECRETION_AND_INACTIVATION_OF_GLP1	15	-0.970081	-1.00436	0.7710843	1	1	1315
KEGG_CHEMOKINE_SIGNALING_PATHWAY	176	-0.681206	-1.004237	0.44970414	1	1	1115
BIOCARTA_INFLAM_PATHWAY	25	-0.924975	-1.002439	0.7646104	1	1	545
BIOCARTA_HSP27_PATHWAY	15	-0.967844	-1.002184	0.81908834	1	1	1413
REACTOME_G1_S_TRANSITION	108	-0.731256	-1.001919	0.46561885	1	1	1498
KEGG_GLYCOXYLATE_AND_DICARBOXYLATE_METABOLISM	16	-0.966657	-0.998224	0.8340307	1	1	1463
REACTOME_SIGNALING_BY_ILS	104	-0.733401	-0.996713	0.49704143	1	1	1153
KEGG_JAK_STAT_SIGNALING_PATHWAY	148	-0.688721	-0.995569	0.47398844	1	1	1566
BIOCARTA_DC_PATHWAY	22	-0.925203	-0.99157	0.7993827	1	1	158
REACTOME_LYSOSOME_VESICLE_BIOGENESIS	23	-0.919102	-0.990112	0.7960725	1	1	966
KEGG_TIGHT_JUNCTION	127	-0.691458	-0.988864	0.4785047	1	1	714
REACTOME_PHOSPHORYLATION_OF_THE_APC_C	17	-0.942827	-0.986318	0.8603269	1	1	153
REACTOME_REGULATION_OF_KIT_SIGNALING	16	-0.942894	-0.986035	0.8744461	1	1	1153
REACTOME_CITRIC_ACID_CYCLE_TCA_CYCLE	20	-0.923309	-0.982983	0.8390093	1	1	609
REACTOME_APC_C_CDC20_MEDIATED_DEGRADATION_OF_CYCLIN_B	20	-0.924557	-0.982173	0.8273616	1	1	1173
REACTOME_LATE_PHASE_OF_HIV_LIFE_CYCLE	94	-0.720912	-0.979127	0.5266055	1	1	1402
REACTOME_HIV_LIFE_CYCLE	109	-0.726722	-0.976693	0.5297398	1	1	1402
REACTOME_RECYCLING_PATHWAY_OF_L1	26	-0.899299	-0.972991	0.7862969	1	1	793
REACTOME_SIGNALING_BY_NODAL	18	-0.919385	-0.971562	0.8531685	1	1	698
REACTOME_CELL_CYCLE_MITOTIC	304	-0.615244	-0.966272	0.5248092	1	1	1532
KEGG_GLYCINE_SERINE_AND_THREONINE_METABOLISM	31	-0.868793	-0.965328	0.74655175	1	1	619
KEGG_GLYCOSAMINOGLYCAN_DEGRADATION	20	-0.917541	-0.961237	0.87253416	1	1	88
BIOCARTA_IL1R_PATHWAY	33	-0.857958	-0.960012	0.73275864	1	1	449
BIOCARTA_MTOR_PATHWAY	23	-0.897312	-0.955363	0.8401254	1	1	1242
BIOCARTA_STATHMIN_PATHWAY	19	-0.895536	-0.950722	0.8489666	1	1	153
REACTOME_AMINO_ACID_AND_OLIGOPEPTIDE_SLC_TRANSPORTERS	48	-0.783316	-0.945492	0.64737797	1	1	453
REACTOME_INTERFERON_SIGNALING	142	-0.656226	-0.943424	0.56037736	1	1	1286
KEGG_TOLL_LIKE_RECEPTOR_SIGNALING_PATHWAY	99	-0.685872	-0.939534	0.58381504	1	1	412
REACTOME_SIGNALING_BY_CONSTITUTIVELY_ACTIVE_EGFR	18	-0.892476	-0.938794	0.8822606	1	1	1153
REACTOME_RECRUITMENT_OF_MITOTIC_CENTROSOME_PROTEINS_AND_COMPLEXES	63	-0.751045	-0.936679	0.609901	1	1	1372
REACTOME_NEGATIVE_REGULATORS_OF_RIG_I_MDA5_SIGNALING	31	-0.835068	-0.932094	0.7599309	1	1	617
REACTOME_RNA_POL_II_TRANSCRIPTION	94	-0.693733	-0.927653	0.62030077	1	1	1444
KEGG_PYRUVATE_METABOLISM	39	-0.800767	-0.924855	0.7092593	1	1	667
CANCER-TESTIS-ANTIGEN	164	-0.635824	-0.924318	0.5864811	1	1	713
REACTOME_APOPTOTIC_EXECUTION_PHASE	50	-0.762226	-0.921834	0.67192984	1	1	765
REACTOME_BASIGIN_INTERACTIONS	25	-0.846071	-0.921287	0.81178397	1	1	784
REACTOME_INSULIN_SYNTHESIS_AND_PROCESSING	18	-0.874473	-0.920062	0.8842593	1	1	927
REACTOME_APC_CDC20_MEDIATED_DEGRADATION_OF_NEK2A	22	-0.858184	-0.919186	0.84294873	1	1	1173
REACTOME_IL_2_SIGNALING	41	-0.78151	-0.909839	0.7209302	1	1	714
KEGG_EPITHELIAL_CELL_SIGNALING_IN_HELICOBACTER_PYLORI_INFECTION	66	-0.712406	-0.905881	0.64480877	1	1	615
KEGG_NATURAL_KILLER_CELL_MEDIATED_CYTOTOXICITY	122	-0.638082	-0.904298	0.6184211	1	1	1464
REACTOME_TGF_BETA_RECEPTOR_SIGNALING_ACTIVATES_SMADS	25	-0.834523	-0.903397	0.83623695	1	1	656
REACTOME_ASSOCIATION_OF_TRIC_CCT_WITH_TARGET_PROTEINS_DURING_BIOSYNTHESIS	26	-0.828922	-0.902554	0.8237288	1	1	1291
KEGG_PROGESTERONE_MEDIATED_OOCYTE_MATURATION	82	-0.687763	-0.900389	0.6397059	1	1	1115
REACTOME_SIGNALING_BY_THE_B_CELL_RECEPTOR_BCR	122	-0.637679	-0.8979	0.6221374	1	1	1498
REACTOME_CLASS_A1_RHODOPSIN_LIKE_RECEPTORS	269	-0.568383	-0.897363	0.6360153	1	1	1522
REACTOME_THROMBIN_SIGNALING_THROUGH_PROTEINASE_ACTIVATED_RECEPTORS_PARS	30	-0.814348	-0.897314	0.7958478	1	1	613
REACTOME_CTNNB1_PHOSPHORYLATION_CASCADE	15	-0.860186	-0.89209	0.9251412	1	1	675
KEGG_CELL_ADHESION_MOLECULES_CAMS	105	-0.647238	-0.890125	0.65346533	1	1	1464
REACTOME_DOWNREGULATION_OF_TGF_BETA_RECEPTOR_SIGNALING	22	-0.834524	-0.889284	0.87741935	1	1	656
REACTOME_SIGNALING_BY_SCF_KIT	74	-0.681661	-0.888998	0.649635	1	1	1153
REACTOME_PERK_REGULATED_GENE_EXPRESSION	27	-0.812484	-0.887594	0.8289703	1	1	106
KEGG_MTOR_SIGNALING_PATHWAY	48	-0.741086	-0.887141	0.69299823	1	1	1242
REACTOME_NEF_MEDIATES_DOWN_MODULATION_OF_CELL_SURFACE_RECEPTORS_BY_RECRUITING_THEM_TO_CLATHRIN_ADAPTERS	18	-0.843055	-0.885876	0.89209723	1	1	47
REACTOME_ACTIVATION_OF_GENES_BY_ATF4	24	-0.812485	-0.880129	0.83686787	1	1	106
REACTOME_DNA_REPLICATION	182	-0.59802	-0.878126	0.67611337	1	1	1617
REACTOME_MITOTIC_M_M_G1_PHASES	162	-0.603085	-0.877434	0.68725866	1	1	1617
BIOCARTA_NTH1_PATHWAY	23	-0.80822	-0.872392	0.8519737	1	1	32
KEGG_MAPK_SIGNALING_PATHWAY	254	-0.56945	-0.871542	0.71146244	1	1	1213
KEGG_HOMOLOGOUS_RECOMBINATION	26	-0.805169	-0.870577	0.8471761	1	1	128
REACTOME_TCR_SIGNALING	43	-0.753119	-0.870258	0.77459747	1	1	47
BIOCARTA_P38MAPK_PATHWAY	39	-0.744559	-0.868279	0.7513612	1	1	343
REACTOME_NEUROTRANSMITTER_RECEPTOR_BINDING_AND_DOWNSTREAM_TRANSMISSION_IN_THE_POSTSYNAPTIC_CELL	132	-0.61511	-0.86736	0.72038835	1	1	1238

REACTOME_THE_ROLE_OF_NEF_IN_HIV1_REPLICATION_AND_DISEASE_PATHOGENESIS	24	-0.797906	-0.866489	0.8416	1	1	47
REACTOME_INHIBITION_OF_THE_PROTEOLYTIC_ACTIVITY_OF_APC_C_REQUIRED_FOR_THE_ONSET_OF_ANAPHAS E_BY_MITOTIC_SPINDLE_CHECKPOINT_COMPONENTS	18	-0.814612	-0.860781	0.8913044	1	1	1173
REACTOME_REGULATION_OF_BETA_CELL_DEVELOPMENT	26	-0.792611	-0.860273	0.8453427	1	1	1388
REACTOME_DNA_REPAIR	102	-0.624709	-0.857582	0.6990476	1	1	1326
KEGG_RNA_POLYMERASE	29	-0.787643	-0.857357	0.8496622	1	1	186
REACTOME_TRANS_GOLGI_NETWORK_VESICLE_BUDDING	57	-0.69469	-0.854874	0.7134935	1	1	966
REACTOME_METABOLISM_OF_AMINO_ACIDS_AND_DERIVATIVES	187	-0.567174	-0.850018	0.7607843	1	1	1575
KEGG_LEISHMANIA_INFECTION	58	-0.691115	-0.844407	0.729927	1	1	482
KEGG_NEUROTROPHIN_SIGNALING_PATHWAY	122	-0.597836	-0.839414	0.7252337	1	1	1072
REACTOME_GLYCOLYSIS	27	-0.760125	-0.836177	0.8322259	1	1	1222
REACTOME_COSTIMULATION_BY_THE_CD28_FAMILY	55	-0.691775	-0.831782	0.75189394	1	1	615
REACTOME_DOWNSTREAM_TCR_SIGNALING	27	-0.753329	-0.828799	0.8476821	1	1	47
KEGG_RETINOL_METABOLISM	57	-0.653935	-0.827264	0.7383721	1	1	1482
BIOCARTA_IL7_PATHWAY	16	-0.79	-0.822385	0.93519884	1	1	545
REACTOME_ANTIGEN_PROCESSING_CROSS_PRESENTATION	68	-0.648722	-0.821279	0.7485605	1	1	1498
KEGG_SPHINGOLIPID_METABOLISM	36	-0.714304	-0.81494	0.8128342	1	1	1291
BIOCARTA_EIF4_PATHWAY	24	-0.750293	-0.814439	0.8536978	1	1	1242
REACTOME_IL1_SIGNALING	38	-0.71261	-0.814341	0.8264015	1	1	449
REACTOME_METABOLISM_OF_CARBOHYDRATES	232	-0.522783	-0.811995	0.81764704	1	1	1287
KEGG_SPLICEOSOME	123	-0.574002	-0.804784	0.7868217	1	1	1553
KEGG_LONG_TERM_POTENTIATION	66	-0.63437	-0.804067	0.7509434	1	1	714
KEGG_NEUROACTIVE_LIGAND_RECEPTOR_INTERACTION	258	-0.516285	-0.803719	0.83514494	1	1	1116
REACTOME_G_ALPHA_Z_SIGNALING_EVENTS	43	-0.682335	-0.80081	0.7935606	1	1	1115
BIOCARTA_CSK_PATHWAY	20	-0.755	-0.797696	0.9296875	1	1	47
KEGG_CARDIAC_MUSCLE_CONTRACTION	70	-0.62462	-0.795503	0.78368795	1	1	1167
REACTOME_AMINE_COMPOUND_SLC_TRANSPORTERS	27	-0.725356	-0.795246	0.85714287	1	1	553
REACTOME_SIGNALING_BY_FGFR_MUTANTS	40	-0.683709	-0.792318	0.8271605	1	1	1152
KEGG_GLYCOSYLPHOSPHATIDYLINOSITOL_GPI_ANCHOR_BIOSYNTHESIS	25	-0.725077	-0.783783	0.885274	1	1	981
BIOCARTA_NKCELLS_PATHWAY	19	-0.738868	-0.781884	0.9253049	1	1	812
REACTOME_CD28_CO_STIMULATION	31	-0.698117	-0.779156	0.86243385	1	1	615
REACTOME_UNFOLDED_PROTEIN_RESPONSE	75	-0.603975	-0.779149	0.8098859	1	1	1657
REACTOME_SIGNALING_BY_FGFR1_FUSION_MUTANTS	18	-0.742135	-0.778057	0.94356006	1	1	1152
REACTOME_ION_CHANNEL_TRANSPORT	83	-0.642717	-0.776743	0.798675	1	1	1249
KEGG_SMALL_CELL_LUNG_CANCER	51	-0.597632	-0.775841	0.798419	1	1	482
BIOCARTA_CARM_ER_PATHWAY	35	-0.681895	-0.771926	0.83652174	1	1	1247
KEGG_DRUG_METABOLISM_OTHER_ENZYMES	47	-0.647934	-0.770553	0.81609195	1	1	1000
REACTOME_GROWTH_HORMONE_RECEPTOR_SIGNALING	24	-0.712471	-0.767953	0.8955224	1	1	615
REACTOME_FACTORS_INVOLVED_IN_MEGAKARYOCYTE_DEVELOPMENT_AND_PLATELET_PRODUCTION	128	-0.539013	-0.766256	0.8593156	1	1	1503
REACTOME_PI3K_EVENTS_IN_ERBB4_SIGNALING	35	-0.679331	-0.761979	0.879646	1	1	202
REACTOME_CD28_DEPENDENT_PI3K_AKT_SIGNALING	21	-0.716119	-0.761404	0.91935486	1	1	47
KEGG_PEROXISOME	78	-0.587109	-0.76089	0.8181818	1	1	1121
BIOCARTA_MAL_PATHWAY	18	-0.719274	-0.757287	0.9375	1	1	500
REACTOME_CHOLESTEROL_BIOSYNTHESIS	21	-0.715355	-0.753668	0.92987806	1	1	1264
REACTOME_LIPID_DIGESTION_MOBILIZATION_AND_TRANSPORT	40	-0.64671	-0.752129	0.83893806	1	1	784
REACTOME_FRS2_MEDIATED_CASCADE	33	-0.672004	-0.751719	0.8687392	1	1	714
REACTOME_INNATE_IMMUNE_SYSTEM	253	-0.494692	-0.748954	0.93495935	1	1	946
KEGG_GLYCEROPHOSPHOLIPID_METABOLISM	67	-0.591615	-0.748113	0.8509804	1	1	1136
REACTOME_LOSS_OF_NLP_FROM_MITOTIC_CENTROSOMES	56	-0.599289	-0.746851	0.84826326	1	1	1372
KEGG_PYRIMIDINE_METABOLISM	95	-0.548067	-0.739831	0.8593156	1	1	1427
BIOCARTA_TNFR1_PATHWAY	29	-0.669891	-0.735232	0.9134126	1	1	1413
REACTOME_GABA_RECEPTOR_ACTIVATION	50	-0.602281	-0.73204	0.8374291	1	1	1115
REACTOME_SHC_MEDIATED_CASCADE	25	-0.672007	-0.730005	0.9081803	1	1	714
REACTOME_A_TETRASACCHARIDE_LINKER_SEQUENCE_IS_REQUIRED_FOR_GAG_SYNTHESIS	24	-0.671256	-0.729514	0.9104	1	1	1287
KEGG_ALDOSTERONE_REGULATED_SODIUM_REABSORPTION	38	-0.639115	-0.7293	0.8813869	1	1	1066
KEGG_BLADDER_CANCER	39	-0.632899	-0.729065	0.88	1	1	822
KEGG_ANTIGEN_PROCESSING_AND_PRESENTATION	61	-0.579318	-0.719777	0.90185183	1	1	966
REACTOME_NA_CL_DEPENDENT_NEUROTRANSMITTER_TRANSPORTERS	17	-0.683894	-0.713518	0.9519651	1	1	453
REACTOME_PKB_MEDIATED_EVENTS	27	-0.648649	-0.71316	0.90084034	1	1	1242
REACTOME_CELL_SURFACE_INTERACTIONS_AT_THE_VASCULAR_WALL	83	-0.537481	-0.708504	0.91698843	1	1	784
REACTOME_ACTIVATED_AMPK_STIMULATES_FATTY_ACID_OXIDATION_IN_MUSCLE	17	-0.675806	-0.707584	0.95224315	1	1	660
REACTOME_RIG_1_MDA5_MEDIATED_INDUCION_OF_IFN_ALPHA_BETA_PATHWAYS	71	-0.559646	-0.706134	0.8897196	1	1	617
REACTOME_IL_3_5_AND_GM-CSF_SIGNALING	42	-0.60709	-0.705159	0.8863233	1	1	1153
REACTOME_SIGNALING_BY_ROBO_RECEPTOR	27	-0.645036	-0.702923	0.91137123	1	1	98
BIOCARTA_GSK3_PATHWAY	27	-0.642029	-0.699752	0.91797554	1	1	412
REACTOME_APOPTOTIC_CLEAVAGE_OF_CELLULAR_PROTEINS	36	-0.588616	-0.6801	0.88729876	1	1	727
REACTOME_GLUCAGON_SIGNALING_IN_METABOLIC_REGULATION	32	-0.607457	-0.677008	0.92413795	1	1	1115
KEGG_INSULIN_SIGNALING_PATHWAY	133	-0.476293	-0.670337	0.994	1	1	1242
KEGG_VIRAL_MYOCARDITIS	50	-0.548646	-0.666183	0.9259259	1	1	1464
REACTOME_GRB2_EVENTS_IN_ERBB2_SIGNALING	21	-0.627814	-0.66405	0.9512579	1	1	714
REACTOME_SIGNAL_TRANSDUCTION_BY_L1	34	-0.580904	-0.661444	0.91296625	1	1	63
KEGG_GNRH_SIGNALING_PATHWAY	96	-0.488497	-0.659222	0.97096187	1	1	1115
BIOCARTA_FAS_PATHWAY	30	-0.598021	-0.656909	0.95238096	1	1	1195
REACTOME_SIGNALING_BY_FGFR1_MUTANTS	28	-0.597628	-0.656559	0.93634844	1	1	1152
KEGG_GLYCOSAMINOGLYCAN_BIOSYNTHESIS_CHONDROITIN_SULFATE	22	-0.60471	-0.6533	0.9424	1	1	124
REACTOME_CONVERSION_FROM_APC_C_CD20_TO_APC_C_CDH1_IN_LATE_ANAPHASE	16	-0.629027	-0.650434	0.9790732	1	1	1173
REACTOME_NOD1_2_SIGNALING_PATHWAY	28	-0.585904	-0.643093	0.93771046	1	1	412
REACTOME_GLYCEROPHOSPHOLIPID_BIOSYNTHESIS	75	-0.496106	-0.642965	0.9609375	1	1	1136
REACTOME_FATTY_ACYL_COA_BIOSYNTHESIS	18	-0.612985	-0.641004	0.96390975	1	1	1121
REACTOME_SMAD2_SMAD3_SMAD4_HETEROTRIMER_REGULATES_TRANSCRIPTION	26	-0.582123	-0.637641	0.9479866	1	1	1247
REACTOME_TAK1_ACTIVATES_NFKB_BY_PHOSPHORYLATION_AND_ACTIVATION_OF_IKKK_COMPLEX	22	-0.585905	-0.636503	0.9328969	1	1	412
REACTOME_CHONDROITIN_SULFATE_DERMATAN_SULFATE_METABOLISM	46	-0.534614	-0.634052	0.9508772	1	1	124
REACTOME_ENERGY_DEPENDENT_REGULATION_OF_MTOR_BY_LKB1_AMPK	16	-0.602106	-0.628349	0.97771174	1	1	660
KEGG_PANCREATIC_CANCER	67	-0.496027	-0.627305	0.9834559	1	1	1096
KEGG_PATHOGENIC_ESCHERICHIA_COLI_INFECTION	56	-0.517754	-0.6201	0.964486	1	1	915
REACTOME_ACTIVATED_TAK1_MEDIATES_P38_MAPK_ACTIVATION	17	-0.585907	-0.615338	0.97337276	1	1	412
REACTOME_POST_TRANSLATIONAL_MODIFICATION_SYNTHESIS_OF_GPI_ANCHORED_PROTEINS	26	-0.561153	-0.612545	0.95408165	1	1	981
KEGG_GLYCOSAMINOGLYCAN_BIOSYNTHESIS_HEPARAN_SULFATE	26	-0.559318	-0.61194	0.9629005	1	1	693
REACTOME_JNK_C_JUN_KINASES_PHOSPHORYLATION_AND_ACTIVATION_MEDIATED_BY_ACTIVATED_HUMAN_TA K1	16	-0.585907	-0.611676	0.9775112	1	1	412
BIOCARTA_NFAT_PATHWAY	51	-0.500462	-0.611049	0.9810964	1	1	675
REACTOME_O_LINKED_GLYCOSYLATION_OF_MUCINS	47	-0.50743	-0.610144	0.96045196	1	1	776
REACTOME_LIPOPROTEIN_METABOLISM	24	-0.559792	-0.603461	0.965625	1	1	429
BIOCARTA_GCR_PATHWAY	19	-0.568246	-0.60326	0.969651	1	1	1393
KEGG_TYROSINE_METABOLISM	34	-0.527049	-0.596639	0.96466434	1	1	1399
REACTOME_ACTIVATED_NOTCH1_TRANSMITS_SIGNAL_TO_THE_NUCLEUS	26	-0.547978	-0.596261	0.9650582	1	1	971
REACTOME_TERMINATION_OF_O_GLYCAN_BIOSYNTHESIS	18	-0.563401	-0.589287	0.98275864	1	1	776
REACTOME_NUCLEAR_SIGNALING_BY_ERBB4	36	-0.520543	-0.587878	0.9678571	1	1	202
KEGG_BASE_EXCISION_REPAIR	34	-0.523273	-0.585933	0.98109967	1	1	215
REACTOME_E2F_MEDIATED_REGULATION_OF_DNA_REPLICATION	34	-0.518298	-0.585327	0.97861844	1	1	1125
REACTOME_CHONDROITIN_SULFATE_BIOSYNTHESIS	18	-0.55427	-0.583039	0.97720367	1	1	74
KEGG_BASAL_TRANSCRIPTION_FACTORS	34	-0.511515	-0.58245	0.9711375	1	1	1039
REACTOME_CROSS_PRESENTATION_OF_SOLUBLE_EXOGENOUS_ANTIGENS_ENDOSOMES	47	-0.489516	-0.576699	0.9911119	1	1	1498
REACTOME_EXTENSION_OF_TELOMERES	27	-0.529226	-0.576037	0.9821718	1	1	862
REACTOME_IL_RECEPTOR_SHC_SIGNALING	27	-0.521274	-0.574516	0.97875816	1	1	158
REACTOME_GAP_JUNCTION_TRAFFICKING	26	-0.498066	-0.544151	0.9897084	1	1	1364
BIOCARTA_NO1_PATHWAY	30	-0.481325	-0.537516	0.9982456	1	1	784
BIOCARTA_IL2_PATHWAY	22	-0.50354	-0.536006	0.9968799	1	1	47
REACTOME_G1_PHASE	36	-0.468986	-0.535083	1	1	1	1687
KEGG_STEROID_BIOSYNTHESIS	16	-0.506189	-0.527849	0.9941349	1	1	1264
REACTOME_TRAFFICKING_OF_AMPA_RECEPTORS	26	-0.478185	-0.518583	1	1	1	1238
BIOCARTA_TID_PATHWAY	19	-0.485499	-0.512902	0.9984375	0.99940956	1	1413

Table S23

GSEA Analysis (Hallmark gene sets) on TCGA HNSC comparing tumors with or without 9p loss, Pathways Depleted

NAME	SIZE	ES	NES	NOM p-value	FDR q-value	FWER p-value	RANK AT MAX
HALLMARK_INTERFERON_GAMMA_RESPONSE	190	-0.855109	-2.744375	0	0	0	1317
HALLMARK_ALLOGRAFT_REJECTION	183	-0.829341	-2.623169	0	0	0	1005
HALLMARK_INTERFERON_ALPHA_RESPONSE	91	-0.885347	-2.578858	0	0	0	1809
HALLMARK_COMPLEMENT	195	-0.728917	-2.34002	0	0	0	1959
HALLMARK_INFLAMMATORY_RESPONSE	197	-0.730056	-2.338272	0	0	0	2367
HALLMARK_IL6_JAK_STAT3_SIGNALING	87	-0.731323	-2.160054	0	0	0	2179
HALLMARK_IL2_STATS_SIGNALING	194	-0.637947	-2.066072	0	0	0	2951
HALLMARK_KRAS_SIGNALING_UP	193	-0.614807	-1.950687	0	0	0	2401
HALLMARK_TNFA_SIGNALING_VIA_NFKB	197	-0.606805	-1.941103	0	0	0	2922
HALLMARK_APOPTOSIS	158	-0.534577	-1.670234	0	0.002546372	0.025	1413
HALLMARK_MYOGENESIS	198	-0.487981	-1.572575	0.001265823	0.011794602	0.118	4426
HALLMARK_COAGULATION	136	-0.498312	-1.516129	0.001408451	0.019545117	0.212	2535
HALLMARK_APICAL_SURFACE	43	-0.554415	-1.448977	0.03301887	0.038945436	0.405	2694
HALLMARK_PI3K_AKT_MTOR_SIGNALING	103	-0.485388	-1.440448	0.015625	0.040478278	0.438	3797
HALLMARK_APICAL_JUNCTION	194	-0.415006	-1.332427	0.030612245	0.11372461	0.825	4265
HALLMARK_EPITHELIAL_MESENCHYMAL_TRANSITION	194	-0.39935	-1.285401	0.04935065	0.16172253	0.934	4265
HALLMARK_P53_PATHWAY	190	-0.402605	-1.283451	0.037958115	0.15477194	0.94	2794
HALLMARK_TGF_BETA_SIGNALING	54	-0.436768	-1.188955	0.19809826	0.31416717	1	3796
HALLMARK_REACTIVE_OXYGEN_SPECIES_PATHWAY	45	-0.437367	-1.164183	0.2257525	0.35447887	1	3287
HALLMARK_ANDROGEN_RESPONSE	95	-0.393577	-1.158838	0.18785311	0.3485101	1	3475
HALLMARK_UV_RESPONSE_DN	137	-0.363454	-1.124269	0.26287264	0.41170365	1	3416
HALLMARK_XENOBIOTIC_METABOLISM	197	-0.334834	-1.068999	0.33462533	0.5457384	1	2441
HALLMARK_KRAS_SIGNALING_DN	183	-0.337534	-1.067487	0.3126649	0.5262501	1	2808
HALLMARK_HEME_METABOLISM	188	-0.316462	-1.016585	0.44530246	0.6528651	1	2828
HALLMARK_UV_RESPONSE_UP	150	-0.327607	-1.01619	0.4238683	0.62860024	1	3125
HALLMARK_ESTROGEN_RESPONSE_EARLY	191	-0.307421	-0.98401	0.47556144	0.70073336	1	2680
HALLMARK_HYPOXIA	190	-0.293301	-0.93711	0.6111111	0.8168293	1	4039
HALLMARK_ANGIOGENESIS	36	-0.36884	-0.933068	0.5620915	0.79852504	1	4928
HALLMARK_NOTCH_SIGNALING	32	-0.368209	-0.924665	0.56053066	0.7947106	1	3159
HALLMARK_BILE_ACID_METABOLISM	112	-0.293459	-0.882431	0.7089136	0.88307863	1	3156
HALLMARK_CHOLESTEROL_HOMEOSTASIS	72	-0.29527	-0.85229	0.72534144	0.9208138	1	2694
HALLMARK_PROTEIN_SECRETION	95	-0.281959	-0.834622	0.7886473	0.9438062	1	1561
HALLMARK_HEDGEHOG_SIGNALING	34	-0.320207	-0.817857	0.75166667	0.9504564	1	1814
HALLMARK_FATTY_ACID_METABOLISM	154	-0.259991	-0.81369	0.87109905	0.93067247	1	2202
HALLMARK_PEROXISOME	101	-0.265368	-0.792086	0.8718704	0.9426724	1	2725
HALLMARK_ESTROGEN_RESPONSE_LATE	195	-0.237139	-0.759483	0.9711286	0.9605489	1	3811
HALLMARK_MITOTIC_SPINDLE	196	-0.206286	-0.651896	0.9987097	0.99242125	1	3740

Table S24

GSEA Analysis (Hallmark gene sets) on HNSC cancer cell lines comparing cell lines with or without 9p loss, Pathways Depleted

NAME	SIZE	ES	NES	NOM p-value	FDR q-value	FWER p-value	RANK AT MAX	LEADING EDGE
HALLMARK_TNFA_SIGNALING_VIA_NFKB	198	-0.619899	-2.170048	0	0	0	4069	tags=42%, list=15%, sig
HALLMARK_COAGULATION	124	-0.590234	-1.9757	0	0	0	4463	tags=34%, list=17%, sig
HALLMARK_INFLAMMATORY_RESPONSE	193	-0.571366	-1.974279	0	0	0	3097	tags=30%, list=12%, sig
HALLMARK_EPITHELIAL_MESENCHYMAL_TRANSITION	198	-0.534657	-1.860491	0	2.16E-04	0.001	1844	tags=17%, list=7%, sign
HALLMARK_KRAS_SIGNALING_UP	187	-0.519257	-1.795184	0	9.94E-04	0.005	3604	tags=28%, list=14%, sig
HALLMARK_ANGIOGENESIS	33	-0.656333	-1.75946	0.00501672	0.0023008	0.014	2975	tags=33%, list=11%, sig
HALLMARK_IL6_JAK_STAT3_SIGNALING	84	-0.544827	-1.711052	0.00150602	0.00354771	0.026	3605	tags=38%, list=14%, sig
HALLMARK_UV_RESPONSE_DN	142	-0.510999	-1.710883	0	0.00310424	0.026	7022	tags=43%, list=27%, sig
HALLMARK_APOPTOSIS	158	-0.48388	-1.654786	0	0.00628327	0.057	5767	tags=36%, list=22%, sig
HALLMARK_INTERFERON_GAMMA_RESPONSE	188	-0.471526	-1.63304	0	0.00712844	0.073	2406	tags=19%, list=9%, sign
HALLMARK_ALLOGRAFT_REJECTION	162	-0.464622	-1.580121	0.00282087	0.01053302	0.116	3066	tags=21%, list=12%, sig
HALLMARK_IL2_STAT5_SIGNALING	192	-0.445174	-1.541696	0.002849	0.0151668	0.168	3882	tags=24%, list=15%, sig
HALLMARK_COMPLEMENT	188	-0.420759	-1.447641	0.00278164	0.03660318	0.388	5168	tags=30%, list=20%, sig
HALLMARK_P53_PATHWAY	196	-0.397632	-1.380204	0.01081081	0.06433246	0.621	3456	tags=20%, list=13%, sig
HALLMARK_MYOGENESIS	183	-0.394919	-1.36761	0.01969058	0.06886461	0.662	2498	tags=18%, list=9%, sign
HALLMARK_CHOLESTEROL_HOMEOSTASIS	72	-0.44087	-1.346827	0.06026059	0.07996611	0.733	2866	tags=18%, list=11%, sig
HALLMARK_APICAL_SURFACE	43	-0.465589	-1.286086	0.11575563	0.13013865	0.901	4443	tags=30%, list=17%, sig
HALLMARK_HYPOXIA	193	-0.366242	-1.275969	0.0455192	0.13387458	0.923	3468	tags=18%, list=13%, sig
HALLMARK_INTERFERON_ALPHA_RESPONSE	95	-0.39273	-1.244748	0.11620795	0.16426632	0.967	4418	tags=20%, list=17%, sig
HALLMARK_ANDROGEN_RESPONSE	97	-0.380451	-1.212907	0.14285715	0.19757609	0.985	5264	tags=21%, list=20%, sig
HALLMARK_PROTEIN_SECRETION	96	-0.371022	-1.187122	0.17204301	0.23100984	0.994	4307	tags=22%, list=16%, sig
HALLMARK_UNFOLDED_PROTEIN_RESPONSE	110	-0.355734	-1.149209	0.2185129	0.28581247	0.997	2230	tags=10%, list=8%, sign
HALLMARK_HEME_METABOLISM	180	-0.328723	-1.130226	0.2168331	0.31082824	0.999	5916	tags=29%, list=22%, sig
HALLMARK_XENOBIOTIC_METABOLISM	190	-0.321674	-1.124744	0.19855073	0.30841008	0.999	3941	tags=17%, list=15%, sig
HALLMARK_KRAS_SIGNALING_DN	170	-0.322385	-1.096166	0.25637394	0.35064724	1	4137	tags=24%, list=16%, sig
HALLMARK_ESTROGEN_RESPONSE_EARLY	197	-0.298795	-1.049508	0.35021707	0.4385567	1	5627	tags=23%, list=21%, sig
HALLMARK_GLYCOLYSIS	196	-0.2988	-1.036344	0.36219338	0.45062795	1	3275	tags=16%, list=12%, sig
HALLMARK_APICAL_JUNCTION	197	-0.298921	-1.03401	0.392022	0.43924826	1	5734	tags=27%, list=22%, sig
HALLMARK_BILE_ACID_METABOLISM	103	-0.31583	-1.022427	0.41097924	0.45043015	1	5617	tags=24%, list=21%, sig
HALLMARK_TGF_BETA_SIGNALING	53	-0.296927	-0.855525	0.6930693	0.83178765	1	6869	tags=25%, list=26%, sig
HALLMARK_HEDGEHOG_SIGNALING	35	-0.305406	-0.823129	0.74429965	0.8723356	1	7394	tags=43%, list=26%, sig
HALLMARK_PI3K_AKT_MTOR_SIGNALING	102	-0.250278	-0.808546	0.8445122	0.8709158	1	3406	tags=13%, list=13%, sig

**Table S25**  
**Cox proportional hazards model for OCFs of the indicated parameters in Real-World Evidence Cohort**

Plot Title	HR	HR_95CI LowerBound	HR_95CI UpperBound	p-value	arm2_name	arm1_name	arm2_n	arm1_n	arm2_median_weeks	arm1_median_weeks
3p - IO	0.781	0.410	1.489	0.449	Loss	No Loss	35	87	43	79
3p - non-IO	0.506	0.239	1.070	0.069	Loss	No Loss	15	59	67	86
17p - IO	1.074	0.426	2.712	0.881	Loss	No Loss	11	111	48	79
17p - non-IO*					Loss	No Loss	2	72	6	72
9p - IO	0.468	0.232	0.944	0.030	Loss	No Loss	19	103	43	79
9p - non-IO	0.988	0.397	2.457	0.980	Loss	No Loss	12	62	83	67
9p13 - IO	0.636	0.342	1.183	0.150	Loss	No Loss	29	93	79	53
9p13 - non-IO	1.020	0.468	2.224	0.960	Loss	No Loss	19	55	174	67
9p21.3 - IO	0.907	0.514	1.603	0.738	Loss	No Loss	45	77	50	80
9p21.3 - non-IO	1.168	0.558	2.444	0.681	Loss	No Loss	26	48	83	49
9p24.1 - IO	0.482	0.249	0.934	0.028	Loss	No Loss	24	98	43	79
9p24.1 - non-IO	0.986	0.439	2.218	0.973	Loss	No Loss	17	57	83	67
PDL1 - IO	0.594	0.336	1.050	0.071	Deletion	No Deletion	37	85	43	79
PDL1 - non-IO	0.752	0.361	1.568	0.446	Deletion	No Deletion	21	53	83	67
PDL2 - IO	0.582	0.321	1.055	0.072	Deletion	No Deletion	32	90	43	79
PDL2 - non-IO	0.649	0.311	1.353	0.245	Deletion	No Deletion	20	54	72	69
JAK2 - IO	0.580	0.313	1.074	0.081	Deletion	No Deletion	33	89	43	79
JAK2 - non-IO	0.715	0.348	1.466	0.358	Deletion	No Deletion	24	50	72	69
PDL1, JAK2 - IO	0.436	0.235	0.810	0.007	Co-Deletion	No Co-Deletion	29	93	27	80
PDL1, JAK2 - non-IO	0.979	0.450	2.133	0.958	Co-Deletion	No Co-Deletion	19	55	83	67
PDL2, JAK2 - IO	0.473	0.252	0.888	0.018	Co-Deletion	No Co-Deletion	28	94	43	79
PDL2, JAK2 - non-IO	0.843	0.387	1.838	0.667	Co-Deletion	No Co-Deletion	18	56	83	67
PDL1, PDL2 - IO	0.554	0.306	1.006	0.050	Co-Deletion	No Co-Deletion	31	91	43	79
PDL1, PDL2 - non-IO	0.649	0.311	1.353	0.245	Co-Deletion	No Co-Deletion	20	54	72	69
PDL1, PDL2, JAK2 - IO**	0.473	0.252	0.888	0.018	Co-Deletion	No Co-Deletion	28	94	43	79
PDL1, PDL2, JAK2 - non-IO**	0.843	0.387	1.838	0.667	Co-Deletion	No Co-Deletion	18	56	83	67

\*Insufficient n in the No Loss arm to perform hazard ratio calculations

\*\*For the 32 PDL2 deletions, PDL1 was always co-deleted resulting in identical numbers in the PDL2, JAK2 and the PDL2, PDL2, JAK2 cohorts. PDL1 was deleted 5 times without PDL2 being co-deleted.